Theses and Dissertations   1. Thesis and Dissertation Collection, all items

1991-12

Ocean bottom modeling for ray acoustics

Jones, Trevor N.

Monterey, California. Naval Postgraduate School

http://hdl.handle.net/10945/26660

NAVAL POSTGRADUATE SCHOOL
Monterey , California

THESIS

OCEAN BOTTOM MODELING
FOR RAY ACOUSTICS

by

Trevor N. Jones

December 1991

Thesis Advisor   Lawrence J. Ziomek

REPORT DOCUMENTATION PAGE

Report Security Classification Unclassified		1b Restrictive Markings			
Security Classification Authority		3 Distribution Availability of Report			
Declassification Downgrading Schedule		Approved for public release; distribution is unlimited.			
Performing Organization Report Number(s)		5 Monitoring Organization Report Number(s)			
Name of Performing Organization val Postgraduate School	6b Office Symbol *(if applicable)* 33	7a Name of Monitoring Organization Naval Postgraduate School			
Address *(city, state, and ZIP code)* onterey, CA 93943-5000		7b Address *(city, state, and ZIP code)* Monterey, CA 93943-5000			
Name of Funding Sponsoring Organization	8b Office Symbol *(if applicable)*	9 Procurement Instrument Identification Number			
Address *(city, state, and ZIP code)*		10 Source of Funding Numbers			
		Program Element No	Project No	Task No	Work Unit Accession No

Title *(include security classification)* OCEAN BOTTOM MODELING FOR RAY ACOUSTICS

Personal Author(s) Trevor N. Jones

Type of Report ister's Thesis	13b Time Covered From To	14 Date of Report *(year, month, day)* December 1991	15 Page Count 142

Supplementary Notation The views expressed in this thesis are those of the author and do not reflect the official policy or po-on of the Department of Defense or the U.S. Government.

Cosati Codes			18 Subject Terms *(continue on reverse if necessary and identify by block number)*
eld	Group	Subgroup	word processing, Script, GML, text processing.

Abstract *(continue on reverse if necessary and identify by block number)*
Akima cubic spline and spatial Fourier series (SFS) techniques for modeling ocean bottom contours from bathymetric a were comparatively analyzed. SFS methods encountered difficulty in ocean bottom reconstruction despite several en-acements to the fundamental technique. Both Akima cubic spline and SFS approaches proved unsatisfactory in re-oducing first and second-order derivatives for several arbitrarily shaped ocean bottom contours.

A simple reflection angle algorithm for arbitrary one-dimensional bottom models was examined and found to be accurate. graphical demonstration of acoustic ray interaction with the ocean bottom using a variety of mathematical ocean bottom dels and the reflection angle algorithm was conducted.

Distribution Availability of Abstract unclassified unlimited ☐ same as report ☐ DTIC users	21 Abstract Security Classification Unclassified	
Name of Responsible Individual wrence J. Ziomek	22b Telephone *(include Area code)* (408) 646-3206	22c Office Symbol 72Zm

FORM 1473,84 MAR   83 APR edition may be used until exhausted   security classification of this page
All other editions are obsolete

Unclassified

Ocean Bottom Modeling
For Ray Acoustics

by

Trevor N. Jones
Lieutenant Commander, Royal Australian Navy
B.Sc., University of New South Wales, Australia, 1980

Submitted in partial fulfillment of the
requirements for the degree of

MASTER OF SCIENCE IN ENGINEERING ACOUSTICS

from the

ABSTRACT

Akima cubic spline and spatial Fourier series (SFS) techniques for modeling ocean bottom contours from bathymetric data were comparatively analyzed. SFS methods encountered difficulty in ocean bottom reconstruction despite several enhancements to the fundamental technique. Both Akima cubic spline and SFS approaches proved unsatisfactory in reproducing first and second-order derivatives for several arbitrarily shaped ocean bottom contours.

A simple reflection angle algorithm for arbitrary one-dimensional bottom models was examined and found to be accurate. A graphical demonstration of acoustic ray interaction with the ocean bottom using a variety of mathematical ocean bottom models and the reflection angle algorithm was conducted.

TABLE OF CONTENTS

LIST OF TABLES

vi

LIST OF FIGURES

I. INTRODUCTION

The primary endeavour of this thesis research was the comparative evaluation of existing numerical cubic spline techniques with spatial Fourier series (SFS) methods for the interpolative modeling of real, discrete, ocean bathymetric data. The Akima cubic spline was chosen for its reported ability to produce ocean bottom contour curves which pass through the original data while minimizing artificial oscillations in the interpolation. The Akima cubic spline logic was implemented via the IMSL Version 10 double precision computer program DCSAKM. First and second-order derivatives of the resulting spline were calculated from a second IMSL Version 10 double precision program DCSDER. The SFS technique was developed as a separate generic computer program subroutine.

Seven differentiable mathematical bathymetric data models were employed in determining the accuracy and relative worth of both the Akima cubic spline and SFS representations of the ocean bottom contour, including the first and second-order derivatives of these contours. A series of numerical enhancements were also applied to both modeling techniques to optimize their utility in accurately reconstructing sampled ocean bottoms.

The second objective of this research was the development and evaluation of a reflection angle algorithm, derived from the principles of the calculus as outlined by Goodman [Ref. 1], which enables the computation of reflection angles for acoustic rays incident upon an ocean bottom whose variation in depth is modeled as a function of down range. This algorithm requires exact first derivatives for angle calculations. Hence the apriori requirement for accurate ocean bottom modeling.

Both of the developments outlined above were then incorporated into an existing acoustic ray trace program and several simple case studies investigated.

II.   THEORETICAL ANALYSIS

A.   SPATIAL FOURIER SERIES REPRESENTATION OF OCEAN BOTTOM CONTOURS

For any ocean region of horizontal range extent Z meters with a one-dimensional, range dependent bathymetry, the ocean bottom contour $y_B(z)$ can be modeled by the following spatial Fourier series (SFS):

$$y_B(z) = |w_0| + 2\sum_{s=1}^{S} |w_s| \cos(2\pi s f_{Z_0} z - \angle w_s) , 0 \leq z \leq Z. \tag{2.1}$$

The magnitude and phase angle of the complex Fourier series coefficient w_s, for spatial harmonic s, are given by $|w_s|$ and $\angle w_s$, respectively. The average value for depth, which corresponds to zero spatial frequency or the "DC component" of the bathymetry data, is represented by $|w_0|$. The fundamental spatial frequency f_{Z_0} is defined as:

$$f_{Z_0} = \frac{1}{N T_{S_z}} \tag{2.2}$$

where N is the total number of bathymetric data points and T_{S_z} is the uniform sampling period in the z direction in meters per sample. The highest spatial harmonic is S and is governed by the number of data points:

$$S = \frac{N}{2} , \text{ for even N} \tag{2.3}$$

and

$$S = \frac{N-1}{2} , \text{ for odd N.} \tag{2.4}$$

The first and second-order derivatives of the SFS representation of discrete ocean bathymetry are readily determined from Equation (2.1):

$$y_B'(z) = -4\pi f_{Z_0} \sum_{s=1}^{S} s |w_s| \sin(2\pi s f_{Z_0} z - \angle w_s) , 0 \leq z \leq Z \tag{2.5}$$

2

and

$$y_B''(z) = - 8\pi^2 f_{Z_0}^2 \sum_{s=1}^{S} s^2 |w_s|^2 \cos(2\pi s f_{Z_0} z - \angle w_s) \, , \, 0 \leq z \leq Z. \tag{2.6}$$

The complex Fourier series coefficients w_s are determined from the spatial discrete Fourier transform (DFT) of the ocean bathymetric data as follows:

$$w_s = \frac{1}{N} \sum_{n=0}^{N-1} y_B(nT_{S_y}) W_N^{sn} \, , \quad s = -S,...,0,...,S \tag{2.7}$$

The term W_N^{sn} is known as the DFT *weighting factor* and is given by

$$W_N^{-sn} = [e^{(+j2\pi/N)}]^{sn} \, , \tag{2.8}$$

where

$$N = 2S + 1 \tag{2.9}$$

when the ocean bottom sampling frequency equals the Nyquist rate.

The reconstruction of any one-dimensional function or contour by a Fourier series of finite extent will be characterized by small oscilliatory deviations from the exact function values in the interpolated region between the discrete samples. These oscillations are often of little consequence due to the small amplitudes involved. However, efforts to model a simple ocean bottom profile of constant non zero slope by SFS methods generate significant amplitude errors at the function extremeties. This development highlights a particular problem that SFS methods have with apparent function discontinuities represented by the boundaries of the discrete data string. This anomoly, first documented by Willard Gibbs in 1899 and known as "Gibbs' phenomenon" [Ref. 2], can be partially redressed by the inclusion of more data samples. This results in the compression of the larger amplitude oscillations toward the discontinuities. However, the peak amplitude of these ripples, being independent of the number of discrete data, remains constant. The problems associated with SFS methods and the "Gibbs' phenomenon" take on greater significance when derivatives of the bottom contour are sought. The ripples generated at the extremities by the Fourier series representation will be magnified in subsequent calculations making reliable determination of function

3

derivatives difficult. Strum and Kirk [Ref. 2] provide a more detailed treatment of "Gibbs' phenomenon".

Lanczos [Ref. 3] argued that the impact of this phenomenon could be minimized by hastening the convergence of the Fourier series and proposed the following modified complex Fourier series coefficient w_{s_L} as a means of achieving this:

$$w_{s_L} = \frac{\sin(s\pi/S)}{s\pi/S} w_s , \; s \neq 0 \qquad (2.10)$$

where w_s is the original coefficient given by Equation (2.7).

An additional modification to Lanczos' formula was suggested by Hamming [Ref. 4] and involved increasing the harmonic S by 1. The final expression for spatial complex Fourier series coefficients employing the Lanczos smoothing methodology therefore becomes

$$w_{s_L} = \frac{\sin(s\pi/(S+1))}{s\pi/(S+1)} w_s , \; s \neq 0. \qquad (2.11)$$

B. THE REFLECTION ANGLE ALGORITHM

Acoustic rays obey the reflection laws applied in optics. Equation (2.12) relates the angle of incidence ζ and angle of reflection ζ' for a sound ray impinging the ocean surface or ocean bottom:

$$\zeta = \zeta'. \qquad (2.12)$$

Consider a ray launched from a sound source with initial angle β_0 and propagating in an isospeed ocean with a perfectly flat sea surface. When the ocean bottom is flat, the angle of incidence ζ will remain constant for successive reflections as shown in Figure 1. The magnitude of the reflection angle is given by

$$\zeta' = \beta_0. \qquad (2.13)$$

When the ocean bottom shoals (up slope) with constant angle of slope γ, the relationship given by Equation (2.13) is invalidated and subsequent acoustic ray reflections become linearly dependent upon the bottom slope. This observation, reported by Officer [Ref. 5] and illustrated in Figure 2, is given by

$$\zeta_n = (\beta_0 - n\gamma) \quad , \; n = 1,2,3,... \qquad (2.14)$$

4

where ($n = 1$) corresponds to the first bottom bounce with higher values for n representing subsequent surface and bottom reflections. Negative values for ζ_n indicate acoustic rays which have been reflected back toward their source. Assigning a negative value to γ in Equation (2.14) yields the relationship for ζ_n after an initial reflection from a bottom contour that deepens (down slope) with constant angle of slope γ. Figure 3 and Equation (2.15) refer to this situation:

$$\zeta_n = (\beta_0 + n\gamma) \quad , n = 1,2,3...$$ (2.15)
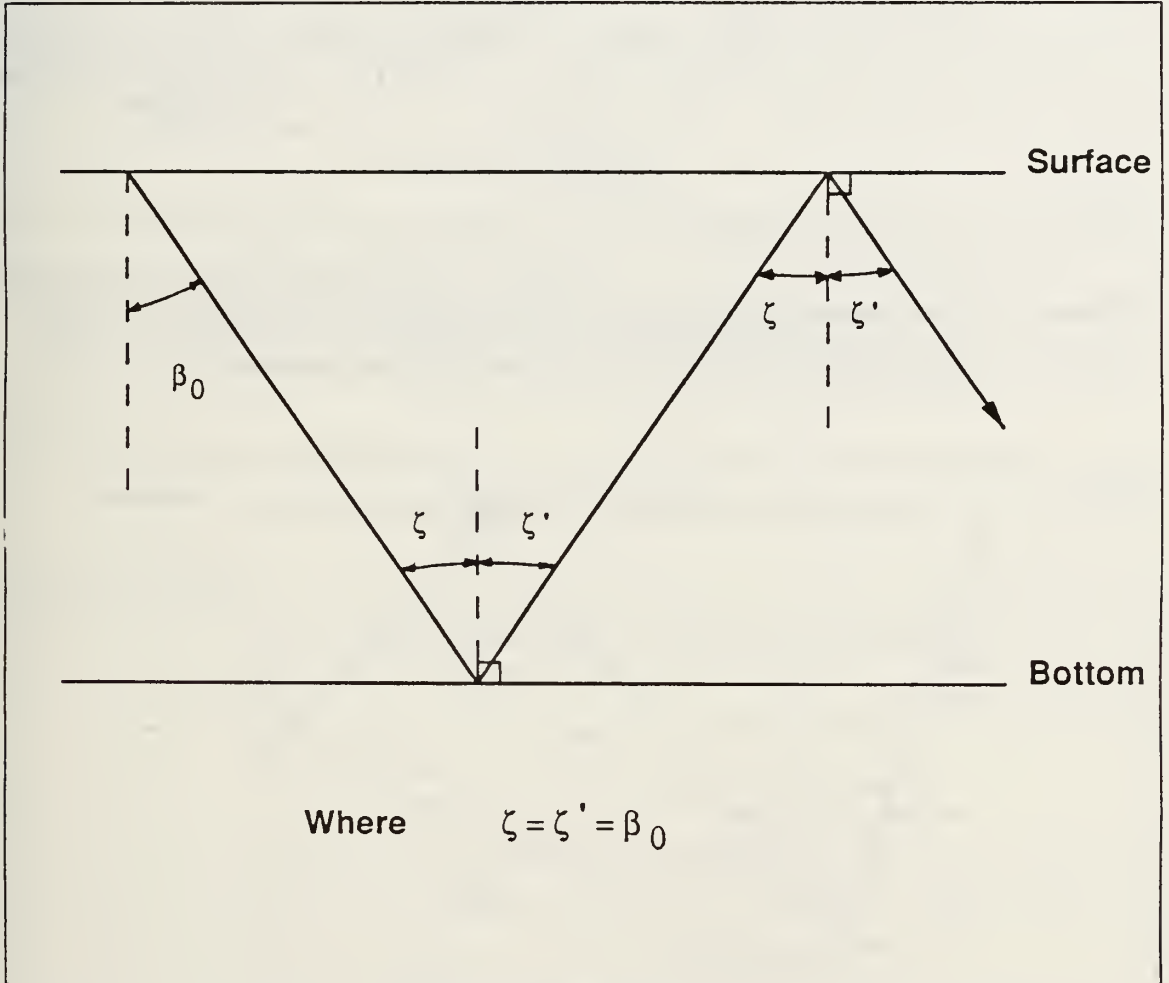
Figure 1.   Acoustic Ray Impinging a Flat Ocean Bottom: This diagram represents an acoustic ray launched with initial angle of propagation β_0 in an isospeed ocean with a flat ocean surface.
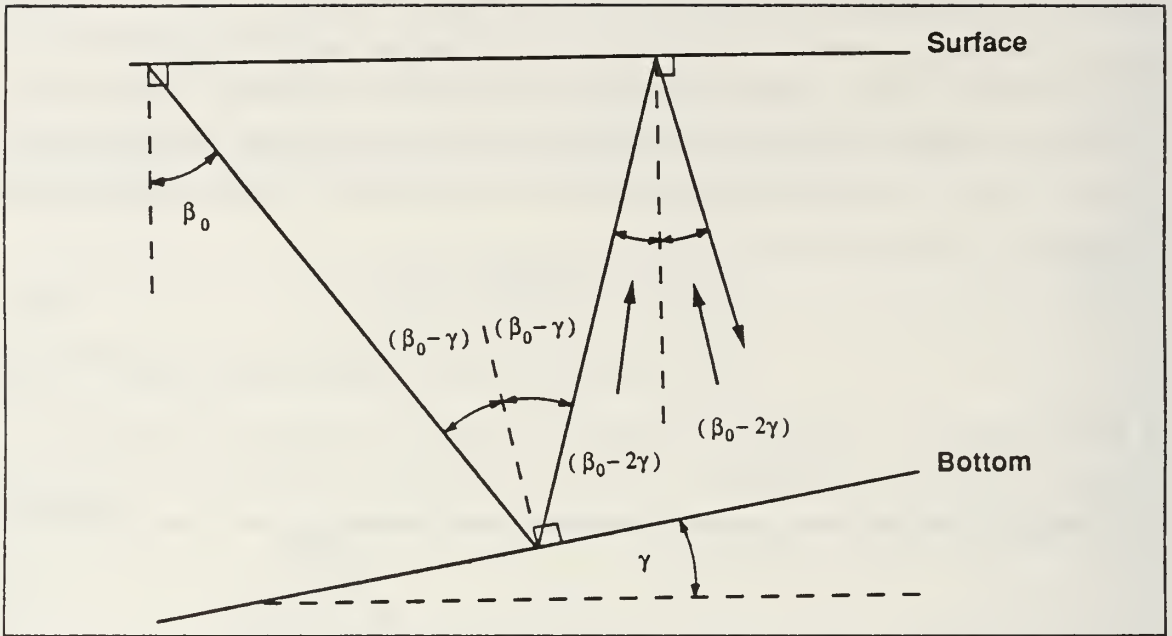
Figure 2. Acoustic Ray Impinging a Constant Up-Slope Ocean Bottom: This diagram represents an acoustic ray launched with initial angle of propagation β_0 in an isospeed ocean with a flat ocean surface.
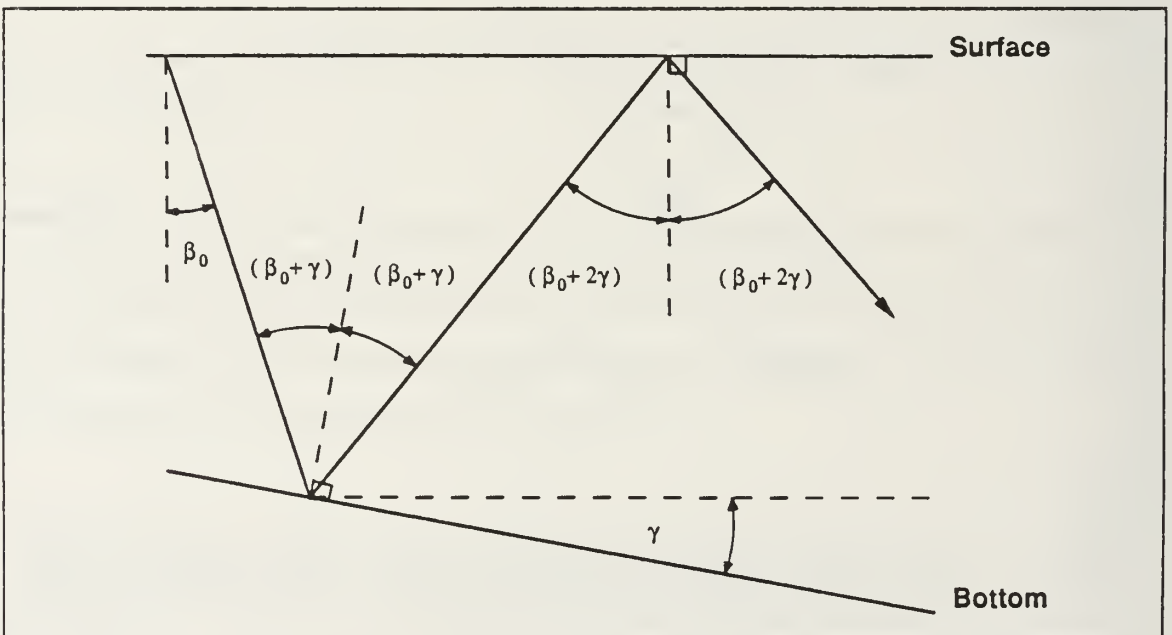
Figure 3. Acoustic Ray Impinging a Constant Down-Slope Ocean Bottom: This diagram represents an acoustic ray launched with initial angle of propagation β_0 in an isospeed ocean with a flat ocean surface.

These laws of reflection are equally valid in more general ocean models. However, their application is correspondingly more complex. In the case of constant sound speed c, acoustic rays travel in straight lines within the initial YZ launch plane making the calculation of ζ relatively simple. However, if sound speed is made to vary with depth such that

$$c = c(y),\tag{2.16}$$

then the acoustic ray will remain in the initial YZ launch plane but travel a curved path. Additionally, if the ocean bottom contour y_B varies arbitrarily with down range z from the sound source where

$$y_B = y_B(z),\tag{2.17}$$

then the relationships given by Equations (2.14) and (2.15) are no longer relevant since the angle of slope γ does not remain constant.

The calculation of ζ in an ocean model characterized by Equations (2.16) and (2.17) is achieved by representing the direction of the acoustic ray at any point along its path by the unit vector

$$\hat{n}(y) = v(y)\,\hat{j} + w(y)\,\hat{k}\tag{2.18}$$

as shown in Figure 4.
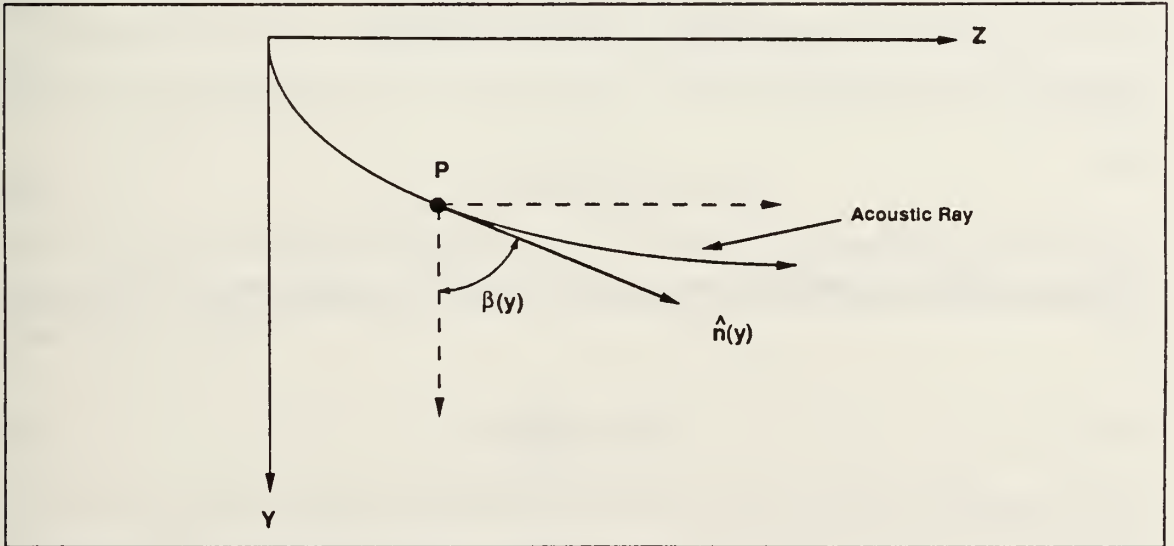
Figure 4.   Vector Representation of an Acoustic Ray: This diagram shows the vector representation of a sound ray travelling in an ocean medium where sound speed is a function of depth y.

7

The vector components $v(y)$ and $w(y)$ are the direction cosines with respect to the Y and Z axes, respectively, describing the direction of propagation of the ray and are given by

$$v(y) = \cos \beta(y) \tag{2.19}$$

and

$$w(y) = \sin \beta(y). \tag{2.20}$$

In addition, the tangent plane and normal vector at any point $P(x_0, z_0)$ on the ocean bottom must be determined.

The tangent plane at a particular point $P(x_0, y_0, z_0)$ on a two-dimensional surface given by

$$y = f(x, z) \tag{2.21}$$

can be determined as follows (see Goodman [Ref. 1]):

$$y - y_0 = f_x(x_0, z_0)(x - x_0) + f_z(x_0, z_0)(z - z_0) \tag{2.22}$$

where

$$f_x(x_0, z_0) = \frac{\partial}{\partial x} f(x, z)\big|_{x = x_0, z = z_0} \tag{2.23}$$

and

$$f_z(x_0, z_0) = \frac{\partial}{\partial z} f(x, z)\big|_{x = x_0, z = z_0}. \tag{2.24}$$

Goodman further showed the unit vector normal to the tangent plane at $P(x_0, y_0, z_0)$ to be

$$\hat{n}_\perp = \frac{\vec{n}_\perp}{|\vec{n}_\perp|} \tag{2.25}$$

where

$$\vec{n}_\perp = -f_x(x_0, z_0)\hat{i} + \hat{j} - f_z(x_0, z_0)\hat{k} \tag{2.26}$$

8

and

$$|\hat{n}_\perp| = \sqrt{f_x(x_0,z_0)^2 + 1 + f_z(x_0,z_0)^2}. \tag{2.27}$$

Substitution of the function y_B given by Equation (2.17) into Equation (2.22) yields the following general expression for the tangent plane at any point $P(y_0,z_0)$ on an ocean bottom which is an arbitrary function of down range z.

$$y - y_0 = y'_B(z)(z - z_0). \tag{2.28}$$

Similarly, substitution of the function y_B into Equation (2.25) provides the following general relationship for the vector normal to the bottom at any point $P(y_0,z_0)$:

$$\hat{n}_{B\perp} = \frac{\vec{n}_{B\perp}}{|\vec{n}_{B\perp}|} \tag{2.29}$$

where

$$\vec{n}_{B\perp} = +\hat{j} - y'_B(z_0)\hat{k} \tag{2.30}$$

and

$$|\vec{n}_{B\perp}| = \sqrt{1 + (y'_B(z_0))^2}. \tag{2.31}$$

The angle of slope γ at any point along the one-dimensional ocean floor y_B can be determined from elementary vector calculus with the use of Equation (2.29) as follows:

$$\gamma = \cos^{-1}(\hat{y} \cdot \hat{n}_{B\perp}) \tag{2.32}$$

where $\hat{y}$ is the unit vector lying along the y axis. The vector representation of an acoustic ray given by Equation (2.18) can be used in defining the sound ray $\hat{n}_i$ incident upon the ocean bottom where

$$\hat{n}_i = v_i\hat{j} + w_i\hat{k}. \tag{2.33}$$

The angle of arrival β_i, which is measured from the y axis to $\hat{n}_i$ and is necessary in the calculation of the angle of incidence ζ, is given by

$$\beta_i = \cos^{-1}(\hat{y} \cdot \hat{n}_i). \tag{2.34}$$

9

Finally, with general expressions determined for γ and β_i, the angle of incidence ζ and the launch angle for the reflected ray β_r can be evaluated from the following relationships:

$$\zeta = \beta_i - \Delta y_B \gamma \tag{2.35}$$

and

$$\beta_r = 180° - (\zeta + \Delta y_B \gamma) \tag{2.36}$$

where

$$\Delta y_B = \frac{y'_B(z_i)}{|y'_B(z_i)|}. \tag{2.37}$$

Figures 5 and 6 illustrate the respective cases of an acoustic ray incident upon an ocean bottom with negative and positive gradients, respectively.

10
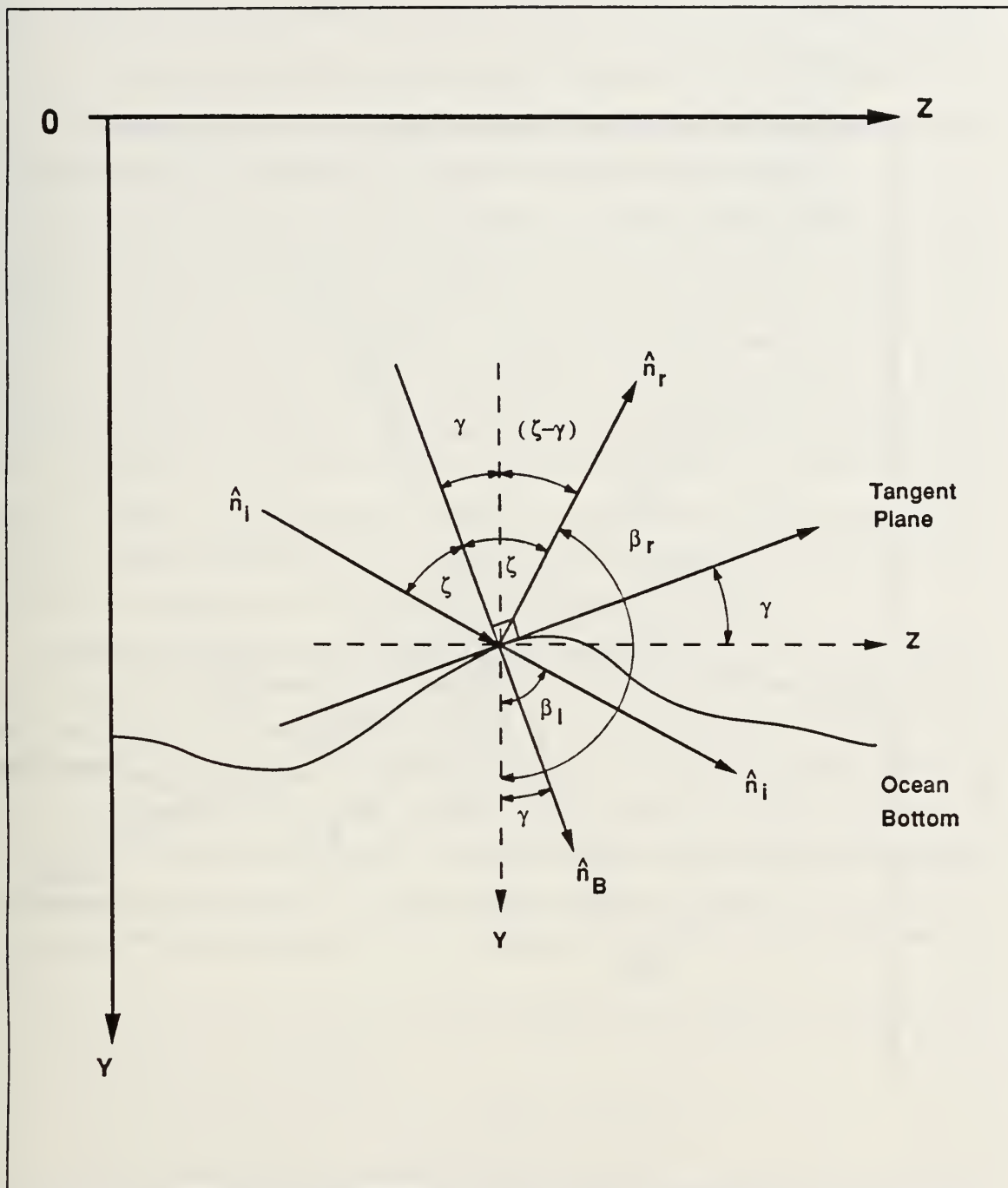
Figure 5. Acoustic Ray Impinging an Arbitrary Ocean Bottom: This diagram represents an acoustic ray incident upon an ocean bottom which is shoaling (up slope) at the point of impact.

11
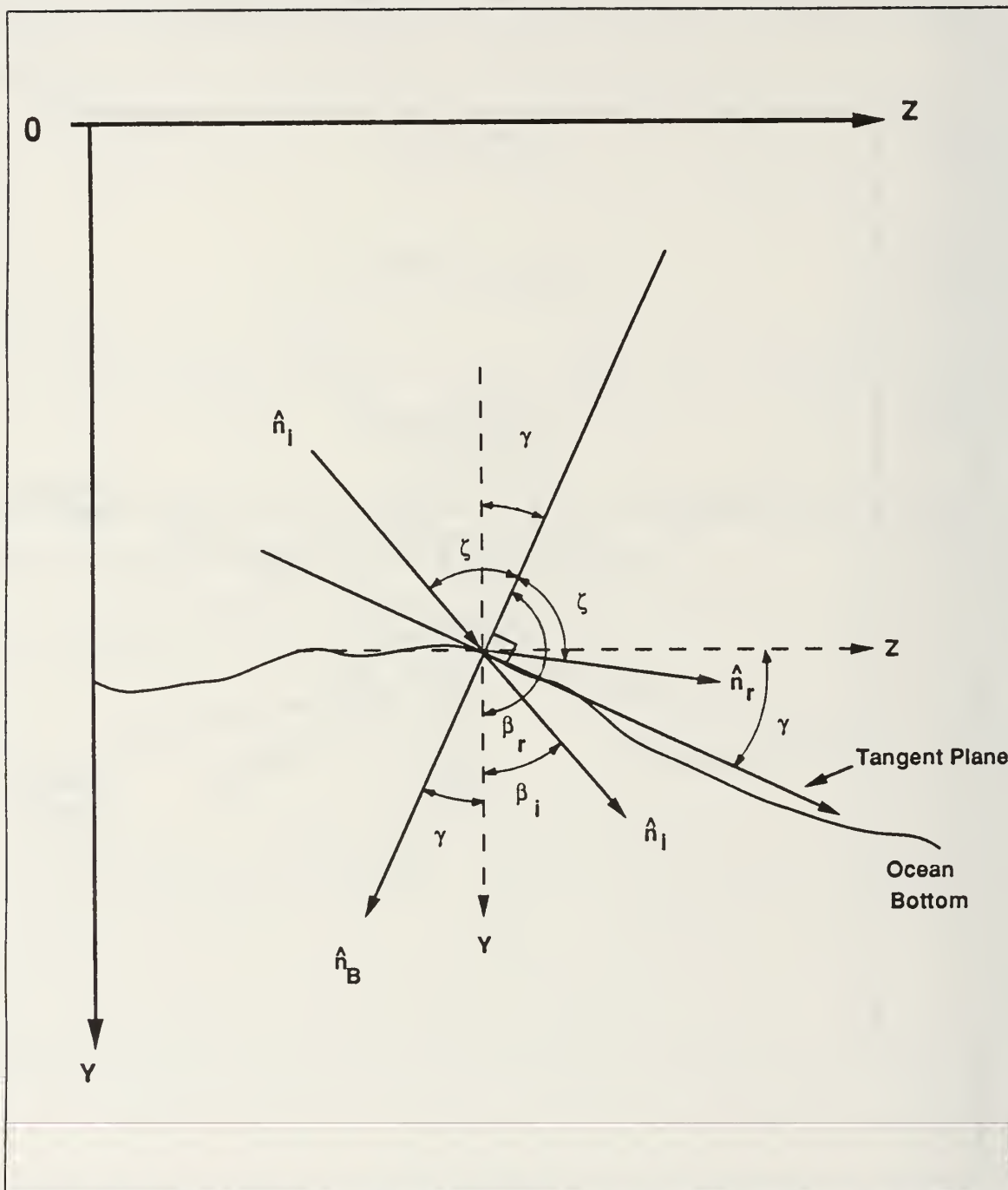
Figure 6. Acoustic Ray Impinging an Arbitrary Ocean Bottom: This diagram re-
presents an acoustic ray incident upon an ocean bottom which is
deepening (down slope) at the point of impact.

12

III. OCEAN BOTTOM MODELING OF DISCRETE BATHYMETRY

A. A COMPARATIVE ANALYSIS OF AKIMA CUBIC SPLINE AND SPATIAL FOURIER SERIES REPRESENTATIONS OF BATHYMETRIC DATA

The Akima Cubic Spline (ACS) algorithm accurately models most continuous functions from discrete data but will frequently return inaccurate first and second-order derivatives. Reliable derivative calculations are crucial for reflection angle and ray acoustic computations and consequently an alternative modeling technique was needed. One of the primary focuses of this thesis, therefore, was the investigation of Spatial Fourier Series (SFS) methods for modeling the ocean bottom from discrete bathymetric data. This particular approach possessed the added attraction in that bottom roughness could be related to spatial frequency components. Furthermore, derivative calculations could be readily determined from the resultant series representation of the contour obviating the requirement to call complex external computer programs.

Synthetic bathymetric profiles comprising 11 equidistant data points over a 1000 meter range were generated from seven exact mathematical functions containing features consistent with real ocean bottoms. ACS and SFS representations of each bottom contour, including their first and second-order derivatives, were then computed. Percentage error calculations were made with respect to the exact function values for each model and its associated derivatives. When the difference between the modeled and exact data was of magnitude less than 10^{-6}, the percentage error was assumed to be zero. Similarly, percentage errors greater than 10^6 were represented in tabular output as a series of asterisks.

The exact functions used to generate the artificial ocean bottom contours were:

- Flat bottom ($y_B(z) = 100$ m)
- Constant downslope bottom ($y_B(z) = 220.0 + 0.2z$ m)
- Constant upslope bottom ($y_B(z) = 420.0 - 0.2z$ m)
- One period cosine bottom ($y_B(z) = 450.0 - 250.0 \cos(0.002\pi z)$ m)
- Modified Witch of Agnesi bottom ($y_B(z) = 100.0 - \dfrac{125000.0}{(0.01z^2 + 2500.0)}$ m)
- Half catenary bottom ($y_B(z) = 315.0 - 30.0(e^{z/600.0} + e^{-z/600.0})$ m)
- Parabolic bottom ($y_B(z) = 50.0 + \dfrac{(z - 5000.0)^2}{2500.0}$ m).

Figures 7, 8 and 9 and Tables 1 and 2 reveal shortcomings associated with the SFS representation of a flat ocean bottom. While both the ACS and SFS techniques replicated precisely the original contour, the latter introduced small errors in both the first and second-order derivatives.

Figures 10, 11 and 12 and Tables 3 and 4 provide a comparison between the ACS and SFS representations of an ocean bottom which deepens (down slope) with constant slope. Table 3 and Figure 10 show that the ACS technique accurately modeled the original function and its derivatives. However, Figure 10 and Table 4 highlight difficulties in the SFS representation of this same contour. This method accurately reproduced the original discrete bathymetric data values but introduced oscilliatory errors in the interpolated region between them. These small oscillations around the true function values were propagated through the subsequent derivative calculations generating large percentage errors.

Figures 13, 14 and 15 and Tables 5 and 6 provide an analogous comparison for an ocean bottom which shoals (up-slope) at a constant rate. The results observed for this model were identical to those for the constant down slope ocean bottom.

Figures 16, 17 and 18 and Tables 7 and 8 pertain to the ACS and SFS representations of the one period cosine ocean bottom. Both techniques accurately reproduced the fundamental function shape as shown by Figure 10 but the ACS approach had trouble with both the first and second-order derivatives. Figures 17 and 18 and Table 7 refer. Additionally, both the ACS and SFS reconstructions of the first and second-order derivatives were characterized by large errors at the contour end points.

Figures 19, 20 and 21 and Tables 9 and 10 provide a comparison between the ACS and SFS representations of the modified Witch of Agnesi ocean (see [Ref. 6]) bottom model. The SFS technique was incapable of reproducing this contour or its derivatives as shown in the referenced Figures and Table 10. Furthermore, the oscilliatory errors first observed with the constant up slope and down slope ocean bottoms were again present. The ACS approach yielded a far more accurate reproduction of the exact bottom function. However, both the first and second-order derivative values, although better than those reproduced by SFS methods, were also unsatisfactory.

Figures 22, 23 and 24 and Tables 11 and 12 relate to the ACS and SFS representations of the half catenary (see [Ref. 6]) ocean bottom. The problems observed with the SFS reconstruction of this contour were identical to those observed for the modified Witch of Agnesi bottom as seen in Table 12. The ACS method again provided a true reproduction of the exact mathematical bottom model. In addition, the first-order
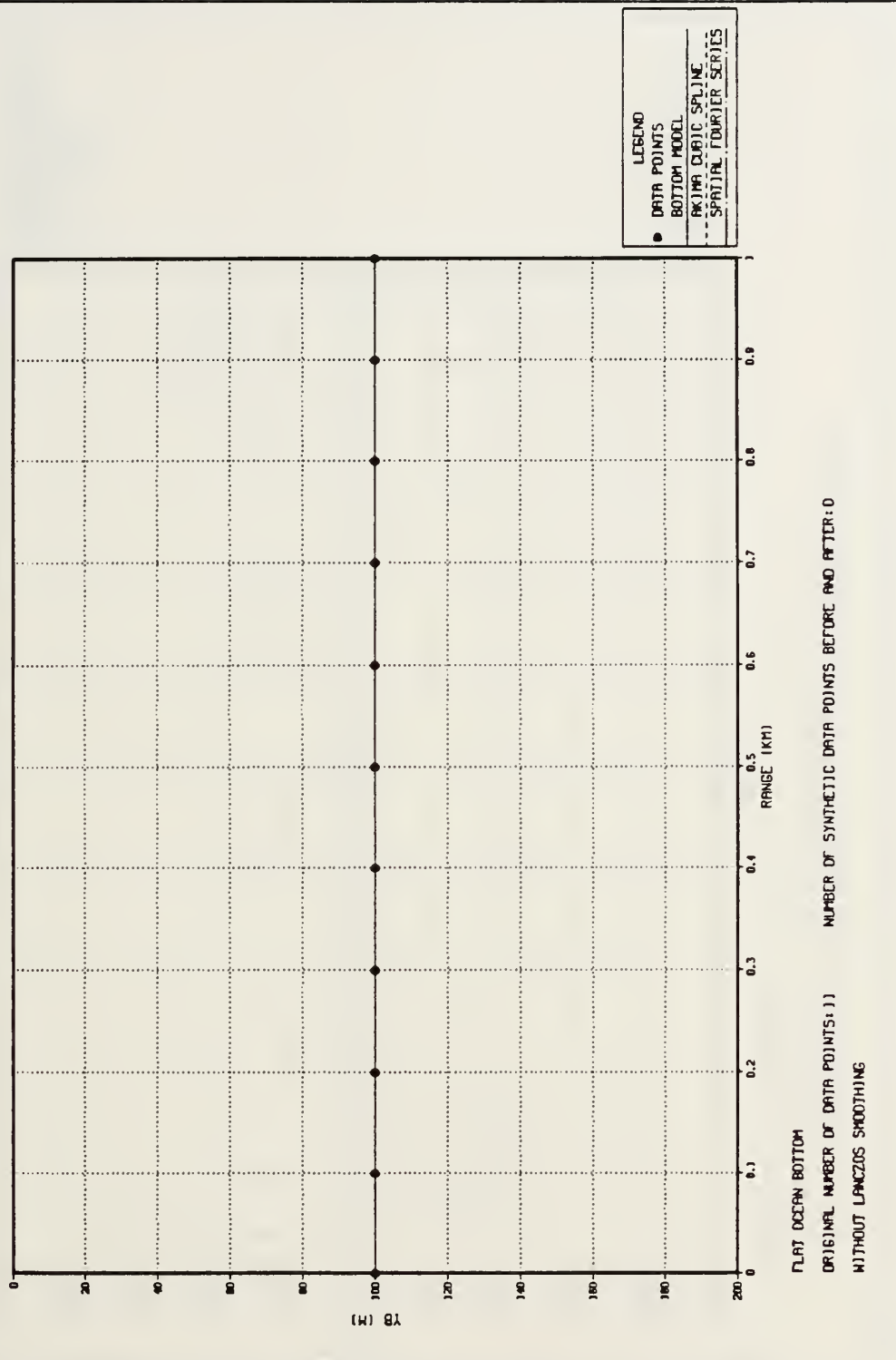
Figure 7.   Flat Ocean Bottom : Contour Reconstruction.

15
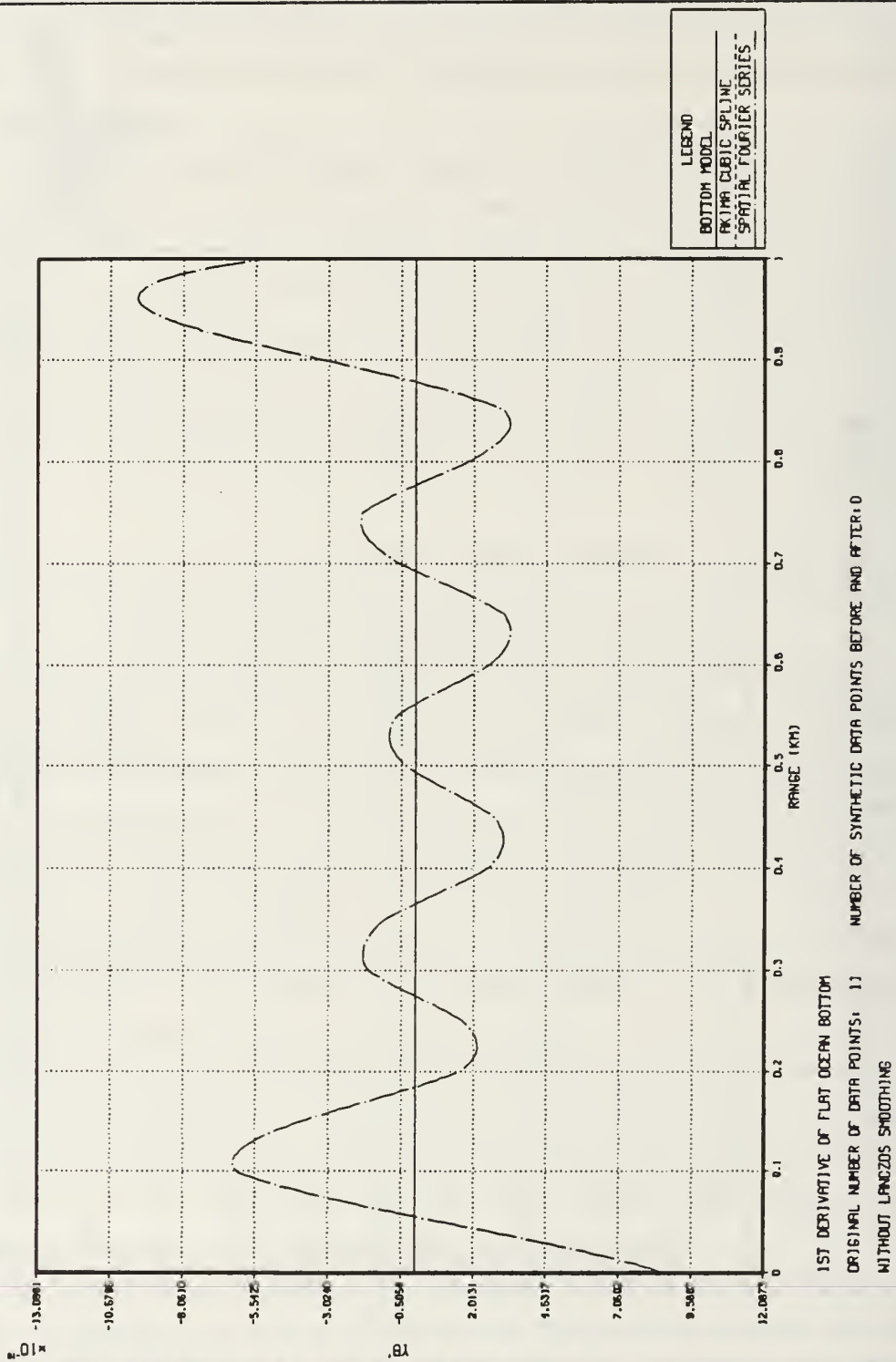
Figure 8.   Flat Ocean Bottom : First-Order Derivatives.

16
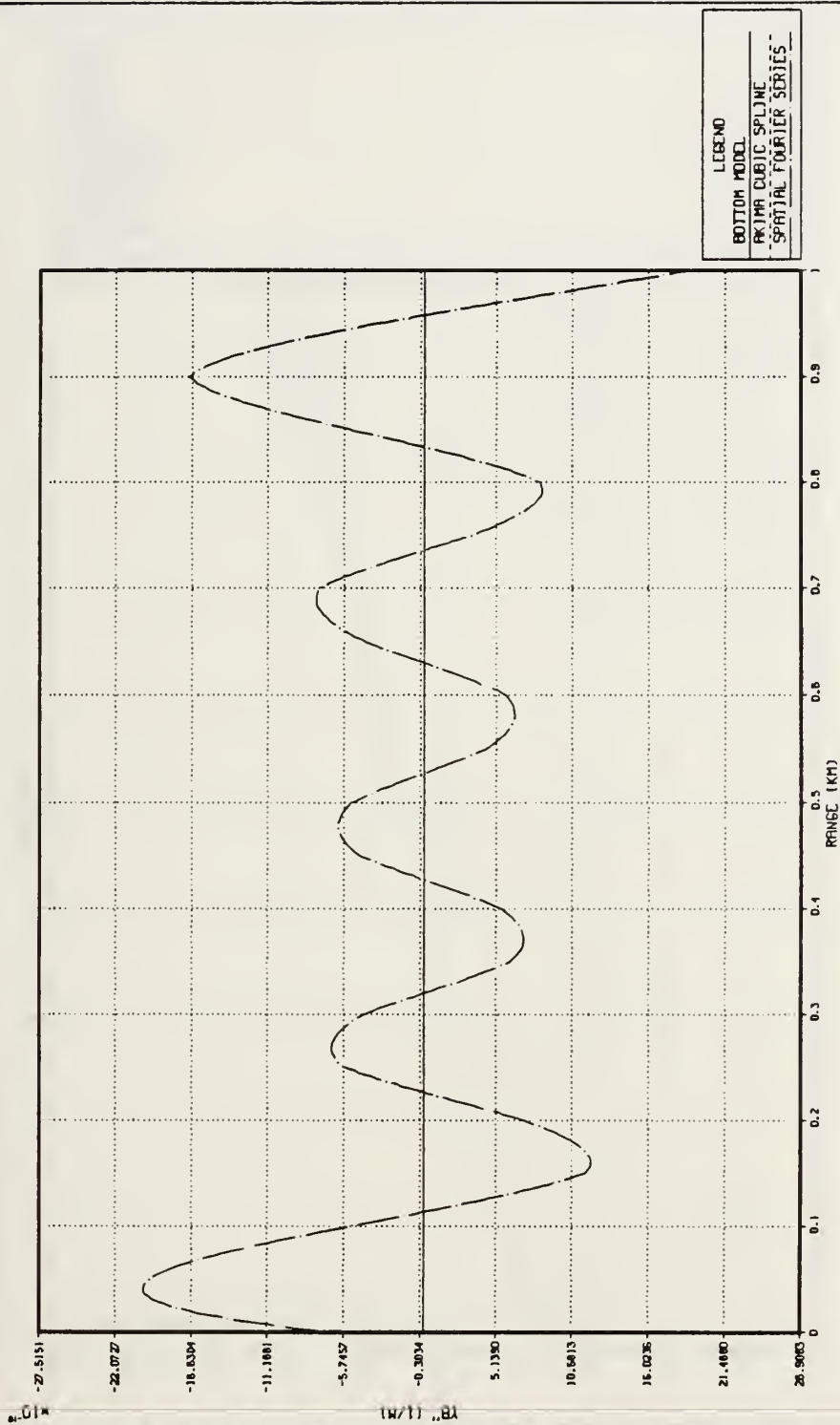
Figure 9.   Flat Ocean Bottom : Second-Order Derivatives.

17
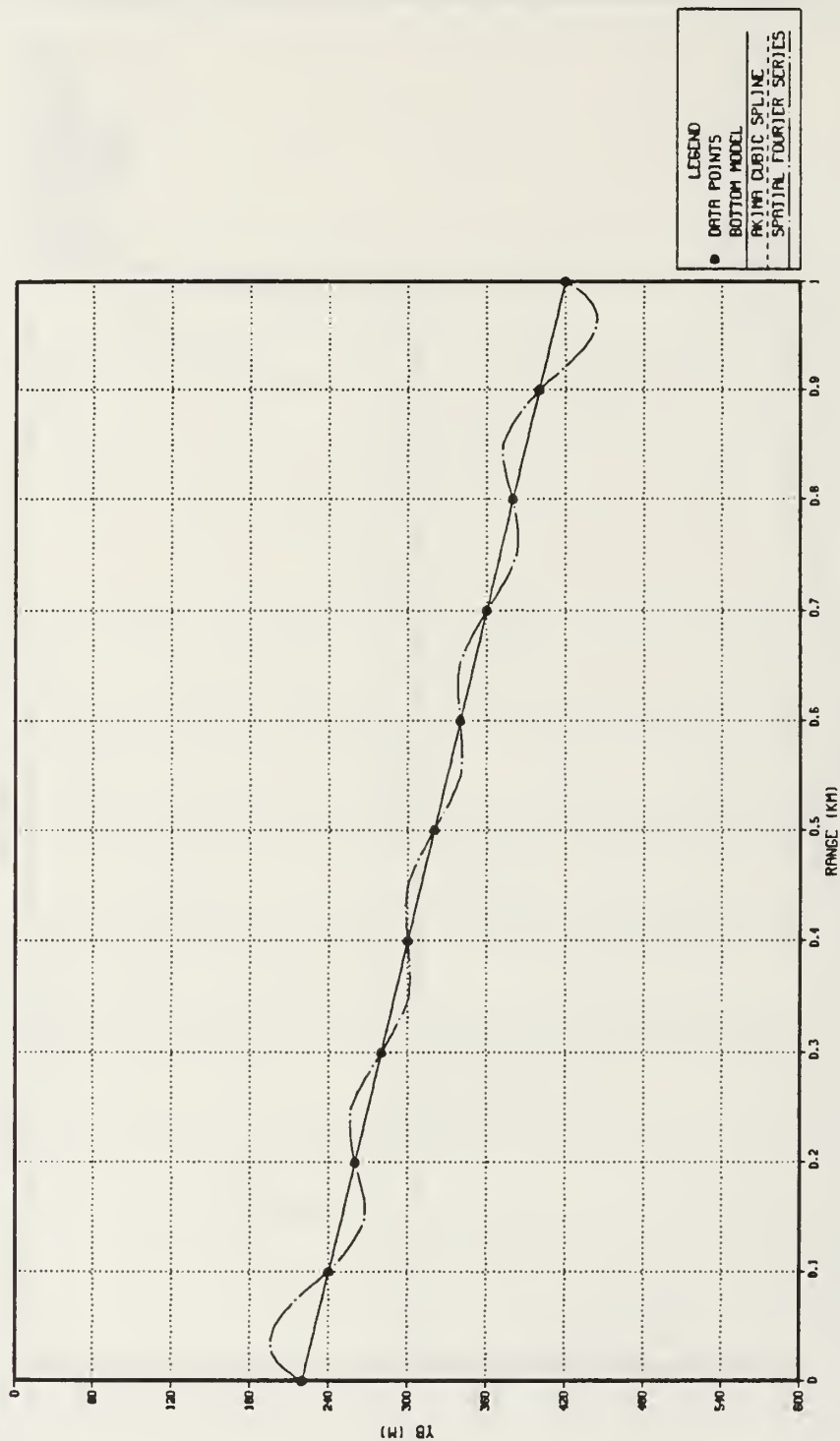
Figure 10.   Down-Slope Ocean Bottom : Contour Reconstruction.
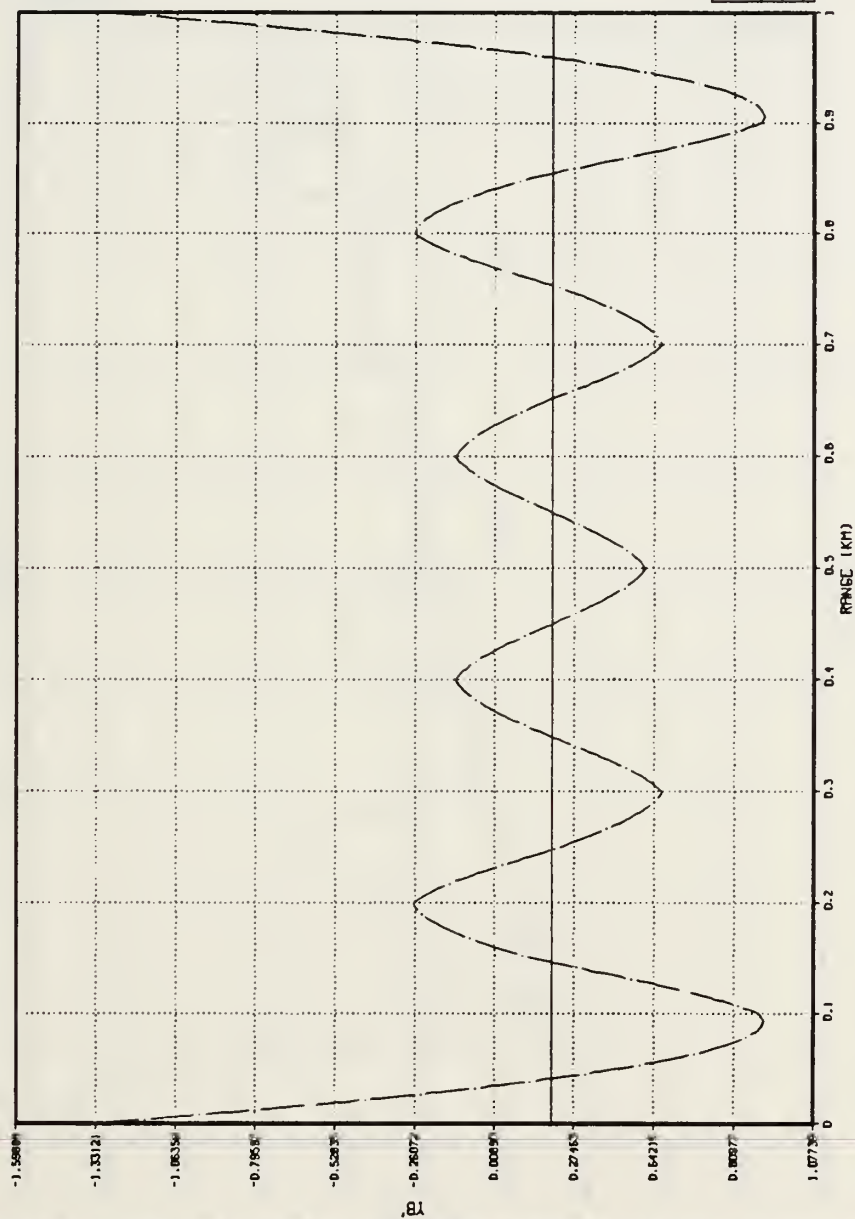
Figure 11.   Down-Slope Ocean Bottom : First-Order Derivatives.

19
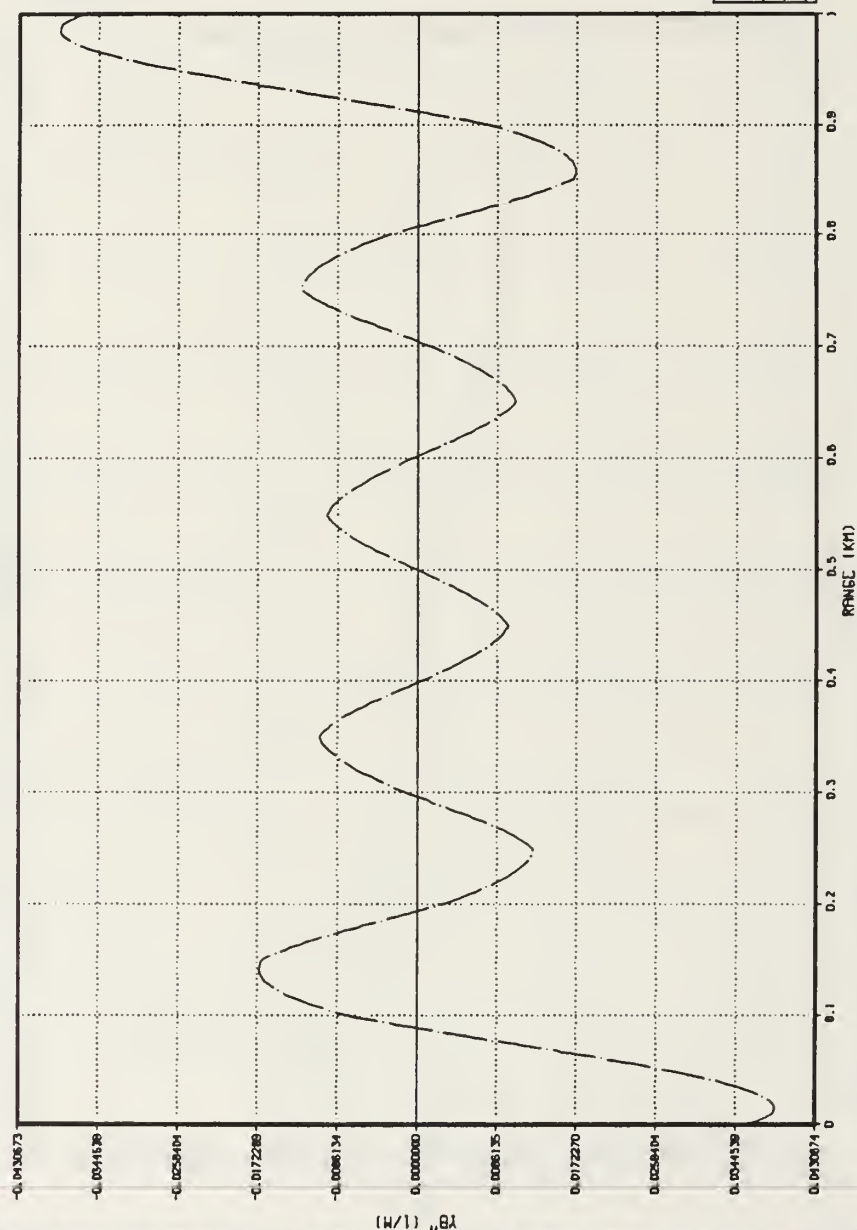
Figure 12.   Down-Slope Ocean Bottom : Second-Order Derivatives.
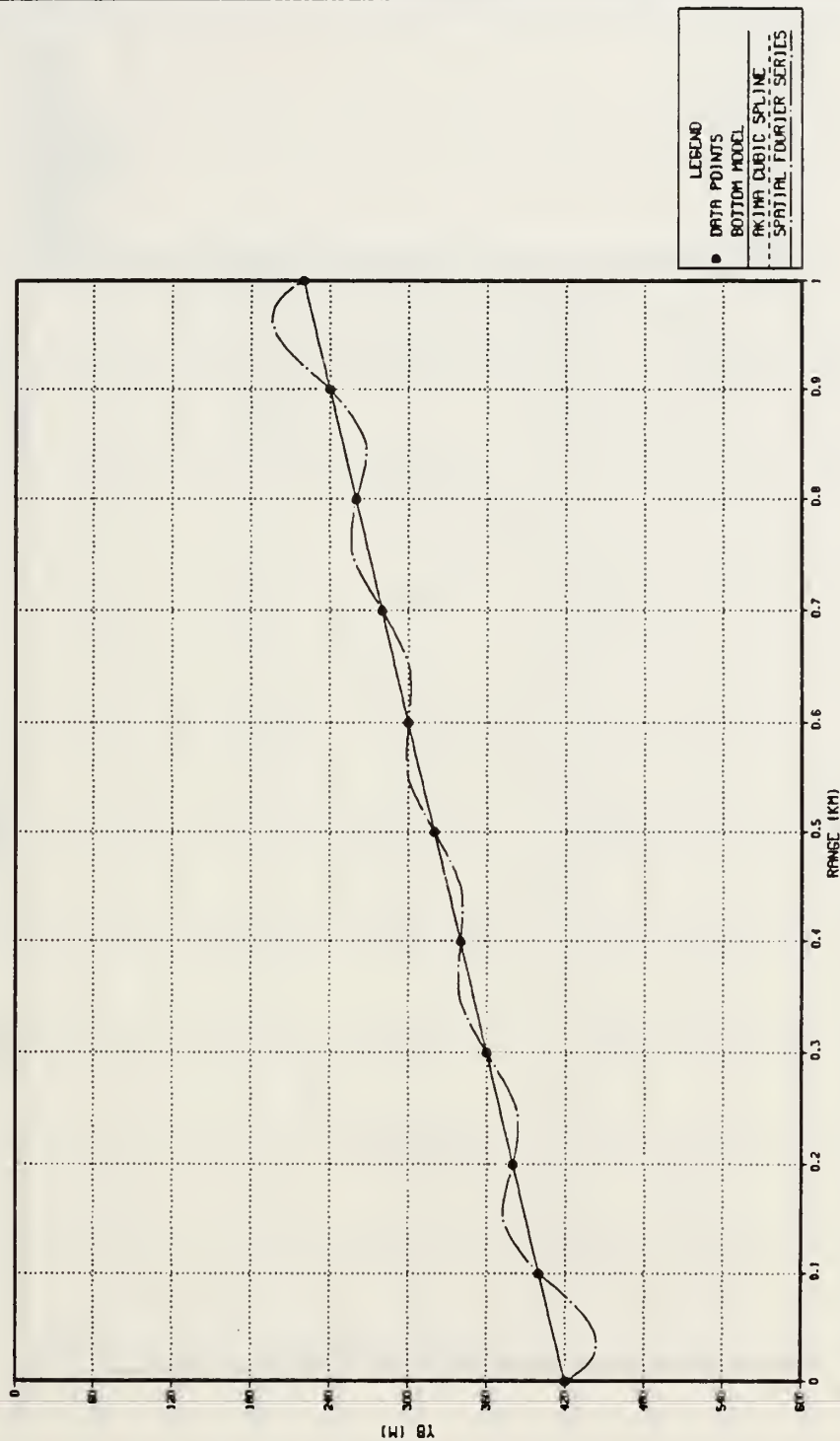
20

Figure 13.   Up-Slope Ocean Bottom : Contour Reconstruction.

21
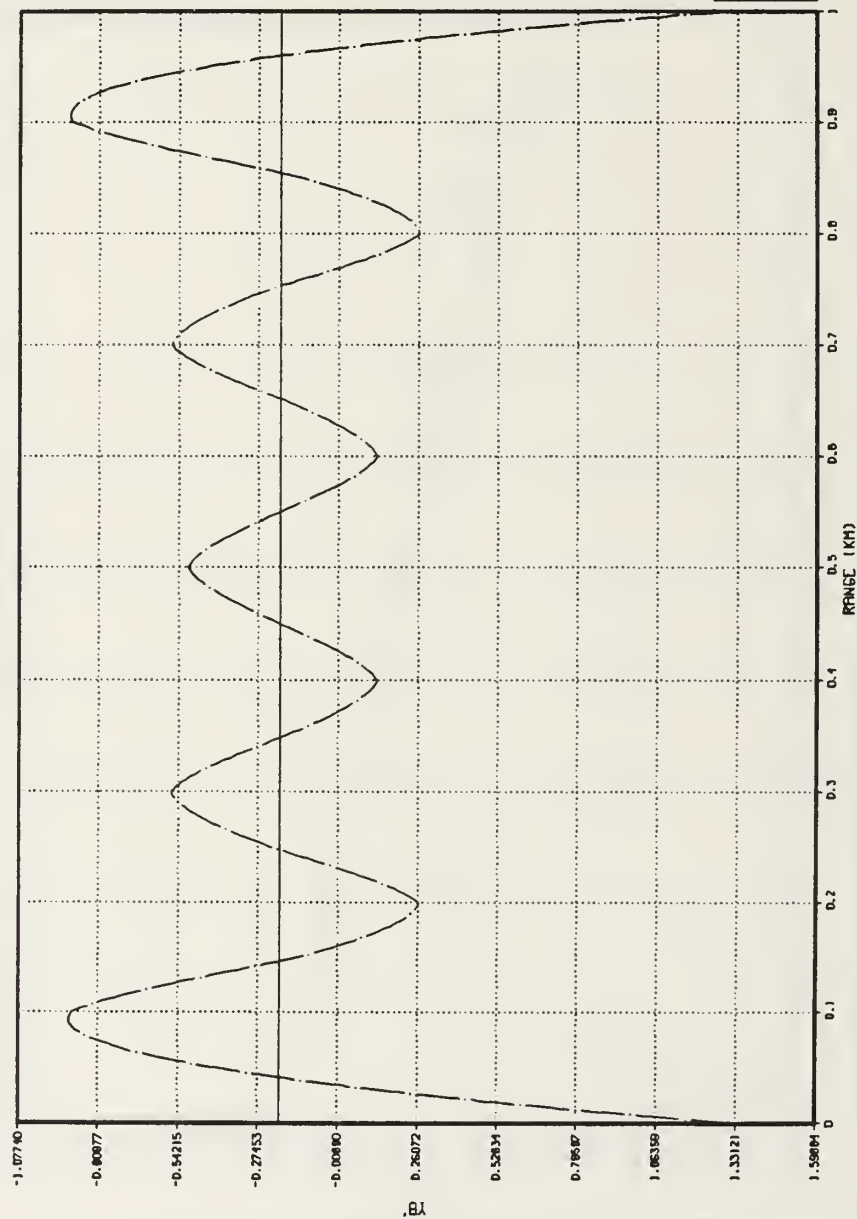
Figure 14.   Up-Slope Ocean Bottom : First-Order Derivatives.

22
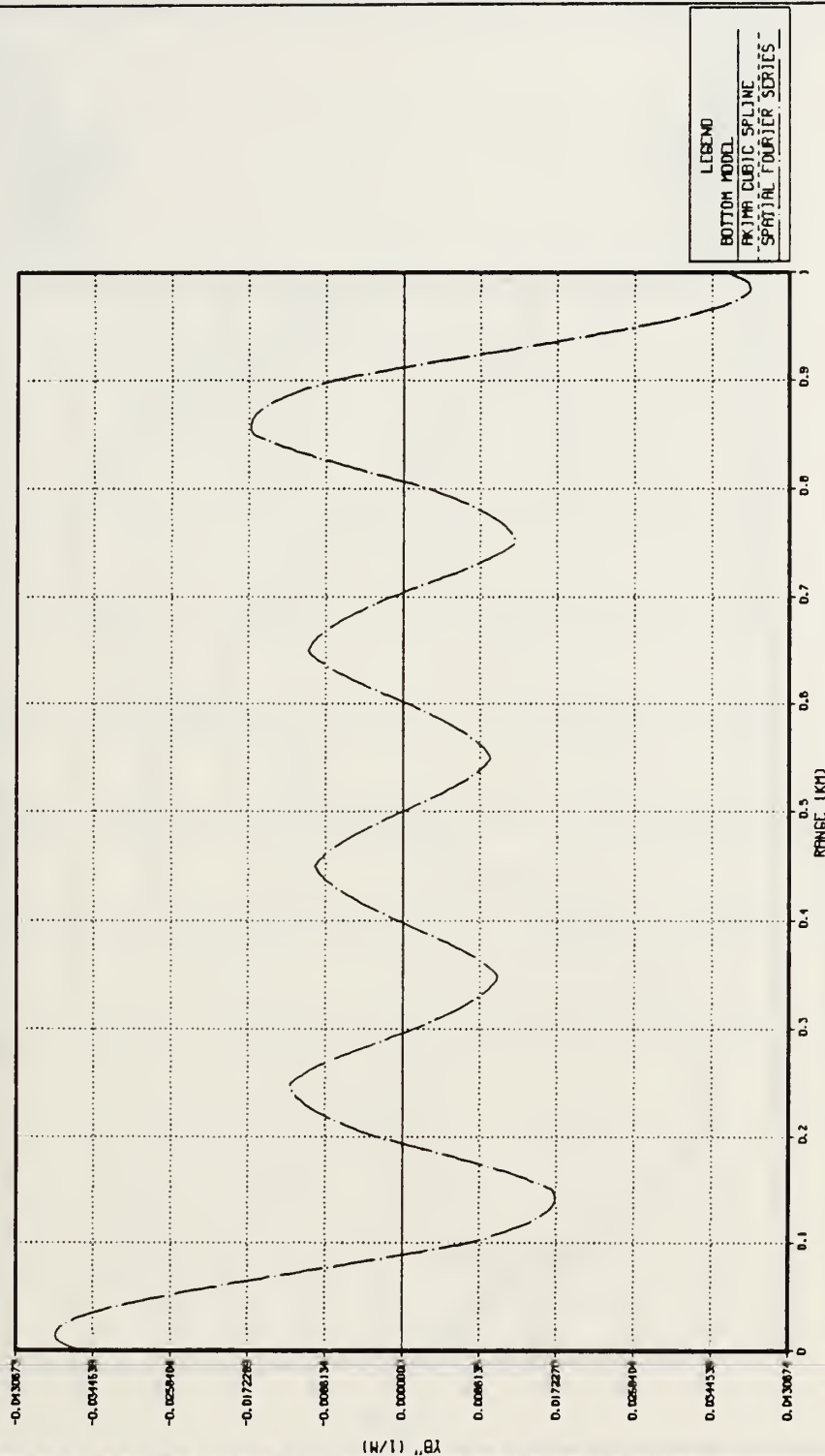
Figure 15.   Up-Slope Ocean Bottom : Second-Order Derivatives.

23
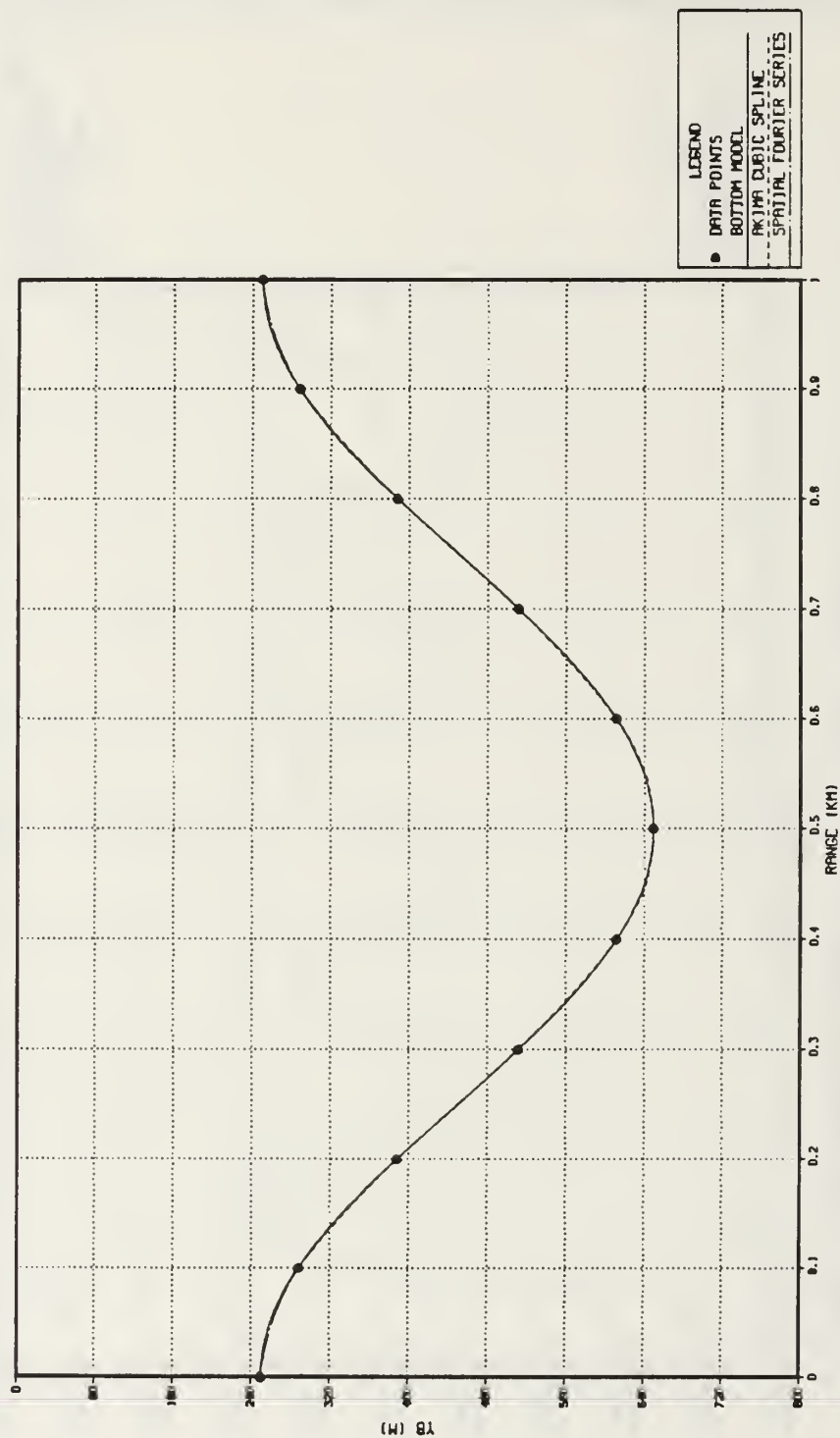
Figure 16.   Cosine Ocean Bottom : Contour Reconstruction.

24
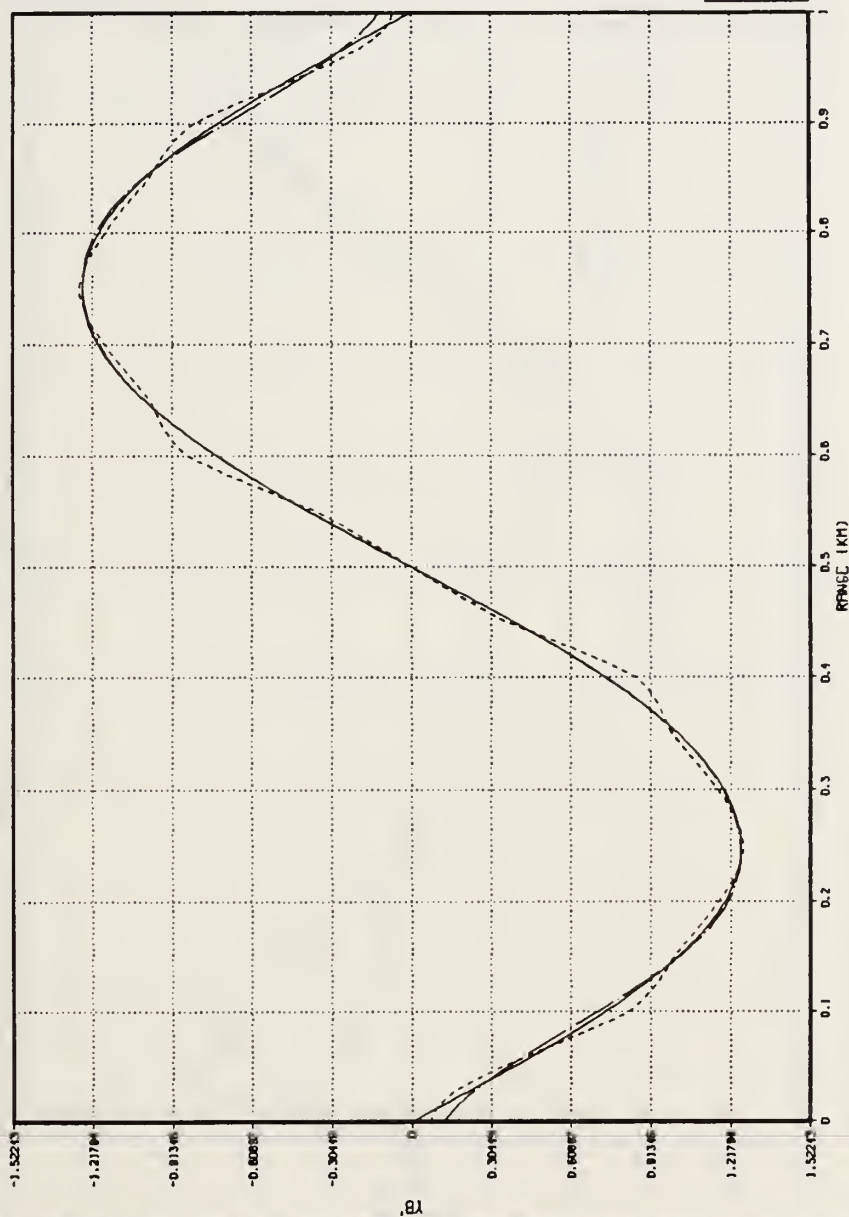
Figure 17.   Cosine Ocean Bottom : First-Order Derivatives.

25
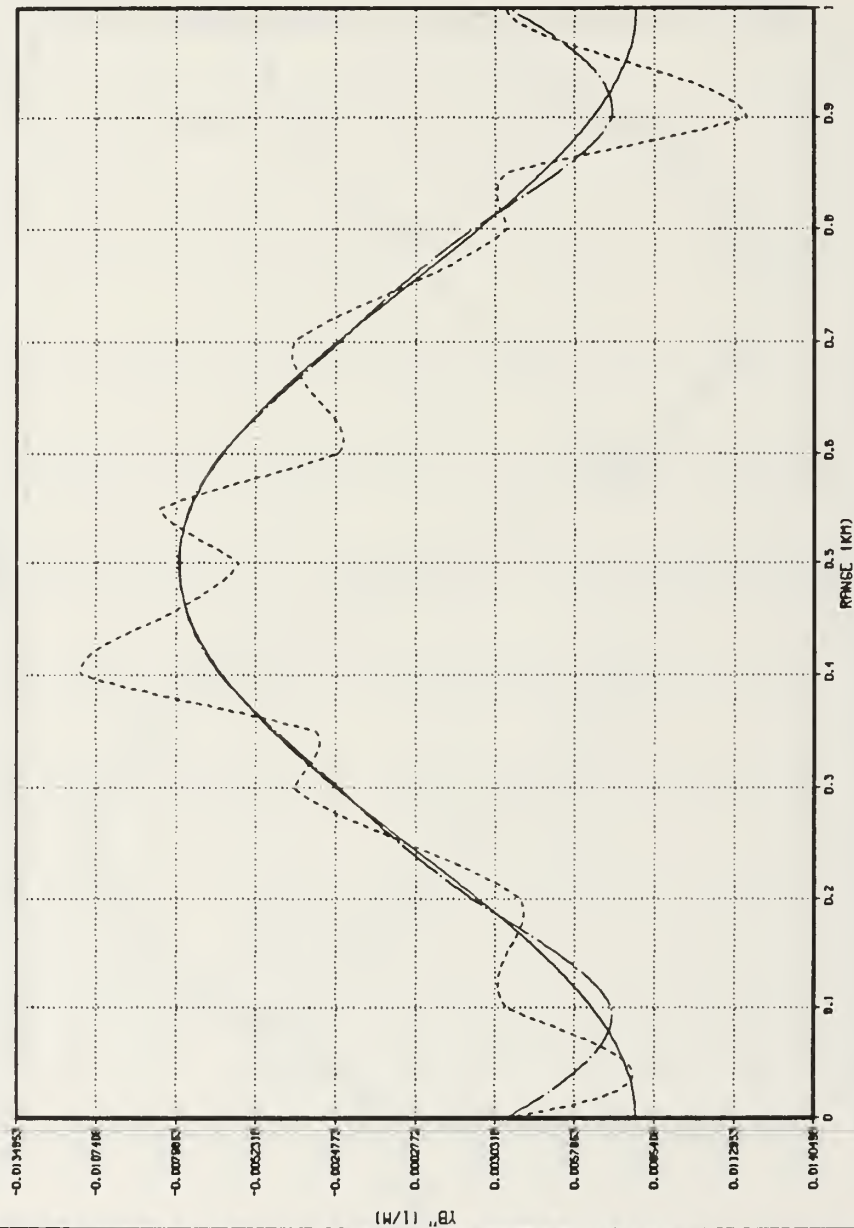
Figure 18.   Cosine Ocean Bottom : Second-Order Derivatives.

26
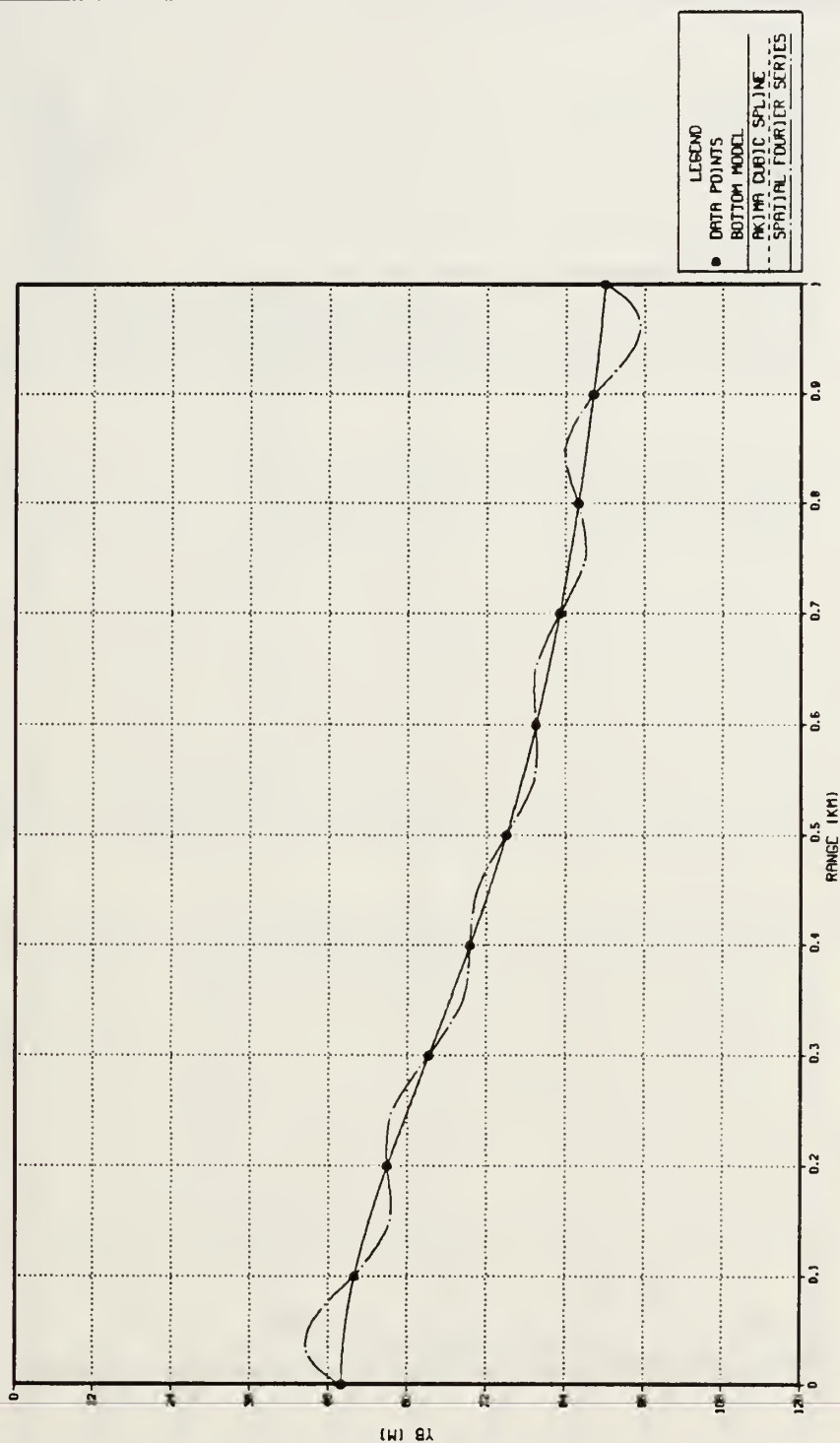
Figure 19.   Modified Witch Of Agnesi Ocean Bottom : Contour Reconstruction.

27
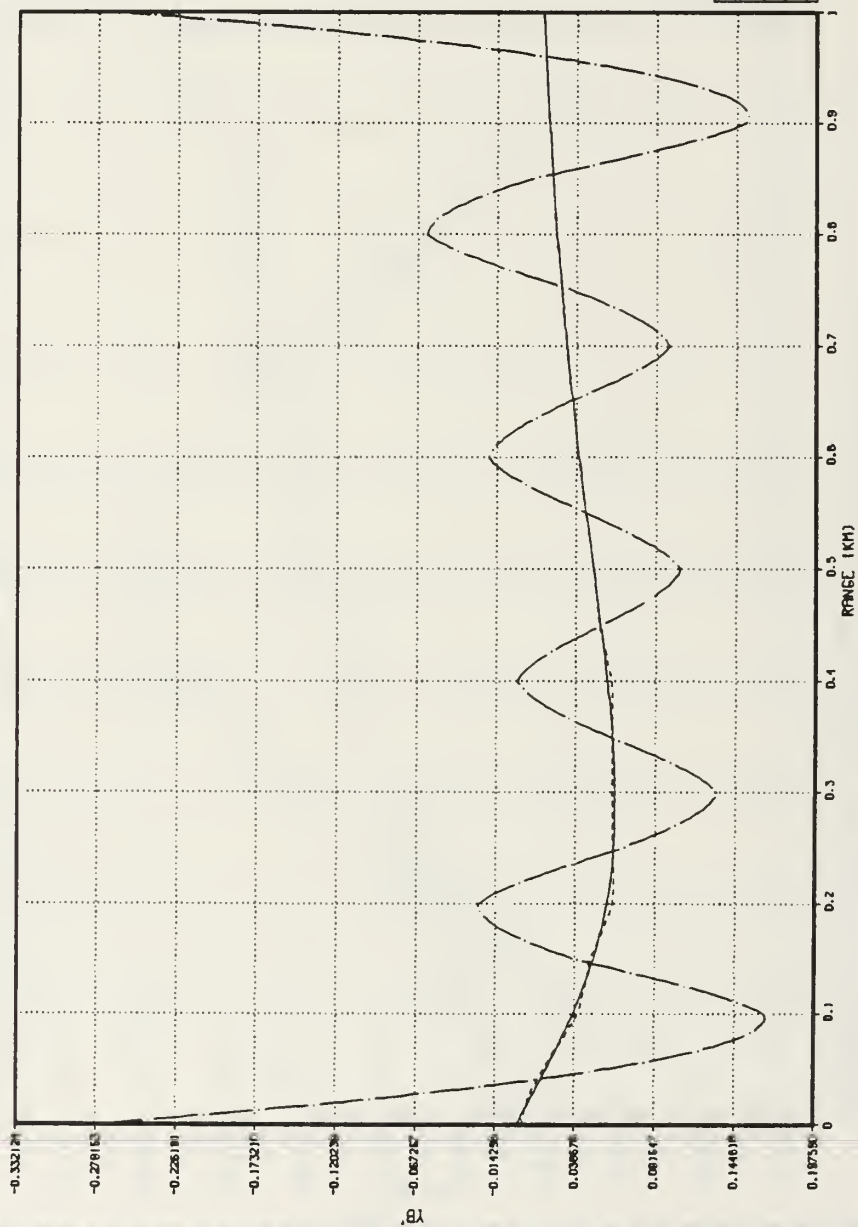
Figure 20.   Modified Witch Of Agnesi Ocean Bottom : First-Order Derivatives.

28
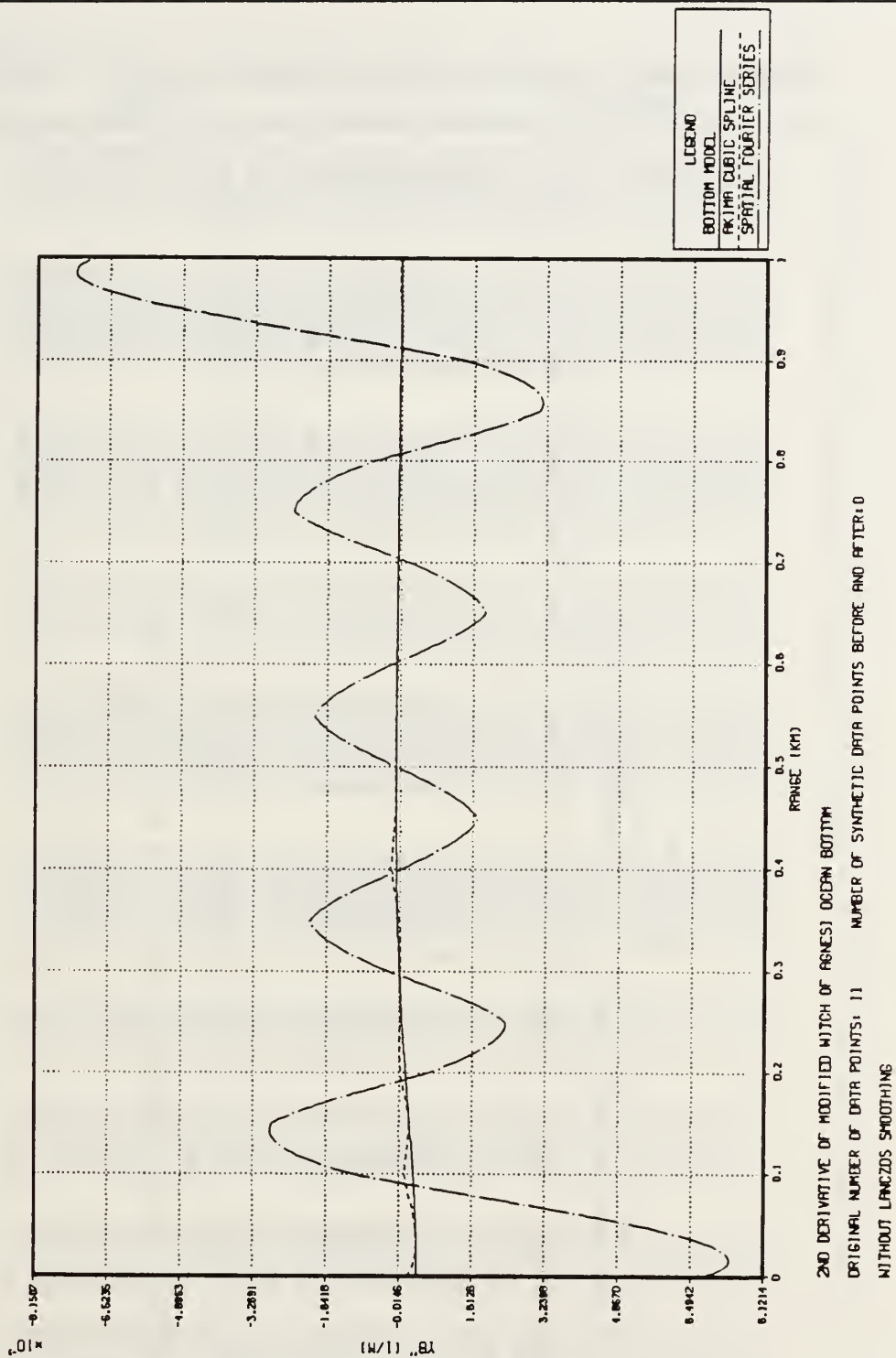
Figure 21.   Modified Witch Of Agnesi Ocean Bottom : Second-Order Derivatives.

29

Table 1. AKIMA CUBIC SPLINE RESULTS : FLAT OCEAN BOTTOM

FLAT BOTTOM

TECHNIQUE: AKIMA CUBIC SPLINE FIT   NO. OF ORIGINAL DATA POINTS: 11

RANGE (KM)	YB(EXACT) (M)	YB(FIT) (M)	% ERROR	YBDOT(EXACT)	YBDOT(FIT)	% ERROR	YBDOT2(EXACT) (1/M)	YBDOT2(FIT) (1/M)	% ERROR
0.00	100.00	100.00	0.000	0.000E+00	0.000E+00	0.000	0.000E+00	0.000E+00	0.000
0.05	100.00	100.00	0.000	0.000E+00	0.000E+00	0.000	0.000E+00	0.000E+00	0.000
0.10	100.00	100.00	0.000	0.000E+00	0.000E+00	0.000	0.000E+00	0.000E+00	0.000
0.15	100.00	100.00	0.000	0.000E+00	0.000E+00	0.000	0.000E+00	0.000E+00	0.000
0.20	100.00	100.00	0.000	0.000E+00	0.000E+00	0.000	0.000E+00	0.000E+00	0.000
0.25	100.00	100.00	0.000	0.000E+00	0.000E+00	0.000	0.000E+00	0.000E+00	0.000
0.30	100.00	100.00	0.000	0.000E+00	0.000E+00	0.000	0.000E+00	0.000E+00	0.000
0.35	100.00	100.00	0.000	0.000E+00	0.000E+00	0.000	0.000E+00	0.000E+00	0.000
0.40	100.00	100.00	0.000	0.000E+00	0.000E+00	0.000	0.000E+00	0.000E+00	0.000
0.45	100.00	100.00	0.000	0.000E+00	0.000E+00	0.000	0.000E+00	0.000E+00	0.000
0.50	100.00	100.00	0.000	0.000E+00	0.000E+00	0.000	0.000E+00	0.000E+00	0.000
0.55	100.00	100.00	0.000	0.000E+00	0.000E+00	0.000	0.000E+00	0.000E+00	0.000
0.60	100.00	100.00	0.000	0.000E+00	0.000E+00	0.000	0.000E+00	0.000E+00	0.000
0.65	100.00	100.00	0.000	0.000E+00	0.000E+00	0.000	0.000E+00	0.000E+00	0.000
0.70	100.00	100.00	0.000	0.000E+00	0.000E+00	0.000	0.000E+00	0.000E+00	0.000
0.75	100.00	100.00	0.000	0.000E+00	0.000E+00	0.000	0.000E+00	0.000E+00	0.000
0.80	100.00	100.00	0.000	0.000E+00	0.000E+00	0.000	0.000E+00	0.000E+00	0.000
0.85	100.00	100.00	0.000	0.000E+00	0.000E+00	0.000	0.000E+00	0.000E+00	0.000
0.90	100.00	100.00	0.000	0.000E+00	0.000E+00	0.000	0.000E+00	0.000E+00	0.000
0.95	100.00	100.00	0.000	0.000E+00	0.000E+00	0.000	0.000E+00	0.000E+00	0.000
1.00	100.00	100.00	0.000	0.000E+00	0.000E+00	0.000	0.000E+00	0.000E+00	0.000

Table 2. FOURIER SERIES RESULTS : FLAT OCEAN BOTTOM

FLAT BOTTOM

TECHNIQUE: SPATIAL FOURIER SERIES FIT   NO. OF ORIGINAL DATA POINTS: 11

RANGE (KM)	YB(EXACT) (M)	YB(FIT) (M)	% ERROR	YBDOT(EXACT) (M)	YBDOT(FIT)	% ERROR	YBOOT2(EXACT) (1/M)	YBDOT2(FIT) (1/M)	% ERROR
0.00	100.00	100.00	0.000	0.000E+00	0.863E-15	0.000	0.000E+00	-0.686E-17	0.000
0.05	100.00	100.00	0.000	0.000E+00	0.849E-16	0.000	0.000E+00	-0.196E-16	0.000
0.10	100.00	100.00	0.000	0.000E+00	-0.620E-15	0.000	0.000E+00	-0.522E-17	0.000
0.15	100.00	100.00	0.000	0.000E+00	-0.401E-15	0.000	0.000E+00	0.115E-16	0.000
0.20	100.00	100.00	0.000	0.000E+00	0.154E-15	0.000	0.000E+00	0.713E-17	0.000
0.25	100.00	100.00	0.000	0.000E+00	0.165E-15	0.000	0.000E+00	-0.573E-17	0.000
0.30	100.00	100.00	0.000	0.000E+00	-0.162E-15	0.000	0.000E+00	-0.435E-17	0.000
0.35	100.00	100.00	0.000	0.000E+00	-0.109E-15	0.000	0.000E+00	0.611E-17	0.000
0.40	100.00	100.00	0.000	0.000E+00	0.249E-15	0.000	0.000E+00	0.552E-17	0.000
0.45	100.00	100.00	0.000	0.000E+00	0.274E-15	0.000	0.000E+00	-0.452E-17	0.000
0.50	100.00	100.00	0.000	0.000E+00	-0.353E-16	0.000	0.000E+00	-0.527E-17	0.000
0.55	100.00	100.00	0.000	0.000E+00	-0.664E-16	0.000	0.000E+00	0.433E-17	0.000
0.60	100.00	100.00	0.000	0.000E+00	0.252E-15	0.000	0.000E+00	0.584E-17	0.000
0.65	100.00	100.00	0.000	0.000E+00	0.306E-15	0.000	0.000E+00	-0.436E-17	0.000
0.70	100.00	100.00	0.000	0.000E+00	-0.564E-16	0.000	0.000E+00	-0.745E-17	0.000
0.75	100.00	100.00	0.000	0.000E+00	-0.186E-15	0.000	0.000E+00	0.344E-17	0.000
0.80	100.00	100.00	0.000	0.000E+00	0.181E-15	0.000	0.000E+00	0.825E-17	0.000
0.85	100.00	100.00	0.000	0.000E+00	0.306E-15	0.000	0.000E+00	-0.546E-17	0.000
0.90	100.00	100.00	0.000	0.000E+00	-0.328E-15	0.000	0.000E+00	-0.168E-16	0.000
0.95	100.00	100.00	0.000	0.000E+00	-0.935E-15	0.000	0.000E+00	-0.335E-17	0.000
1.00	100.00	100.00	0.000	0.000E+00	-0.498E-15	0.000	0.000E+00	0.192E-16	0.000

31

Table 3. AKIMA CUBIC SPLINE RESULTS : CONSTANT
DOWN-SLOPE BOTTOM

CONSTANT DOWNSLOPE BOTTOM

TECHNIQUE: AKIMA CUBIC SPLINE FIT   NO. OF ORIGINAL DATA POINTS: 11

RANGE (KM)	YB(EXACT) (M)	YB(FIT) (M)	% ERROR	YBDOT(EXACT)	YBDOT(FIT)	% ERROR	YBDOT2(EXACT) (1/M)	YBDOT2(FIT) (1/M)	% ERROR
0.00	220.00	220.00	0.000	0.200E+00	0.200E+00	0.000	0.000E+00	-0.583E-17	0.000
0.05	230.00	230.00	0.000	0.200E+00	0.200E+00	0.000	0.000E+00	-0.500E-17	0.000
0.10	240.00	240.00	0.000	0.200E+00	0.200E+00	0.000	0.000E+00	-0.214E-16	0.000
0.15	250.00	250.00	0.000	0.200E+00	0.200E+00	0.000	0.000E+00	0.278E-17	0.000
0.20	260.00	260.00	0.000	0.200E+00	0.200E+00	0.000	0.000E+00	0.000E+00	0.000
0.25	270.00	270.00	0.000	0.200E+00	0.200E+00	0.000	0.000E+00	0.000E+00	0.000
0.30	280.00	280.00	0.000	0.200E+00	0.200E+00	0.000	0.000E+00	-0.278E-18	0.000
0.35	290.00	290.00	0.000	0.200E+00	0.200E+00	0.000	0.000E+00	0.139E-18	0.000
0.40	300.00	300.00	0.000	0.200E+00	0.200E+00	0.000	0.000E+00	-0.833E-18	0.000
0.45	310.00	310.00	0.000	0.200E+00	0.200E+00	0.000	0.000E+00	-0.132E-33	0.000
0.50	320.00	320.00	0.000	0.200E+00	0.200E+00	0.000	0.000E+00	-0.132E-33	0.000
0.55	330.00	330.00	0.000	0.200E+00	0.200E+00	0.000	0.000E+00	-0.132E-33	0.000
0.60	340.00	340.00	0.000	0.200E+00	0.200E+00	0.000	0.000E+00	-0.833E-18	0.000
0.65	350.00	350.00	0.000	0.200E+00	0.200E+00	0.000	0.000E+00	-0.132E-33	0.000
0.70	360.00	360.00	0.000	0.200E+00	0.200E+00	0.000	0.000E+00	-0.833E-18	0.000
0.75	370.00	370.00	0.000	0.200E+00	0.200E+00	0.000	0.000E+00	-0.132E-33	0.000
0.80	380.00	380.00	0.000	0.200E+00	0.200E+00	0.000	0.000E+00	-0.833E-18	0.000
0.85	390.00	390.00	0.000	0.200E+00	0.200E+00	0.000	0.000E+00	-0.132E-33	0.000
0.90	400.00	400.00	0.000	0.200E+00	0.200E+00	0.000	0.000E+00	-0.833E-18	0.000
0.95	410.00	410.00	0.000	0.200E+00	0.200E+00	0.000	0.000E+00	-0.132E-33	0.000
1.00	420.00	420.00	0.000	0.200E+00	0.200E+00	0.000	0.000E+00	0.833E-18	0.000

32

Table 4. FOURIER SERIES RESULTS : CONSTANT DOWN-SLOPE BOTTOM

CONSTANT DOWNSLOPE BOTTOM

TECHNIQUE: SPATIAL FOURIER SERIES FIT   NO. OF ORIGINAL DATA POINTS: 11

RANGE (KM)	YB(EXACT) (M)	YB(FIT) (M)	% ERROR	YBDOT(EXACT)	YBDOT(FIT)	% ERROR	YBDOT2(EXACT) (1/M)	YBDOT2(FIT) (1/M)	% ERROR
0.00	220.00	220.00	0.000	0.200E+00	-0.133E+01	-766.183	0.000E+00	0.359E-01	*********
0.05	230.00	199.47	-13.275	0.200E+00	0.431E+00	115.265	0.000E+00	0.267E-01	*********
0.10	240.00	240.00	0.000	0.200E+00	0.898E+00	348.915	0.000E+00	-0.750E-02	*********
0.15	250.00	267.61	7.044	0.200E+00	0.129E+00	-35.278	0.000E+00	-0.167E-01	*********
0.20	260.00	260.00	0.000	0.200E+00	-0.264E+00	-232.172	0.000E+00	0.283E-02	*********
0.25	270.00	257.07	-4.789	0.200E+00	0.230E+00	15.054	0.000E+00	0.125E-01	*********
0.30	280.00	280.00	0.000	0.200E+00	0.567E+00	183.520	0.000E+00	-0.128E-02	*********
0.35	290.00	300.84	3.739	0.200E+00	0.186E+00	-6.764	0.000E+00	-0.106E-01	*********
0.40	300.00	300.00	0.000	0.200E+00	-0.124E+00	-161.850	0.000E+00	0.521E-03	*********
0.45	310.00	300.00	-3.226	0.200E+00	0.204E+00	1.976	0.000E+00	0.979E-02	*********
0.50	320.00	320.00	0.000	0.200E+00	0.511E+00	155.540	0.000E+00	-0.846E-17	0.000
0.55	330.00	340.00	3.030	0.200E+00	0.204E+00	1.976	0.000E+00	-0.979E-02	*********
0.60	340.00	340.00	0.000	0.200E+00	-0.124E+00	-161.850	0.000E+00	-0.521E-03	*********
0.65	350.00	339.16	-3.098	0.200E+00	0.186E+00	-6.764	0.000E+00	0.106E-01	*********
0.70	360.00	360.00	0.000	0.200E+00	0.567E+00	183.520	0.000E+00	0.128E-02	*********
0.75	370.00	382.93	3.495	0.200E+00	0.230E+00	15.054	0.000E+00	-0.125E-01	*********
0.80	380.00	380.00	0.000	0.200E+00	-0.264E+00	-232.172	0.000E+00	-0.283E-02	*********
0.85	390.00	372.39	-4.516	0.200E+00	0.129E+00	-35.278	0.000E+00	0.167E-01	*********
0.90	400.00	400.00	0.000	0.200E+00	0.898E+00	348.915	0.000E+00	0.750E-02	*********
0.95	410.00	440.53	7.447	0.200E+00	0.431E+00	115.265	0.000E+00	-0.267E-01	*********
1.00	420.00	420.00	0.000	0.200E+00	-0.133E+01	-766.183	0.000E+00	-0.359E-01	*********

Table 5. AKIMA CUBIC SPLINE RESULTS : CONSTANT UP-SLOPE BOTTOM.

TECHNIQUE: AKIMA CUBIC SPLINE FIT

CONSTANT UPSLOPE BOTTOM

NO. OF ORIGINAL DATA POINTS: 11

RANGE (KM)	YB(EXACT) (M)	YB(FIT) (M)	% ERROR	YBDOT(EXACT)	YBDOT(FIT)	% ERROR	YBDOT2(EXACT) (1/M)	YBDOT2(FIT) (1/M)	% ERROR
0.00	420.00	420.00	0.000	-0.200E+00	-0.200E+00	0.000	0.000E+00	0.833E-18	0.000
0.05	410.00	410.00	0.000	-0.200E+00	-0.200E+00	0.000	0.000E+00	0.132E-33	0.000
0.10	400.00	400.00	0.000	-0.200E+00	-0.200E+00	0.000	0.000E+00	0.833E-18	0.000
0.15	390.00	390.00	0.000	-0.200E+00	-0.200E+00	0.000	0.000E+00	0.132E-33	0.000
0.20	380.00	380.00	0.000	-0.200E+00	-0.200E+00	0.000	0.000E+00	0.833E-18	0.000
0.25	370.00	370.00	0.000	-0.200E+00	-0.200E+00	0.000	0.000E+00	0.132E-33	0.000
0.30	360.00	360.00	0.000	-0.200E+00	-0.200E+00	0.000	0.000E+00	0.833E-18	0.000
0.35	350.00	350.00	0.000	-0.200E+00	-0.200E+00	0.000	0.000E+00	0.132E-33	0.000
0.40	340.00	340.00	0.000	-0.200E+00	-0.200E+00	0.000	0.000E+00	0.833E-18	0.000
0.45	330.00	330.00	0.000	-0.200E+00	-0.200E+00	0.000	0.000E+00	0.132E-33	0.000
0.50	320.00	320.00	0.000	-0.200E+00	-0.200E+00	0.000	0.000E+00	0.132E-33	0.000
0.55	310.00	310.00	0.000	-0.200E+00	-0.200E+00	0.000	0.000E+00	0.833E-18	0.000
0.60	300.00	300.00	0.000	-0.200E+00	-0.200E+00	0.000	0.000E+00	0.132E-33	0.000
0.65	290.00	290.00	0.000	-0.200E+00	-0.200E+00	0.000	0.000E+00	0.132E-33	0.000
0.70	280.00	280.00	0.000	-0.200E+00	-0.200E+00	0.000	0.000E+00	0.833E-18	0.000
0.75	270.00	270.00	0.000	-0.200E+00	-0.200E+00	0.000	0.000E+00	0.132E-33	0.000
0.80	260.00	260.00	0.000	-0.200E+00	-0.200E+00	0.000	0.000E+00	0.250E-17	0.000
0.85	250.00	250.00	0.000	-0.200E+00	-0.200E+00	0.000	0.000E+00	0.416E-18	0.000
0.90	240.00	240.00	0.000	-0.200E+00	-0.200E+00	0.000	0.000E+00	-0.111E-17	0.000
0.95	230.00	230.00	0.000	-0.200E+00	-0.200E+00	0.000	0.000E+00	-0.278E-18	0.000
1.00	220.00	220.00	0.000	-0.200E+00	-0.200E+00	0.000	0.000E+00	0.555E-18	0.000

CONSTANT UPSLOPE BOTTOM

TECHNIQUE: SPATIAL FOURIER SERIES FIT   NO. OF ORIGINAL DATA POINTS: 11

RANGE (KM)	YB(EXACT) (M)	YB(FIT) (M)	% ERROR	YBDOT(EXACT)	YBDOT(FIT)	% ERROR	YBDOT2(EXACT) (1/M)	YBDOT2(FIT) (1/M)	% ERROR
0.00	420.00	420.00	0.000	-0.200E+00	0.133E+01	-766.183	0.000E+00	-0.359E-01	*********
0.05	410.00	440.53	7.447	-0.200E+00	-0.431E+00	115.265	0.000E+00	-0.267E-01	*********
0.10	400.00	400.00	0.000	-0.200E+00	-0.898E+00	348.915	0.000E+00	0.750E-02	*********
0.15	390.00	372.39	-4.516	-0.200E+00	-0.129E+00	-35.278	0.000E+00	0.167E-01	*********
0.20	380.00	380.00	0.000	-0.200E+00	0.264E+00	-232.172	0.000E+00	-0.283E-02	*********
0.25	370.00	382.93	3.495	-0.200E+00	-0.230E+00	15.054	0.000E+00	-0.125E-01	*********
0.30	360.00	360.00	0.000	-0.200E+00	-0.567E+00	183.520	0.000E+00	0.128E-02	*********
0.35	350.00	339.16	-3.098	-0.200E+00	-0.186E+00	-6.764	0.000E+00	0.106E-01	*********
0.40	340.00	340.00	0.000	-0.200E+00	0.124E+00	-161.850	0.000E+00	-0.521E-03	*********
0.45	330.00	340.00	3.030	-0.200E+00	-0.204E+00	1.976	0.000E+00	-0.979E-02	*********
0.50	320.00	320.00	0.000	-0.200E+000	-0.511E+00	155.540	0.000E+00	-0.226E-16	0.000
0.55	310.00	300.00	-3.226	-0.200E+00	-0.204E+00	1.976	0.000E+00	0.979E-02	*********
0.60	300.00	300.00	0.000	-0.200E+00	0.124E+00	-161.850	0.000E+00	0.521E-03	*********
0.65	290.00	300.84	3.739	-0.200E+00	-0.186E+00	-6.764	0.000E+00	-0.106E-01	*********
0.70	280.00	280.00	0.000	-0.200E+00	-0.567E+00	183.520	0.000E+00	-0.128E-02	*********
0.75	270.00	257.07	-4.789	-0.200E+00	-0.230E+00	15.054	0.000E+00	0.125E-01	*********
0.80	260.00	260.00	0.000	-0.200E+00	0.264E+00	-232.172	0.000E+00	0.283E-02	*********
0.85	250.00	267.61	7.044	-0.200E+00	-0.129E+00	-35.278	0.000E+00	-0.167E-01	*********
0.90	240.00	240.00	0.000	-0.200E+00	-0.898E+00	348.915	0.000E+00	-0.750E-02	*********
0.95	230.00	199.47	-13.275	-0.200E+00	-0.431E+00	115.265	0.000E+00	0.267E-01	*********
1.00	220.00	220.00	0.000	-0.200E+00	0.133E+01	-766.183	0.000E+00	0.359E-01	*********

Table 6. FOURIER SERIES RESULTS : CONSTANT UP-SLOPE BOTTOM.

Table 7. AKIMA CUBIC SPLINE RESULTS : ONE PERIOD COSINE OCEAN BOTTOM

ONE PERIOD COSINE WAVE BOTTOM

TECHNIQUE: AKIMA CUBIC SPLINE FIT   NO. OF ORIGINAL DATA POINTS: 11

RANGE (KM)	YB(EXACT) (M)	YB(FIT) (M)	% ERROR	YBDOT(EXACT)	YBDOT(FIT)	% ERROR	YBDOT2(EXACT) (1/M)	YBDOT2(FIT) (1/M)	% ERROR
0.00	250.00	250.00	0.000	0.000E+00	0.729E-01	********	0.790E-02	0.342E-02	-56.731
0.05	259.79	259.65	-0.055	0.388E+00	0.347E+00	-10.534	0.751E-02	0.756E-02	0.707
0.10	288.20	288.20	0.000	0.739E+00	0.829E+00	12.259	0.639E-02	0.342E-02	-46.516
0.15	332.44	333.93	0.446	0.102E+01	0.100E+01	-1.637	0.464E-02	0.342E-02	-26.386
0.20	388.20	368.20	0.000	0.120E+01	0.117E+01	-2.034	0.244E-02	0.391E-02	60.451
0.25	450.00	450.00	0.000	0.126E+01	0.127E+01	0.959	0.224E-17	0.000E+00	0.000
0.30	511.80	511.80	0.000	0.120E+01	0.117E+01	-2.034	-0.244E-02	-0.391E-02	60.451
0.35	567.56	565.76	-0.316	0.102E+01	0.994E+00	-2.250	-0.464E-02	-0.317E-02	-31.756
0.40	611.80	611.80	0.000	0.739E+00	0.854E+00	15.633	-0.639E-02	-0.112E-01	76.058
0.45	640.21	641.58	0.213	0.388E+00	0.359E+00	-7.442	-0.751E-02	-0.854E-02	13.740
0.50	650.00	650.00	0.000	0.154E-15	0.741E-15	0.000	-0.790E-02	-0.584E-02	-26.087
0.55	640.21	641.58	0.213	-0.388E+00	-0.359E+00	-7.442	-0.751E-02	-0.854E-02	13.740
0.60	611.80	611.80	0.000	-0.739E+00	-0.854E+00	15.633	-0.639E-02	-0.242E-02	-62.123
0.65	567.56	565.76	-0.316	-0.102E+01	-0.994E+00	-2.250	-0.464E-02	-0.317E-02	-31.756
0.70	511.80	511.80	0.000	-0.120E+01	-0.117E+01	-2.034	-0.244E-02	-0.391E-02	60.451
0.75	450.00	450.00	0.000	-0.126E+01	-0.127E+01	0.959	-0.145E-17	-0.260E-17	0.000
0.80	388.20	388.20	0.000	-0.120E+01	-0.117E+01	-2.034	0.244E-02	0.342E-02	40.022
0.85	332.44	333.93	0.446	-0.102E+01	-0.100E+01	-1.637	0.464E-02	0.342E-02	-26.386
0.90	288.20	288.20	0.000	-0.739E+00	-0.829E+00	12.259	0.639E-02	0.117E-01	83.292
0.95	259.79	259.65	-0.055	-0.388E+00	-0.347E+00	-10.534	0.751E-02	0.756E-02	0.707
1.00	250.00	250.00	0.000	-0.866E-15	-0.729E-01	********	0.790E-02	0.342E-02	-56.731

36

Table 8.   FOURIER SERIES RESULTS : ONE PERIOD COSINE OCEAN BOTTOM

ONE PERIOD COSINE WAVE BOTTOM

TECHNIQUE: SPATIAL FOURIER SERIES FIT   NO. OF ORIGINAL DATA POINTS: 11

RANGE (KM)	YB(EXACT) (M)	YB(FIT) (M)	% ERROR	YBDOT(EXACT)	YBDOT(FIT)	% ERROR	YBDOT2(EXACT) (1/M)	YBDOT2(FIT) (1/M)	% ERROR
0.00	250.00	250.00	0.000	0.000E+00	0.122E+00	********	0.790E-02	0.343E-02	-56.561
0.05	259.79	261.58	0.691	0.388E+00	0.364E+00	-6.140	0.751E-02	0.618E-02	-17.705
0.10	288.20	288.20	0.000	0.739E+00	0.707E+00	-4.230	0.639E-02	0.705E-02	10.362
0.15	332.44	331.83	-0.184	0.102E+01	0.102E+01	0.541	0.464E-02	0.518E-02	11.616
0.20	388.20	388.20	0.000	0.120E+01	0.121E+01	1.053	0.244E-02	0.224E-02	-8.290
0.25	450.00	450.27	0.060	0.126E+01	0.125E+01	-0.164	0.224E-17	-0.251E-03	********
0.30	511.80	511.80	0.000	0.120E+01	0.119E+01	-0.488	-0.244E-02	-0.235E-02	-3.681
0.35	567.56	567.43	-0.022	0.102E+01	0.102E+01	0.105	-0.464E-02	-0.452E-02	-2.521
0.40	611.80	611.80	0.000	0.739E+00	0.741E+00	0.325	-0.639E-02	-0.644E-02	0.845
0.45	640.21	640.25	0.006	0.388E+00	0.388E+00	-0.194	-0.751E-02	-0.754E-02	0.461
0.50	650.00	650.00	0.000	0.154E-15	-0.223E-16	0.000	-0.790E-02	-0.785E-02	-0.572
0.55	640.21	640.25	0.006	-0.389E+00	-0.388E+00	-0.194	-0.751E-02	-0.754E-02	0.461
0.60	611.80	611.80	0.000	-0.739E+00	-0.741E+00	0.325	-0.639E-02	-0.644E-02	0.845
0.65	567.56	567.43	-0.022	-0.102E+01	-0.102E+01	0.105	-0.464E-02	-0.452E-02	-2.521
0.70	511.80	511.80	0.000	-0.120E+01	-0.119E+01	-0.488	-0.244E-02	-0.235E-02	-3.681
0.75	450.00	450.27	0.060	-0.126E+01	-0.125E+01	-0.164	-0.145E-17	-0.251E-03	********
0.80	388.20	388.20	0.000	-0.120E+01	-0.121E+01	1.053	0.244E-02	0.224E-02	-8.290
0.85	332.44	331.83	-0.184	-0.102E+01	-0.102E+01	0.541	0.464E-02	0.518E-02	11.616
0.90	288.20	288.20	0.000	-0.739E+00	-0.707E+00	-4.230	0.639E-02	0.705E-02	10.362
0.95	259.79	261.58	0.691	-0.388E+00	-0.364E+00	-6.140	0.751E-02	0.618E-02	-17.705
1.00	250.00	250.00	0.000	-0.866E-15	-0.122E+00	********	0.790E-02	0.343E-02	-56.561

Table 9. AKIMA CUBIC SPLINE RESULTS : WITCH OF AGNESI OCEAN BOTTOM

WITCH OF AGNESI BOTTOM

TECHNIQUE: AKIMA CUBIC SPLINE FIT   NO. OF ORIGINAL DATA POINTS: 11

RANGE (KM)	YB(EXACT) (M)	YB(FIT) (M)	% ERROR	YBDOT(EXACT)	YBDOT(FIT)	% ERROR	YBDOT2(EXACT) (1/M)	YBDOT2(FIT) (1/M)	% ERROR
0.00	50.00	50.00	0.000	0.000E+00	0.398E-02	********	0.400E-03	0.189E-03	-52.843
0.05	50.50	50.51	0.025	0.196E-01	0.178E-01	-9.335	0.377E-03	0.363E-03	-3.543
0.10	51.92	51.92	0.000	0.370E-01	0.403E-01	8.980	0.313E-03	0.110E-03	-64.966
0.15	54.13	54.12	-0.007	0.505E-01	0.487E-01	-3.472	0.225E-03	0.228E-03	1.176
0.20	56.90	56.90	0.000	0.595E-01	0.631E-01	6.161	0.133E-03	0.187E-04	-85.975
0.25	60.00	60.07	0.112	0.640E-01	0.636E-01	-0.698	0.512E-04	-0.121E-05	-102.356
0.30	63.24	63.24	0.000	0.649E-01	0.630E-01	-2.903	-0.127E-04	0.311E-06	-102.444
0.35	66.44	66.30	-0.091	0.631E-01	0.628E-01	-0.366	-0.568E-04	-0.695E-05	-87.770
0.40	69.51	69.51	0.000	0.595E-01	0.623E-01	4.727	-0.834E-04	-0.206E-03	146.694
0.45	72.33	72.41	0.042	0.549E-01	0.542E-01	-1.424	-0.965E-04	-0.120E-03	24.157
0.50	75.00	75.00	0.000	0.500E-01	0.503E-01	0.648	-0.100E-03	-0.107E-03	6.969
0.55	77.38	77.38	0.011	0.450E-01	0.451E-01	0.025	-0.975E-04	-0.104E-03	6.476
0.60	79.51	79.51	0.000	0.403E-01	0.399E-01	-0.906	-0.914E-04	-0.669E-04	-26.849
0.65	81.41	81.41	0.002	0.359E-01	0.362E-01	0.610	-0.836E-04	-0.850E-04	1.611
0.70	83.11	83.11	0.000	0.320E-01	0.314E-01	-1.595	-0.753E-04	-0.453E-04	-39.758
0.75	84.62	84.61	-0.001	0.284E-01	0.286E-01	0.863	-0.670E-04	-0.667E-04	-0.469
0.80	85.96	85.96	0.000	0.252E-01	0.248E-01	-1.861	-0.592E-04	-0.383E-04	-35.307
0.85	87.15	87.14	-0.005	0.225E-01	0.226E-01	0.627	-0.521E-04	-0.405E-04	-6.986
0.90	88.21	83.21	0.000	0.200E-01	0.199E-01	-0.466	-0.458E-04	-0.343E-04	-25.096
0.95	89.15	89.16	0.004	0.179E-01	0.180E-01	0.656	-0.401E-04	-0.431E-04	7.320
1.00	90.00	90.00	0.000	0.160E-01	0.156E-01	-2.348	-0.352E-04	-0.519E-04	47.352

38

Table 10. FOURIER SERIES RESULTS : WITCH OF AGNESI OCEAN BOTTOM

WITCH OF AGNESI BOTTOM

TECHNIQUE: SPATIAL FOURIER SERIES FIT   NO. OF ORIGINAL DATA POINTS: 11

RANGE (KM)	YB(EXACT) (M)	YB(FIT) (M)	% ERROR	YBDOT(EXACT)	YBDOT(FIT)	% ERROR	YBDOT2(EXACT) (1/M)	YBDOT2(FIT) (1/M)	% ERROR
0.00	50.00	50.00	0.000	0.000E+00	-0.277E+00	********	0.400E-03	0.677E-02	1591.965
0.05	50.50	44.94	-11.009	0.196E-01	0.609E-01	210.604	0.377E-03	0.525E-02	1292.983
0.10	51.92	51.92	0.000	0.370E-01	0.165E+00	345.236	0.313E-03	-0.104E-02	-431.765
0.15	54.13	57.36	5.972	0.505E-01	0.377E-01	-25.294	0.225E-03	-0.284E-02	********
0.20	56.90	56.90	0.000	0.595E-01	-0.260E-01	-143.710	0.133E-03	0.648E-03	386.147
0.25	60.00	57.62	-3.972	0.640E-01	0.695E-01	8.553	0.512E-04	0.236E-02	4510.553
0.30	63.24	63.24	0.000	0.649E-01	0.133E+00	104.432	-0.127E-04	-0.246E-03	1830.481
0.35	66.44	68.45	3.016	0.631E-01	0.606E-01	-3.895	-0.568E-04	-0.201E-02	3442.647
0.40	69.51	69.51	0.000	0.595E-01	-0.399E-03	-100.670	-0.834E-04	0.107E-04	-112.807
0.45	72.33	70.52	-2.559	0.549E-01	0.556E-01	1.272	-0.965E-04	0.172E-02	********
0.50	75.00	75.00	0.000	0.500E-01	0.108E+00	115.311	-0.100E-03	-0.901E-04	-1.935
0.55	77.38	79.23	2.397	0.450E-01	0.458E-01	1.694	-0.975E-04	-0.191E-02	1862.860
0.60	79.51	79.51	0.000	0.403E-01	-0.190E-01	-149.070	-0.914E-04	-0.190E-03	108.013
0.65	81.41	79.40	-2.475	0.359E-01	0.334E-01	-7.090	-0.836E-04	0.188E-02	********
0.70	83.11	83.11	0.000	0.320E-01	0.100E+00	213.577	-0.753E-04	0.165E-03	-319.618
0.75	84.62	87.02	2.844	0.284E-01	0.341E-01	19.896	-0.670E-04	-0.240E-02	3479.000
0.80	85.96	85.96	0.000	0.252E-01	-0.613E-01	-342.659	-0.592E-04	-0.591E-03	898.206
0.85	87.15	83.86	-3.770	0.225E-01	0.922E-02	-58.954	-0.521E-04	0.306E-02	********
0.90	88.21	88.21	0.000	0.200E-01	0.150E+00	650.993	-0.458E-04	0.136E-02	********
0.95	89.15	94.87	6.409	0.179E-01	0.612E-01	242.451	-0.401E-04	-0.502E-02	********
1.00	90.00	90.00	0.000	0.160E-01	-0.271E+00	********	-0.352E-04	-0.679E-02	********

derivative results were accurate with a uniformly small percentage error as reflected in Table 11. Second-order derivative values generated by the ACS approach were unsatisfactory, although this is not immediately evident from Figure 24 because of the plot scale.

Figures 25, 26 and 27 and Tables 13 and 14 give the ACS and SFS results for the parabolic ocean bottom model. The ACS method matched both the original function and its first and second-order derivatives precisely as shown in Table 13. The SFS representation was reasonably accurate although some oscillations were again in evidence at the contour end points. These oscillations account for the large boundary errors in the subsequent first and second-order derivative computations as reflected in Table 14 and illustrated by Figures 26 and 27.

B. NUMERICAL ENHANCEMENT OF THE SPATIAL FOURIER SERIES TECHNIQUE

The results of the previous section clearly showed that the elementary SFS approach was unsatisfactory. Modifications to the fundamental SFS technique were therefore investigated and applied where appropriate to improve overall performance.

The following numerical enhancements were studied for each of the original seven exact mathematical models. For purposes of brevity, interim results for the modified Witch of Agnesi contour only have been included, as this function reflected the greatest improvement.

1. Lanczos Smoothing.

The modified expression for the SFS coefficients given by Equation (2.11) and incorporating Lanczos smoothing was introduced into the SFS computer algorithm and the modeling process repeated.

Figure 28 and Table 15 show that Lanczos smoothing was effective in the suppression of the between data point oscillations witnessed previously in Table 10 and Figure 19. The corresponding reduction in the magnitude of error for the first and second-order derivatives can be seen in Figures 29 and 30. One undesirable effect of this smoothing technique was the introduction of artificial curvatures at the end points of the bottom contour. The cause of this phenomenon is attributed to the apparent discontinuity of the function generated by the immediate commencement and cessation of data at either end.
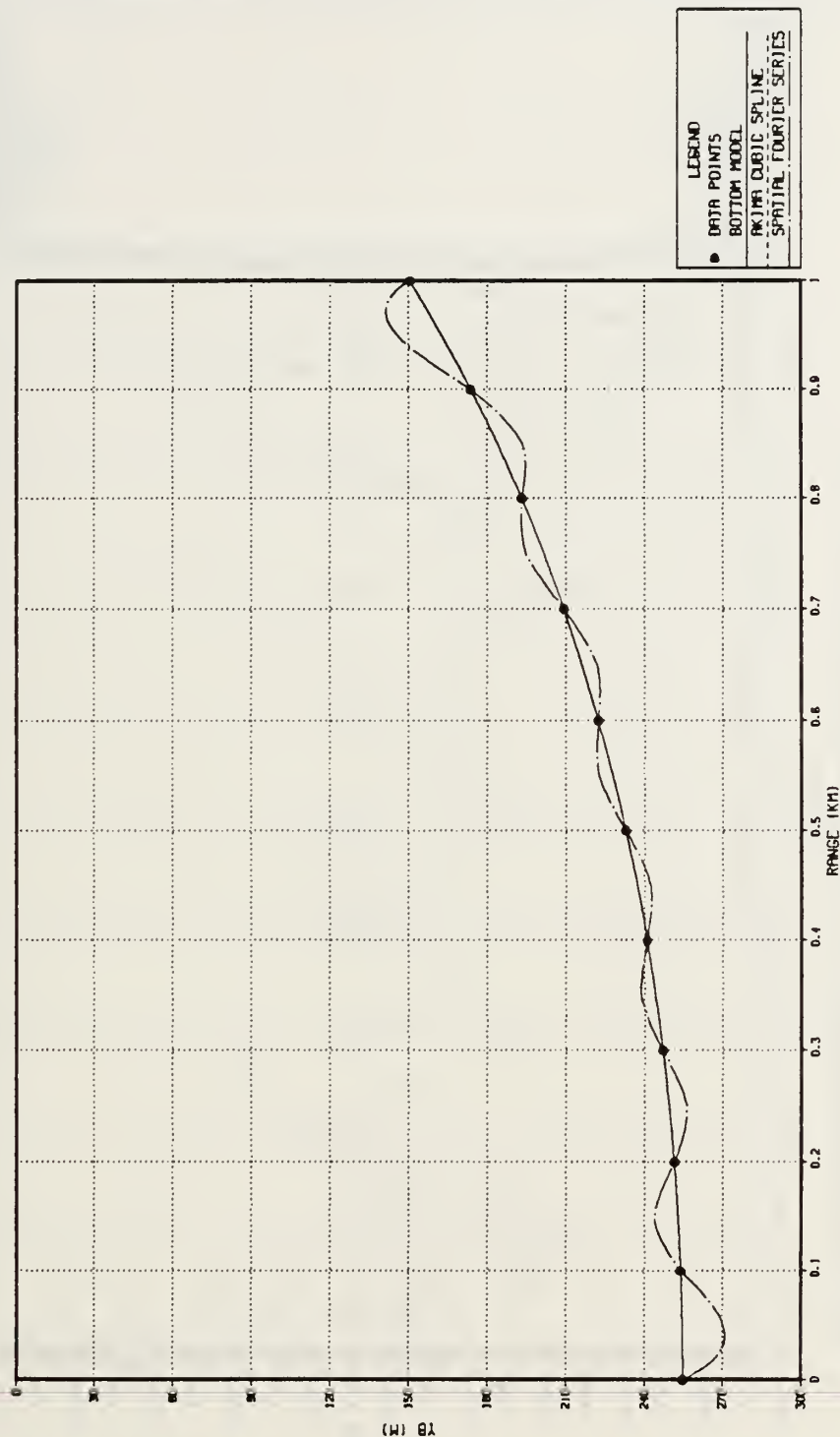
Figure 22.   Half Catenary Ocean Bottom : Contour Reconstruction.

41

Figure 23.　Half Catenary Ocean Bottom : First-Order Derivatives.

42
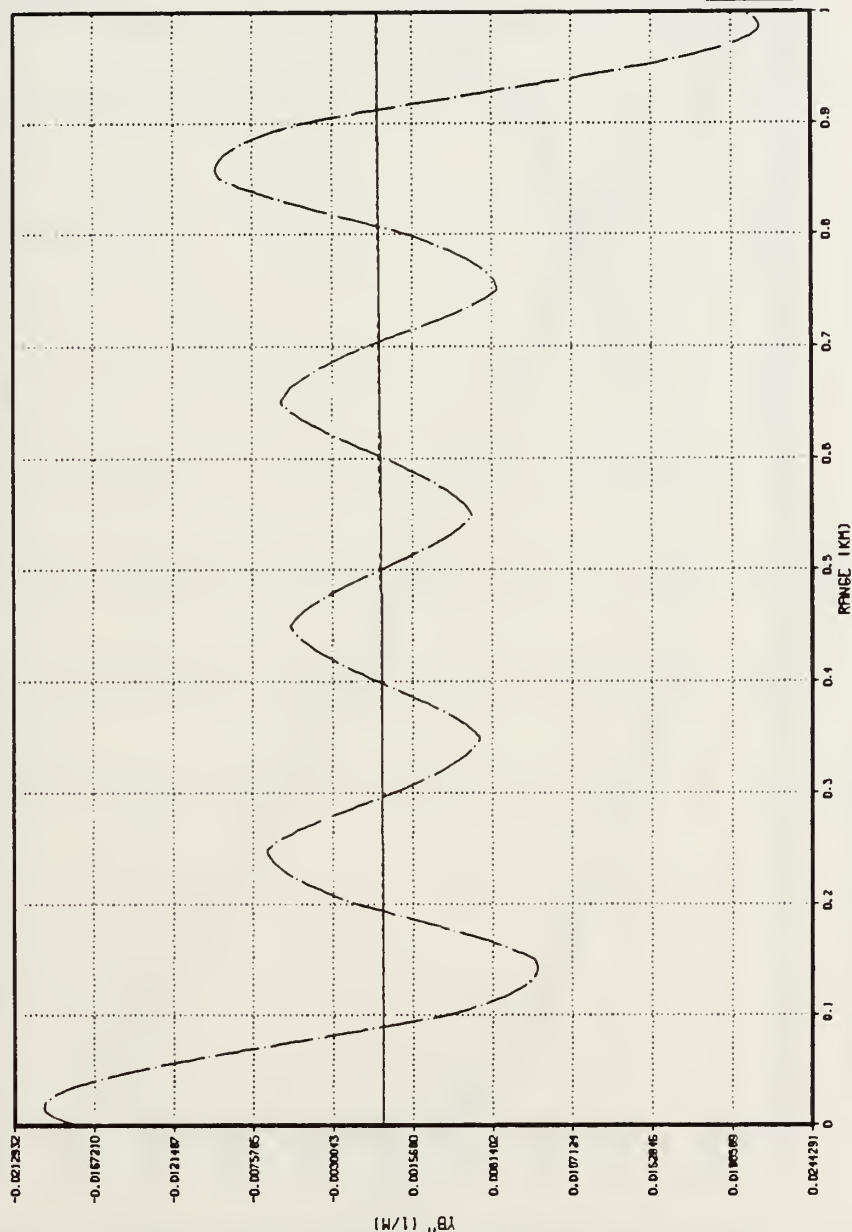
Figure 24. Half Catenary Ocean Bottom : Second-Order Derivatives.

43
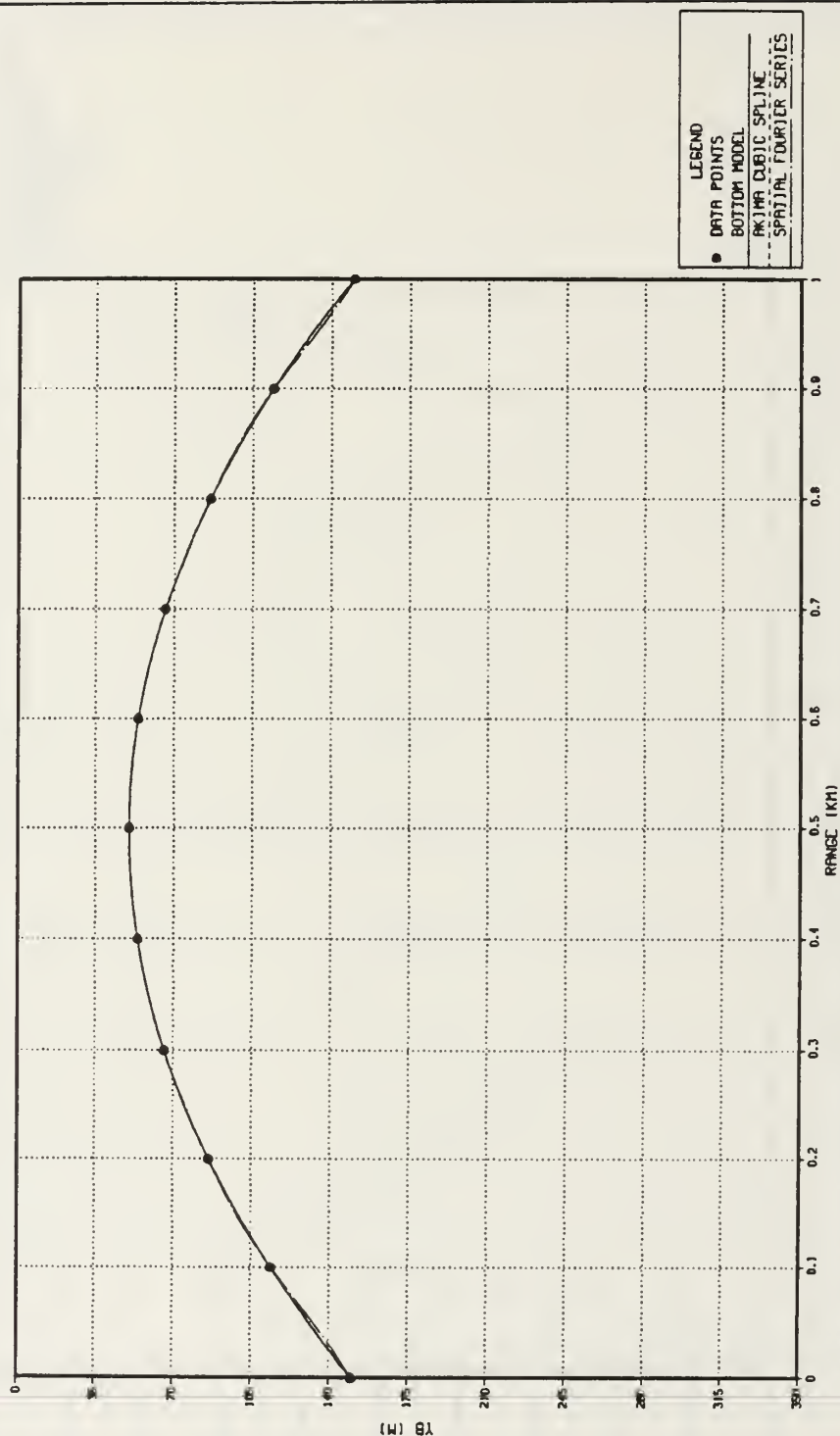
Figure 25. Parabolic Ocean Bottom : Contour Reconstruction.
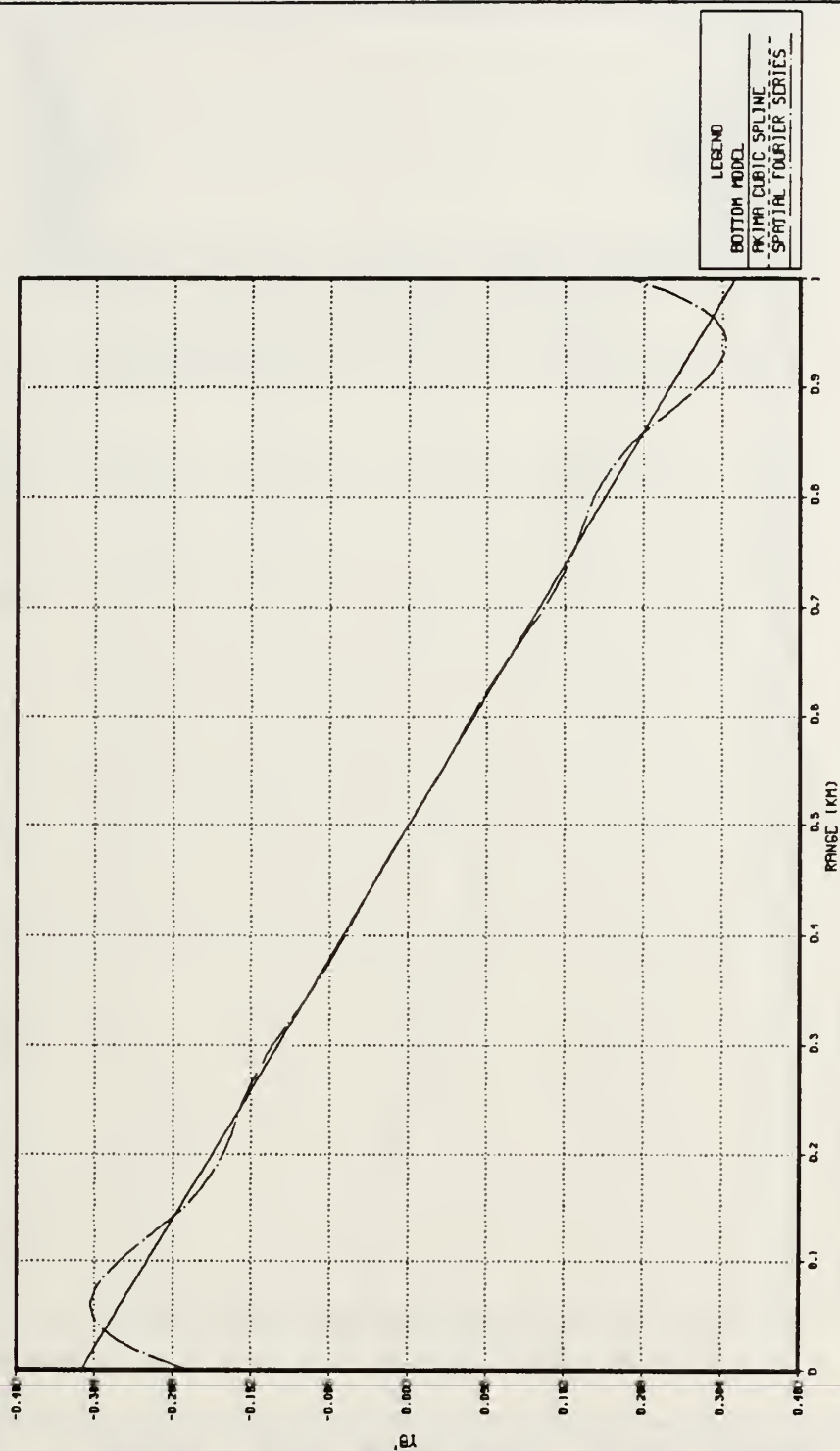
Figure 26. Parabolic Ocean Bottom : First-Order Derivatives.
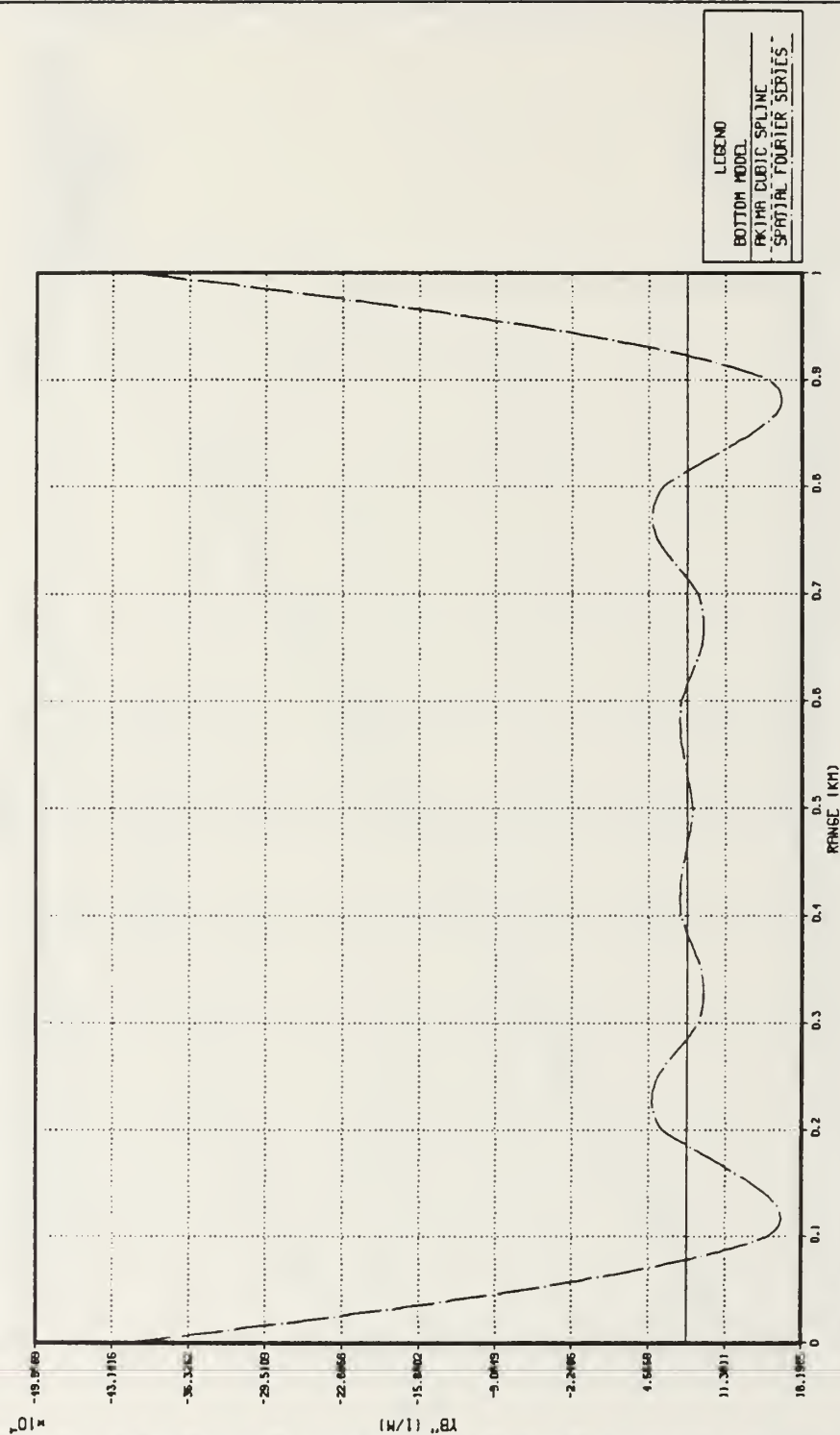
Figure 27.   Parabolic Ocean Bottom : Second-Order Derivatives.
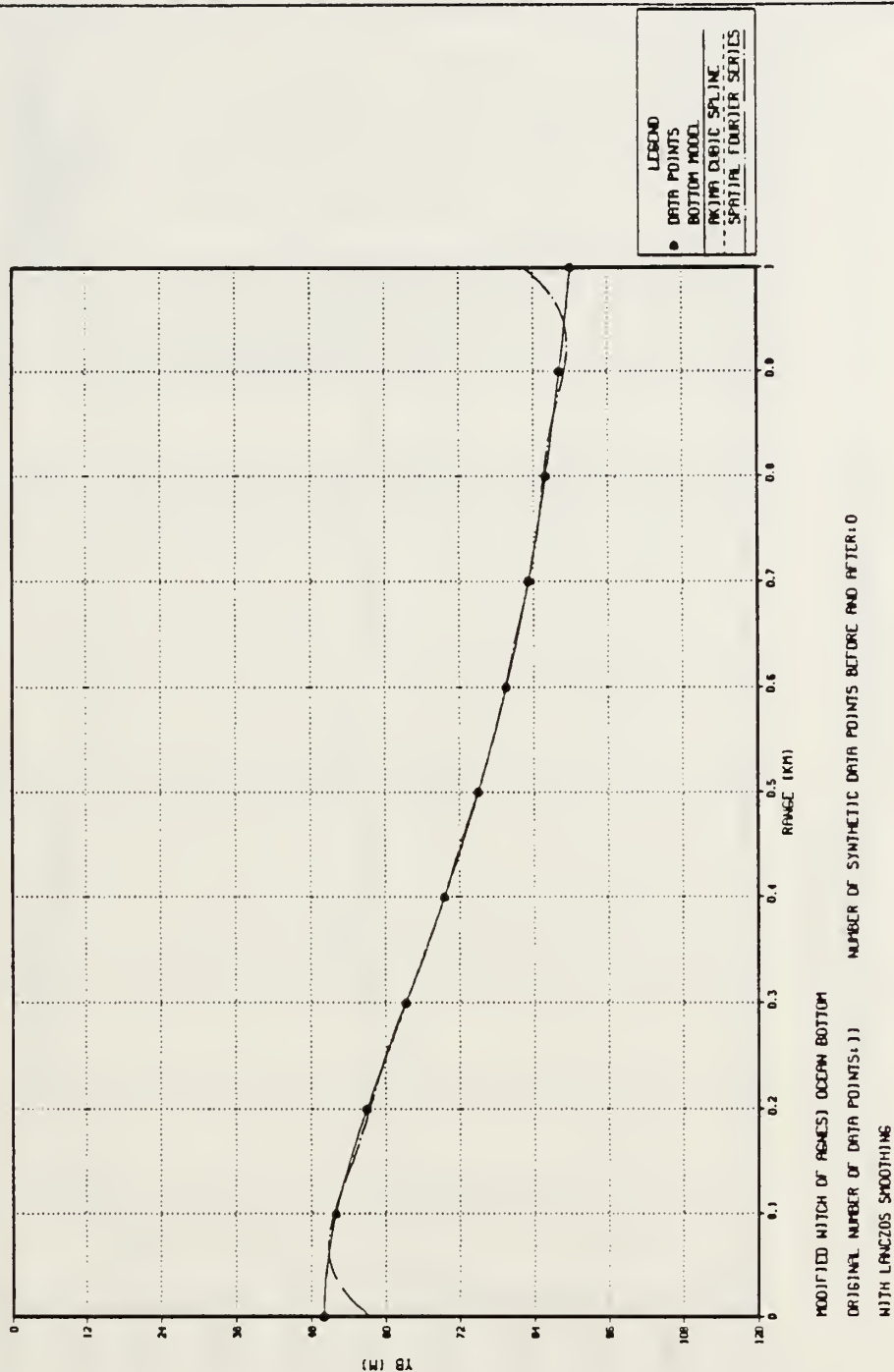
Figure 28.   Modified   Witch   Of   Agnesi   Ocean   Bottom   Contour
Reconstruction: Fourier Series reconstruction with Lanczos smooth-
ing.
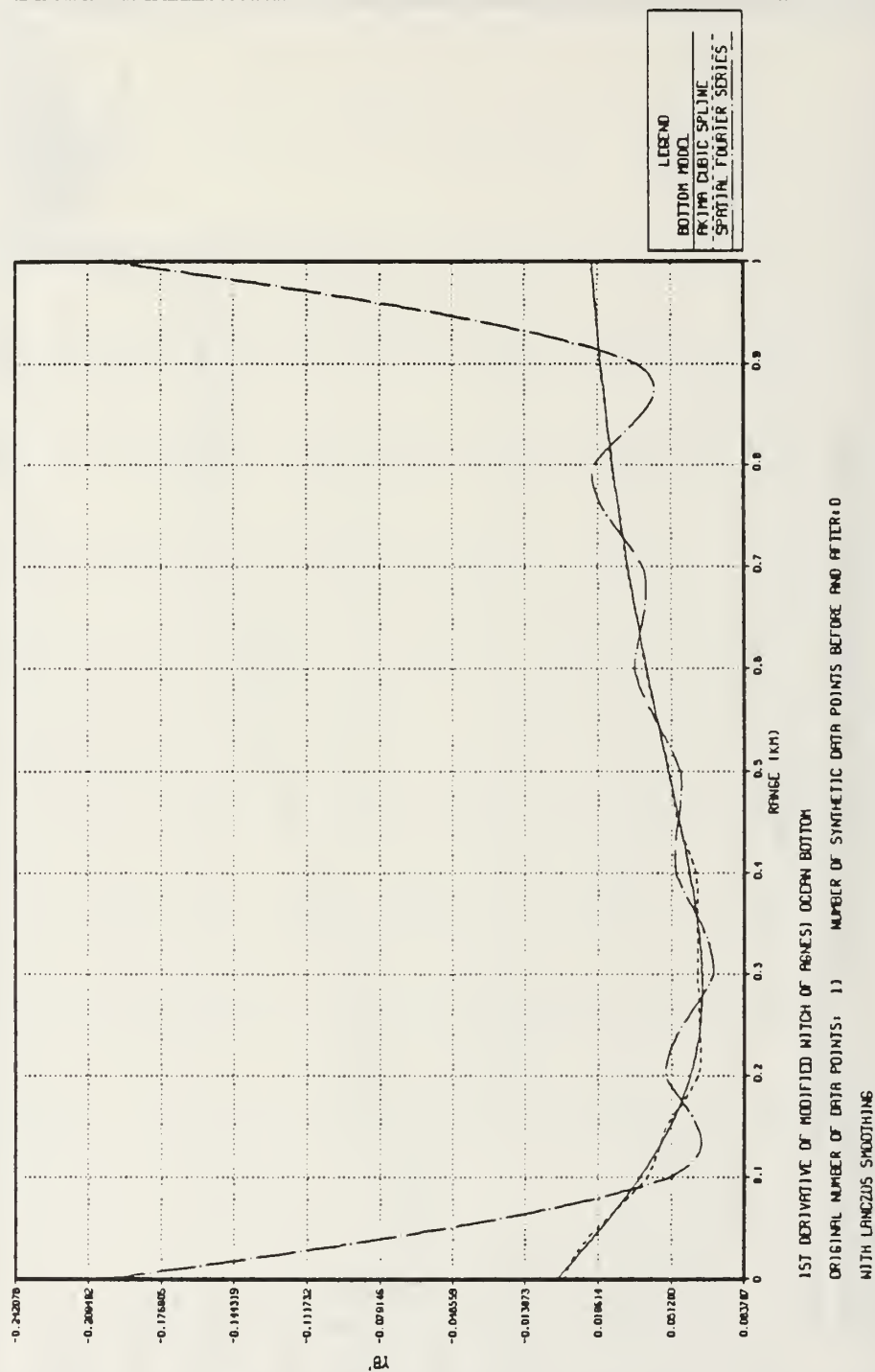
Figure 29.   Modified   Witch   Of   Agnesi   Ocean   Bottom   First-Order
Derivatives: Fourier Series reconstruction with Lanczos smoothing.

48
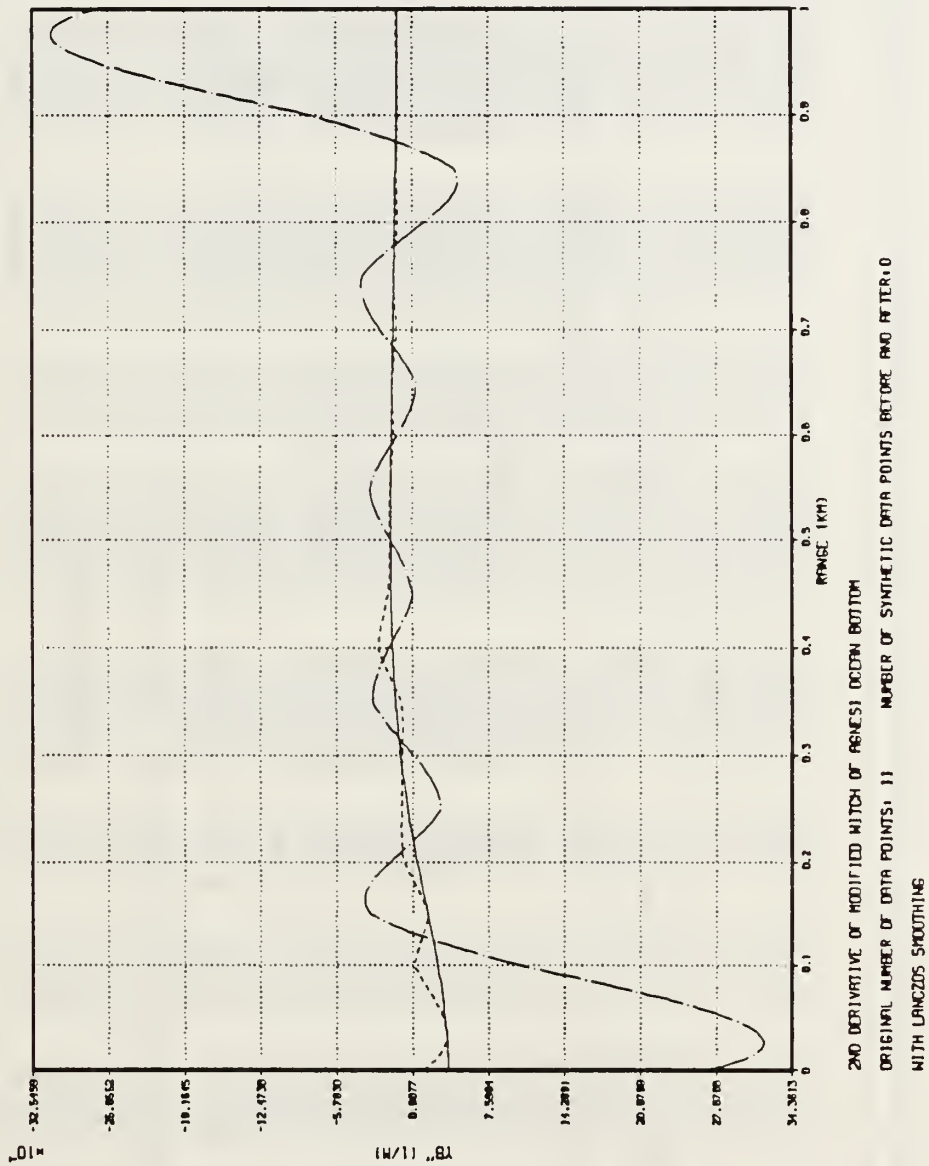
Figure 30.   Modified Witch Of Agnesi Ocean Bottom Second-Order Derivatives: Fourier Series reconstruction with Lanczos smoothing.

49

Table 11. AKIMA CUBIC SPLINE RESULTS : HALF CATENARY OCEAN BOTTOM

HALF CATENARY BOTTOM

TECHNIQUE: AKIMA CUBIC SPLINE FIT   NO. OF ORIGINAL DATA POINTS: 11

RANGE (KM)	YB(EXACT) (M)	YB(FIT) (M)	% ERROR	YBDOT(EXACT)	YBDOT(FIT)	% ERROR	YBDOT2(EXACT) (1/M)	YBDOT2(FIT) (1/M)	% ERROR
0.00	255.00	255.00	0.000	0.000E+00	0.116E-03	********	-0.167E-03	-0.173E-03	3.701
0.05	254.79	254.79	0.000	-0.834E-02	-0.840E-02	0.633	-0.167E-03	-0.168E-03	0.248
0.10	254.16	254.16	0.000	-0.167E-01	-0.166E-01	-0.566	-0.169E-03	-0.179E-03	5.694
0.15	253.12	253.11	-0.001	-0.253E-01	-0.254E-01	0.402	-0.172E-03	-0.170E-03	-1.137
0.20	251.64	251.64	0.000	-0.340E-01	-0.336E-01	-0.916	-0.176E-03	-0.198E-03	12.256
0.25	249.72	249.71	-0.001	-0.429E-01	-0.431E-01	0.459	-0.181E-03	-0.180E-03	-0.797
0.30	247.34	247.34	0.000	-0.521E-01	-0.516E-01	-0.916	-0.188E-03	-0.220E-03	16.911
0.35	244.50	244.50	-0.001	-0.617E-01	-0.620E-01	0.459	-0.196E-03	-0.194E-03	-0.797
0.40	241.17	241.17	0.000	-0.717E-01	-0.711E-01	-0.916	-0.205E-03	-0.248E-03	20.906
0.45	237.32	237.32	-0.001	-0.822E-01	-0.826E-01	0.459	-0.216E-03	-0.214E-03	-0.797
0.50	232.93	232.93	0.000	-0.933E-01	-0.925E-01	-0.916	-0.228E-03	-0.283E-03	24.199
0.55	227.98	227.97	-0.001	-0.105E+00	-0.106E+00	0.459	-0.242E-03	-0.240E-03	-0.797
0.60	222.42	222.42	0.000	-0.118E+00	-0.116E+00	-0.916	-0.257E-03	-0.326E-03	26.825
0.65	216.21	216.21	-0.001	-0.131E+00	-0.131E+00	0.459	-0.274E-03	-0.272E-03	-0.797
0.70	209.32	209.32	0.000	-0.145E+00	-0.144E+00	-0.916	-0.294E-03	-0.378E-03	28.865
0.75	201.69	201.69	-0.002	-0.160E+00	-0.161E+00	0.459	-0.315E-03	-0.312E-03	-0.797
0.80	193.28	193.28	0.000	-0.177E+00	-0.175E+00	-0.916	-0.338E-03	-0.411E-03	21.632
0.85	184.02	184.04	0.008	-0.194E+00	-0.195E+00	0.268	-0.364E-03	-0.376E-03	3.285
0.90	173.86	173.86	0.000	-0.213E+00	-0.212E+00	-0.218	-0.392E-03	-0.451E-03	15.051
0.95	162.71	162.69	-0.012	-0.233E+00	-0.234E+00	0.271	-0.423E-03	-0.407E-03	-3.670
1.00	150.50	150.50	0.000	-0.255E+00	-0.253E+00	-0.810	-0.457E-03	-0.364E-03	-20.352

Table 12. FOURIER SERIES RESULTS : HALF CATENARY OCEAN BOTTOM

HALF CATENARY BOTTOM

TECHNIQUE: SPATIAL FOURIER SERIES FIT   NO. OF ORIGINAL DATA POINTS: 11

RANGE (KM)	YB(EXACT) (M)	YB(FIT) (M)	% ERROR	YBDOT(EXACT)	YBDOT(FIT)	% ERROR	YBDOT2(EXACT) (1/M)	YBDOT2(FIT) (1/M)	% ERROR
0.00	255.00	255.00	0.000	0.000E+00	0.775E+00	********	-0.167E-03	-0.177E-01	********
0.05	254.79	270.45	6.146	-0.834E-02	-0.123E+00	1374.383	-0.167E-03	-0.139E-01	8223.905
0.10	254.16	254.16	0.000	-0.167E-01	-0.378E+00	2157.725	-0.169E-03	0.360E-02	********
0.15	253.12	243.94	-3.626	-0.253E-01	0.105E-01	-141.452	-0.172E-03	0.855E-02	********
0.20	251.64	251.64	0.000	-0.340E-01	0.209E+00	-716.281	-0.176E-03	-0.162E-02	819.266
0.25	249.72	256.51	2.723	-0.429E-01	-0.582E-01	35.787	-0.181E-03	-0.677E-02	3634.071
0.30	247.34	247.34	0.000	-0.521E-01	-0.246E+00	371.595	-0.188E-03	0.464E-03	-346.949
0.35	244.50	238.76	-2.347	-0.617E-01	-0.548E-01	-11.100	-0.196E-03	0.541E-02	********
0.40	241.17	241.17	0.000	-0.717E-01	0.100E+00	-239.419	-0.205E-03	-0.465E-03	126.542
0.45	237.32	242.64	2.241	-0.822E-01	-0.841E-01	2.250	-0.216E-03	-0.542E-02	2412.173
0.50	232.93	232.93	0.000	-0.933E-01	-0.259E+00	177.662	-0.228E-03	-0.243E-03	6.764
0.55	227.98	222.63	-2.343	-0.105E+00	-0.107E+00	2.250	-0.242E-03	0.499E-02	********
0.60	222.42	222.42	0.000	-0.110E+00	0.558E-01	-147.499	-0.257E-03	0.393E-04	-115.267
0.65	216.21	222.03	2.693	-0.131E+00	-0.123E+00	-5.795	-0.274E-03	-0.596E-02	2070.535
0.70	209.32	209.32	0.000	-0.145E+00	-0.343E+00	136.302	-0.294E-03	-0.101E-02	243.167
0.75	201.69	194.71	-3.463	-0.160E+00	-0.177E+00	10.469	-0.315E-03	0.645E-02	********
0.80	193.28	193.28	0.000	-0.177E+00	0.754E-01	-142.696	-0.338E-03	0.124E-02	-467.997
0.85	184.02	193.62	5.217	-0.194E+00	-0.154E+00	-20.393	-0.364E-03	-0.946E-02	2499.017
0.90	173.86	173.86	0.000	-0.213E+00	-0.596E+00	179.874	-0.392E-03	-0.463E-02	1080.160
0.95	162.71	145.79	-10.399	-0.233E+00	-0.365E+00	56.439	-0.423E-03	0.143E-01	********
1.00	150.50	150.50	0.000	-0.255E+00	0.606E+00	-337.529	-0.457E-03	0.204E-01	********

Table 13. AKIMA CUBIC SPLINE RESULTS : PARABOLIC OCEAN BOTTOM

PARABOLIC BOTTOM

TECHNIQUE: AKIMA CUBIC SPLINE FIT   NO. OF ORIGINAL DATA POINTS: 11

RANGE (KM)	YB(EXACT) (M)	YB(FIT) (M)	% ERROR	YBDOT(EXACT)	YBDOT(FIT)	% ERROR	YBDOT2(EXACT) (1/M)	YBDOT2(FIT) (1/M)	% ERROR
0.00	150.00	150.00	0.000	-0.400E+00	-0.400E+00	0.000	0.800E-03	0.800E-03	0.000
0.05	131.00	131.00	0.000	-0.360E+00	-0.360E+00	0.000	0.800E-03	0.800E-03	0.000
0.10	114.00	114.00	0.000	-0.320E+00	-0.320E+00	0.000	0.800E-03	0.800E-03	0.000
0.15	99.00	99.00	0.000	-0.280E+00	-0.280E+00	0.000	0.800E-03	0.800E-03	0.000
0.20	86.00	86.00	0.000	-0.240E+00	-0.240E+00	0.000	0.800E-03	0.800E-03	0.000
0.25	75.00	75.00	0.000	-0.200E+00	-0.200E+00	0.000	0.800E-03	0.600E-03	0.000
0.30	66.00	66.00	0.000	-0.160E+00	-0.160E+00	0.000	0.800E-03	0.800E-03	0.000
0.35	59.00	59.00	0.000	-0.120E+00	-0.120E+00	0.000	0.800E-03	0.800E-03	0.000
0.40	54.00	54.00	0.000	-0.800E-01	-0.800E-01	0.000	0.800E-03	0.800E-03	0.000
0.45	51.00	51.00	0.000	-0.400E-01	-0.400E-01	0.000	0.800E-03	0.800E-03	0.000
0.50	50.00	50.00	0.000	0.000E+00	0.000E+00	0.000	0.800E-03	0.800E-03	0.000
0.55	51.00	51.00	0.000	0.400E-01	0.400E-01	0.000	0.800E-03	0.800E-03	0.000
0.60	54.00	54.00	0.000	0.800E-01	0.800E-01	0.000	0.800E-03	0.800E-03	0.000
0.65	59.00	59.00	0.030	0.120E+00	0.120E+00	0.000	0.800E-03	0.800E-03	0.000
0.70	66.00	66.00	0.000	0.160E+00	0.160E+00	0.000	0.800E-03	0.800E-03	0.000
0.75	75.00	75.00	0.000	0.200E+00	0.200E+00	0.000	0.800E-03	0.800E-03	0.000
0.80	86.00	86.00	0.000	0.240E+00	0.240E+00	0.000	0.800E-03	0.800E-03	0.000
0.85	99.00	99.00	0.000	0.280E+00	0.280E+00	0.000	0.800E-03	0.800E-03	0.000
0.90	114.00	114.00	0.000	0.320E+00	0.320E+00	0.000	0.800E-03	0.800E-03	0.000
0.95	131.00	131.00	0.000	0.360E+00	0.360E+00	0.000	0.800E-03	0.800E-03	0.000
1.00	150.00	150.00	0.000	0.400E+00	0.400E+00	0.000	0.800E-03	0.800E-03	0.000

52

Table 14. FOURIER SERIES RESULTS : PARABOLIC OCEAN BOTTOM

PARABOLIC BOTTOM

TECHNIQUE: SPATIAL FOURIER SERIES FIT   NO. OF ORIGINAL DATA POINTS: 11

RANGE (KM)	YB(EXACT) (M)	YB(FIT) (M)	% ERROR	YBDOT(EXACT)	YBDOT(FIT)	% ERROR	YBDOT2(EXACT) (1/M)	YBDOT2(FIT) (1/M)	% ERROR
0.00	150.00	150.00	0.000	-0.400E+00	-0.266E+00	-33.382	0.800E-03	-0.416E-02	-620.314
0.05	131.00	132.93	1.477	-0.360E+00	-0.386E+00	7.249	0.800E-03	-0.618E-03	-177.302
0.10	114.00	114.00	0.000	-0.320E+00	-0.353E+00	10.431	0.800E-03	0.152E-02	89.547
0.15	99.00	98.35	-0.656	-0.280E+00	-0.274E+00	-2.107	0.800E-03	0.137E-02	71.398
0.20	86.00	86.00	0.000	-0.240E+00	-0.227E+00	-5.549	0.800E-03	0.584E-03	-26.970
0.25	75.00	75.29	0.382	-0.200E+00	-0.202E+00	1.095	0.800E-03	0.535E-03	-33.111
0.30	66.00	66.00	0.000	-0.160E+00	-0.166E+00	3.840	0.800E-03	0.895E-03	11.876
0.35	59.00	58.87	-0.221	-0.120E+00	-0.119E+00	-0.938	0.800E-03	0.923E-03	15.379
0.40	54.00	54.00	0.000	-0.800E-01	-0.775E-01	-3.155	0.800E-03	0.743E-03	-7.104
0.45	51.00	51.04	0.075	-0.400E-01	-0.408E-01	1.976	0.800E-03	0.764E-03	-4.549
0.50	50.00	50.00	0.000	0.000E+00	-0.358E-15	0.000	0.800E-03	0.847E-03	5.929
0.55	51.00	51.04	0.075	0.400E-01	0.408E-01	1.976	0.800E-03	0.764E-03	-4.549
0.60	54.00	54.00	0.000	0.800E-01	0.775E-01	-3.155	0.800E-03	0.743E-03	-7.104
0.65	59.00	58.87	-0.221	0.120E+00	0.119E+00	-0.938	0.800E-03	0.923E-03	15.379
0.70	66.00	66.00	0.000	0.160E+00	0.166E+00	3.840	0.800E-03	0.895E-03	11.876
0.75	75.00	75.29	0.382	0.200E+00	0.202E+00	1.095	0.800E-03	0.535E-03	-33.111
0.80	86.00	86.00	0.000	0.240E+00	0.227E+00	-5.549	0.800E-03	0.584E-03	-26.970
0.85	99.00	98.35	-0.656	0.280E+00	0.274E+00	-2.107	0.800E-03	0.137E-02	71.398
0.90	114.00	114.00	0.000	0.320E+00	0.353E+00	10.431	0.800E-03	0.152E-02	89.547
0.95	131.00	132.93	1.477	0.360E+00	0.386E+00	7.249	0.800E-03	-0.618E-03	-177.302
1.00	150.00	150.00	0.000	0.400E+00	0.266E+00	-33.382	0.800E-03	-0.416E-02	-620.314

Table 15.   FOURIER SERIES RESULTS : LANCZOS SMOOTH-
ING.

WITCH OF AGNESI BOTTOM

TECHNIQUE: SPATIAL FOURIER SERIES FIT WITH LANCZOS SMOOTHING   NO. OF ORIGINAL DATA POINTS: 11

RANGE (KM)	YB(EXACT) (M)	YB(FIT) (M)	% ERROR	YBDOT(EXACT)	YBDOT(FIT)	% ERROR	YBDOT2(EXACT) (1/M)	YBDOT2(FIT) (1/M)	% ERROR
0.00	50.00	57.49	14.980	0.000E+00	-0.202E+00	********	0.400E-03	0.270E-02	574.979
0.05	50.50	51.15	1.305	0.196E-01	-0.505E-01	-357.357	0.377E-03	0.286E-02	660.364
0.10	51.92	51.54	-0.743	0.370E-01	0.501E-01	35.605	0.313E-03	0.104E-02	230.929
0.15	54.13	54.64	0.941	0.505E-01	0.628E-01	24.278	0.225E-03	-0.279E-03	-223.848
0.20	56.90	57.38	0.844	0.595E-01	0.484E-01	-18.546	0.133E-03	-0.110E-03	-182.768
0.25	60.00	59.89	-0.178	0.640E-01	0.561E-01	-12.290	0.512E-04	0.338E-03	560.257
0.30	63.24	63.09	-0.225	0.649E-01	0.698E-01	7.619	-0.127E-04	0.107E-03	-938.194
0.35	66.44	66.53	0.134	0.631E-01	0.646E-01	2.449	-0.568E-04	-0.256E-03	350.322
0.40	69.51	69.45	-0.089	0.595E-01	0.533E-01	-10.336	-0.834E-04	-0.119E-03	42.672
0.45	72.38	72.09	-0.399	0.549E-01	0.540E-01	-1.721	-0.965E-04	0.943E-04	-197.746
0.50	75.00	74.86	-0.183	0.500E-01	0.553E-01	10.686	-0.100E-03	-0.974E-04	-2.561
0.55	77.38	77.40	0.026	0.450E-01	0.444E-01	-1.463	-0.975E-04	-0.281E-03	188.634
0.60	79.51	79.33	-0.229	0.403E-01	0.349E-01	-13.450	-0.914E-04	-0.451E-04	-50.680
0.65	81.41	81.13	-0.347	0.359E-01	0.383E-01	7.950	-0.836E-04	0.127E-03	-252.095
0.70	83.11	83.14	0.033	0.320E-01	0.387E-01	21.104	-0.753E-04	-0.187E-03	149.005
0.75	84.62	84.70	0.106	0.284E-01	0.226E-01	-20.399	-0.670E-04	-0.349E-03	420.421
0.80	85.96	85.57	-0.447	0.252E-01	0.167E-01	-33.711	-0.592E-04	0.198E-03	-434.581
0.85	87.15	86.88	-0.307	0.225E-01	0.380E-01	69.275	-0.521E-04	0.465E-03	-991.978
0.90	88.21	89.00	0.897	0.200E-01	0.359E-01	79.468	-0.458E-04	-0.816E-03	1684.241
0.95	89.15	88.93	-0.254	0.179E-01	-0.550E-01	-407.644	-0.401E-04	-0.271E-02	6656.401
1.00	90.00	82.50	-8.328	0.160E-01	-0.202E+00	********	-0.352E-04	-0.266E-02	7469.706

2. Lanczos Smoothing With Synthetic Data.

The ability of Lanczos smoothing to suppress oscillations generated by the SFS technique gave it great utility. However, the artificial curvature at the end points of the contour was an undesirable effect which needed to be eliminated. It was unlikely that the problems associated with Lanczos smoothing could be countered by further modifying the expression for the SFS coefficients. Extension of the original bathymetric array by adding equally spaced synthetic data points was, however, viewed as a possible solution. The rationale of this procedure was to force the undesirable features generated by Lanczos smoothing beyond the actual region of interest.

Let each data point y_{B_i} be represented as a function of incremented range such that

$$y_{B_i} = y_B(z_i) \,, \quad i = 0,1,2,...,(NZBPTS - 1) \tag{3.1}$$

with

$$z_i = i\Delta z \,, \quad i = 0,1,2,...,(NZBPTS - 1) \tag{3.2}$$

where Δz is the distance between each data point and $NZBPTS$ is the total number of original discrete data. Now let

$$m_S = \frac{y_B(z_1) - y_B(z_0)}{\Delta z} \tag{3.3}$$

and

$$m_F = \frac{y_B(z_{(NZBPTS-1)}) - y_B(z_{(NZBPTS-2)})}{\Delta z} . \tag{3.4}$$

Synthetic data points were then created by linear extrapolation, that is,

$$y_B(z_{-i}) = y_B(z_0) + m_s \, z_{-i} \,, \quad i = 1,2,...,SYNTHP \tag{3.5}$$

where

$$z_{-i} = -z_i \tag{3.6}$$

and

$$y_B(z_{(NZBPTS-1+i)}) = y_B(z_{(NZBPTS-1)}) + m_F \, z_{(NZBPTS-1+i)} \,, \quad i = 1,2,..., SYNTHP. \tag{3.7}$$

55

SYNTHP is the number of synthetic points to be generated. Figure 31 provides a diagramatic representation of this methodology.
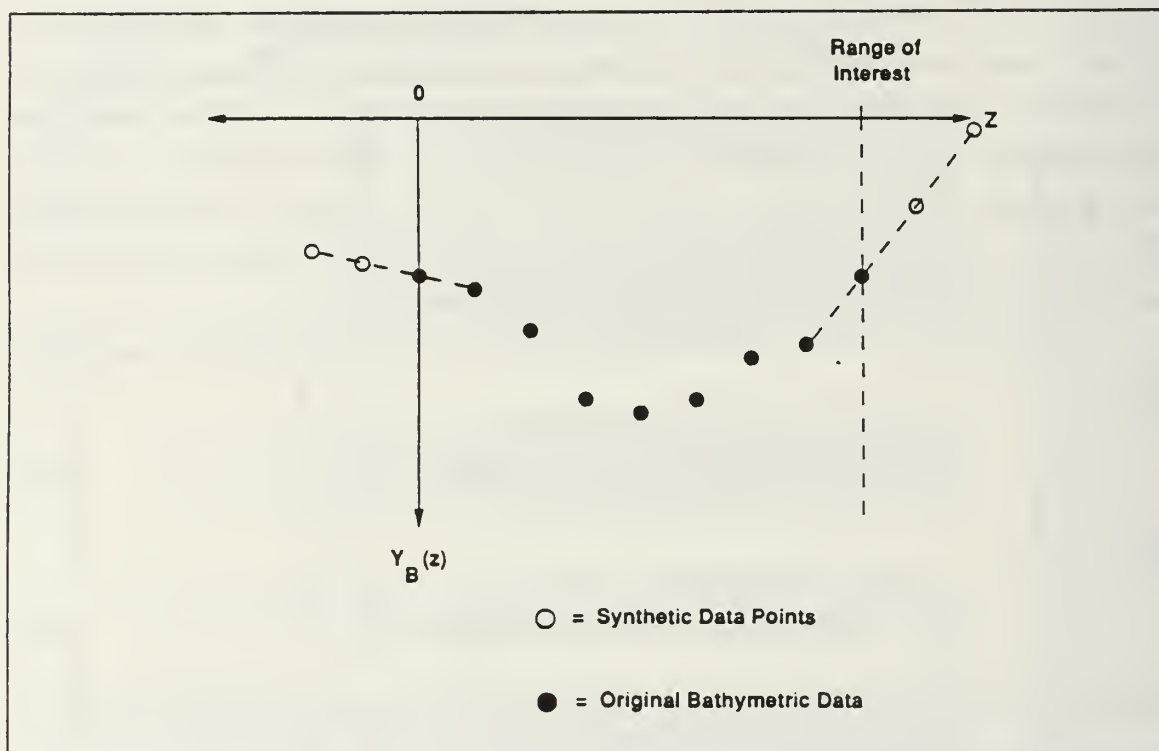
Figure 31.   Generation Of Synthetic Data: Synthetic data points are generated by linear extrapolation.

Figures 32, 33 and 34 and Table 16 reveal that the addition of five synthetic points to either end of the original data array was successful in shifting the end effects induced by Lanczos smoothing outside the horizontal range of interest. This resulted in a better curve fit for the modified Witch of Agnesi bottom and smaller errors in the subsequent first and second-order derivatives. One undesirable feature of the linear extrapolation method for simulating data was its tendency to suppress the natural curvature of the function being modeled. This phenomenon is observed in Figure 32.

Generating synthetic data by linear extrapolation was a valid technique when the nature of the function being modeled was relatively featureless. However, it was not suited to functions with substantial variation in shape. Consequently, an alternative method involving the mirroring of the original data about the end points of the contour was created. This method is described by

$$y_B(-z_i) = y_B(z_i) \ , \ i = 1,2,...,SYNTHP \tag{3.8}$$

56

Figure 32.   Modified   Witch   Of   Agnesi   Ocean   Bottom   Contour
Reconstruction: Fourier Series reconstruction with Lanczos smooth-
ing and linear extrapolation.

57

Figure 33.   Modified   Witch   Of   Agnesi   Ocean   Bottom   First-Order
Derivatives: Fourier Series reconstruction with Lanczos smoothing
and linear extrapolation.

Figure 34.   Modified   Witch   Of   Agnesi   Ocean   Bottom   Second-Order
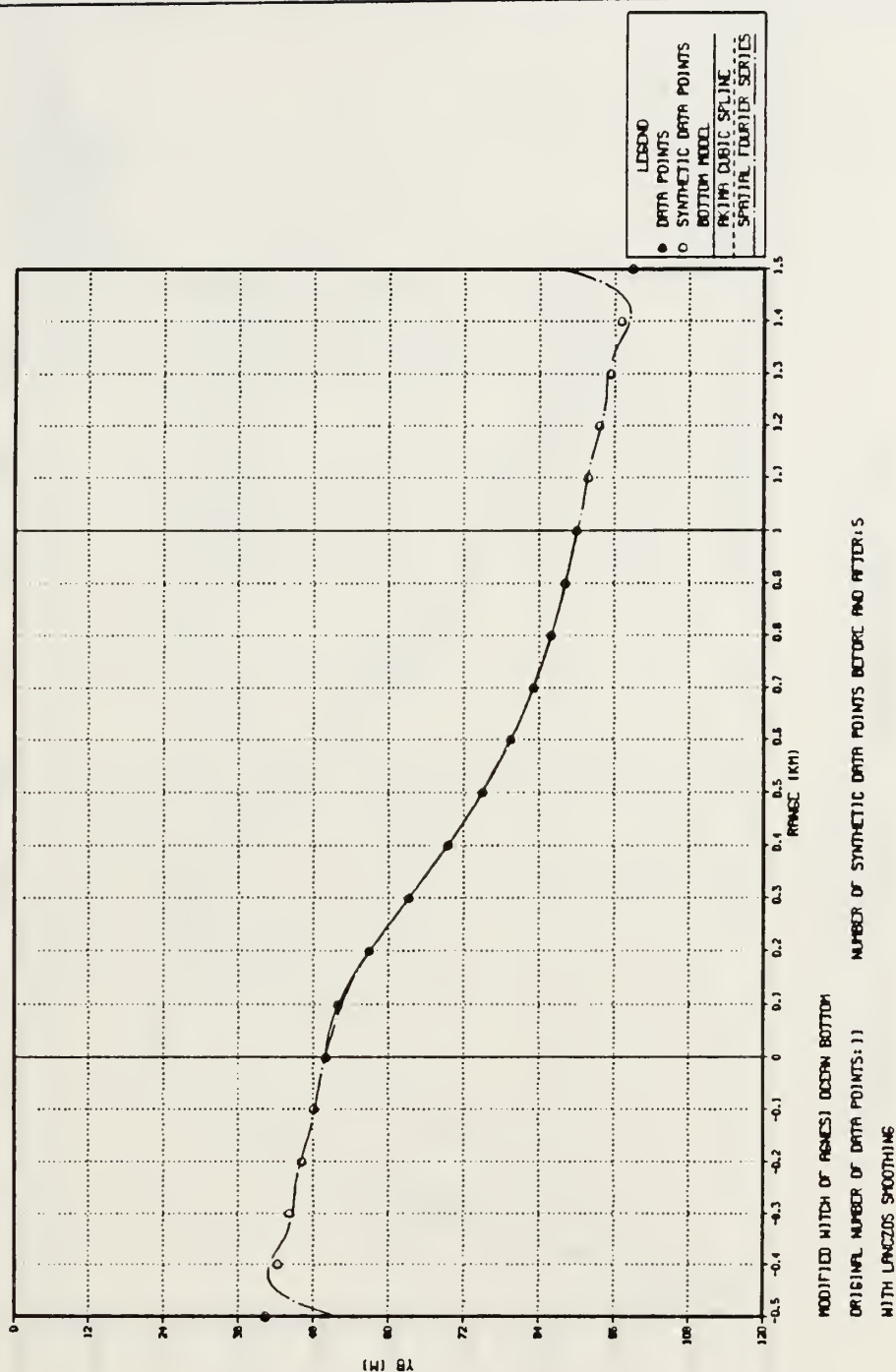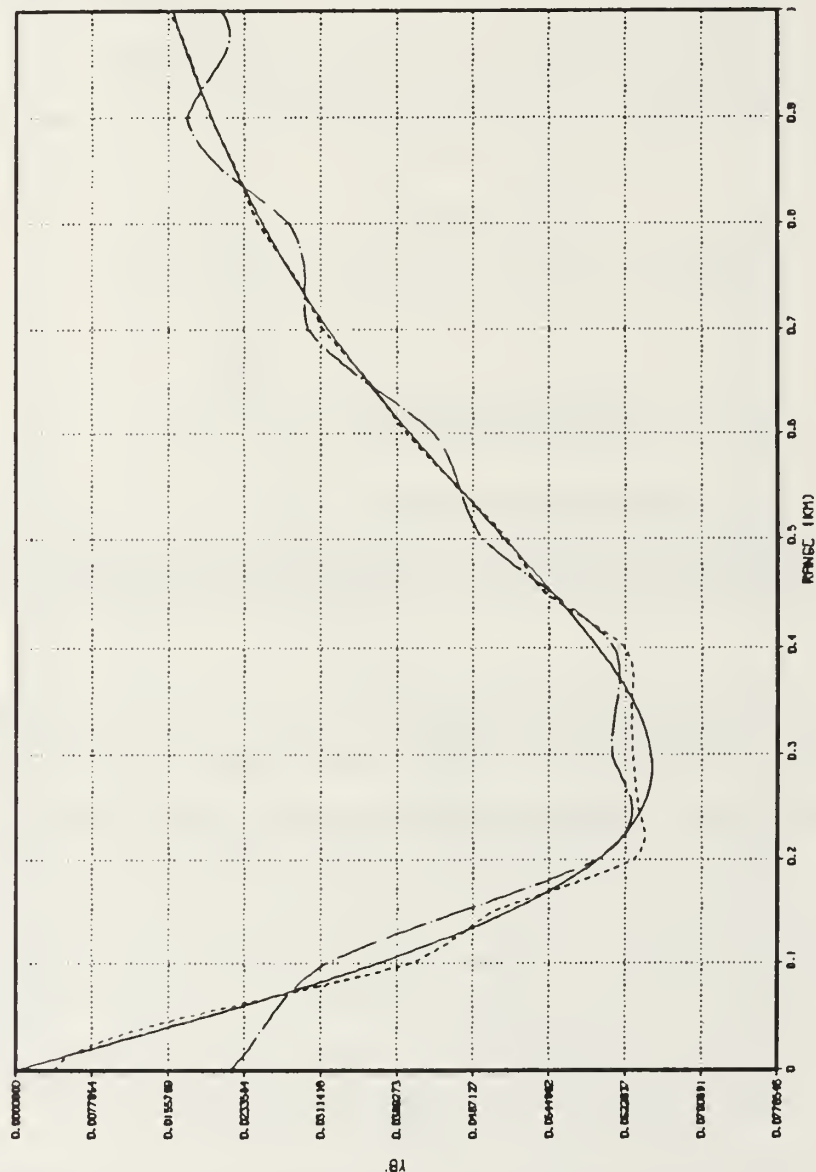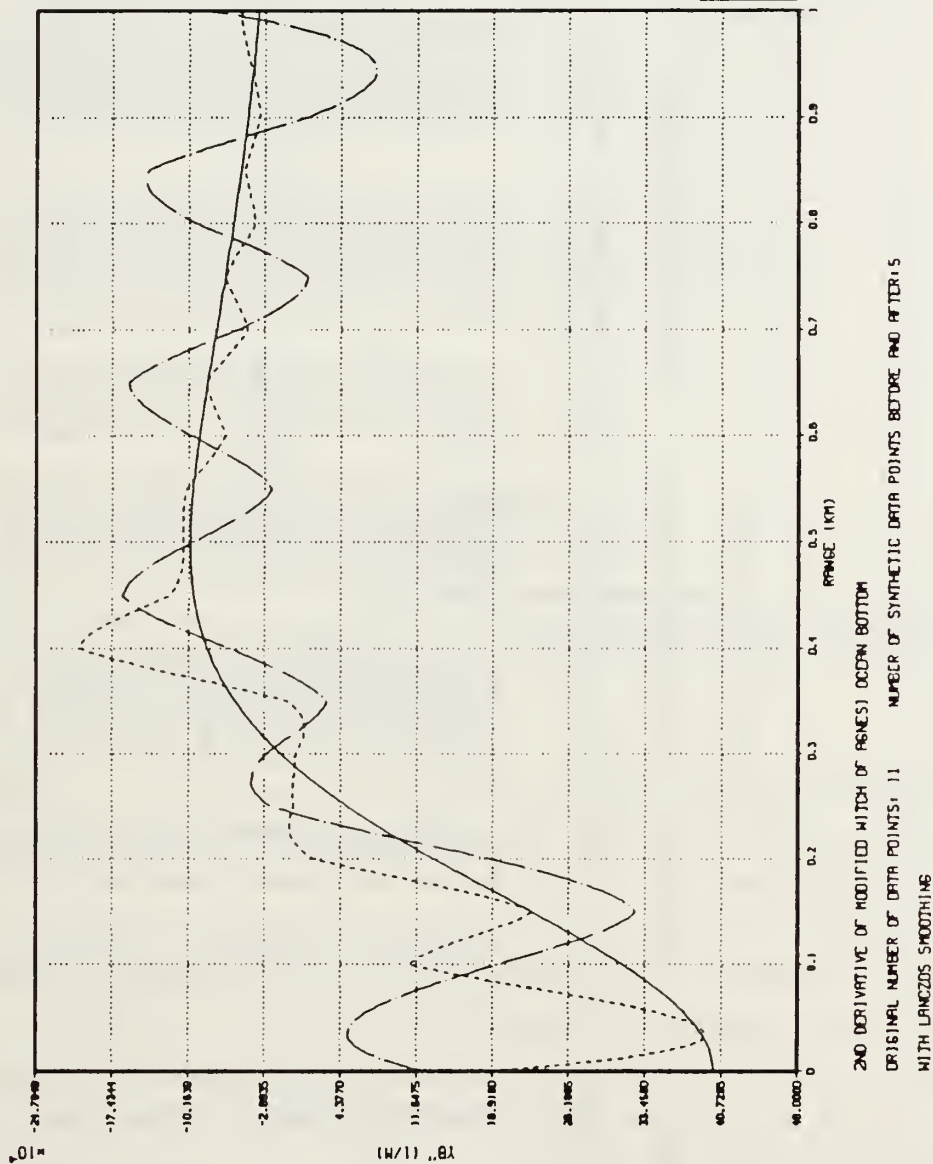Derivatives: Fourier Series reconstruction with Lanczos smoothing
and linear extrapolation.

59

Table 16. FOURIER SERIES RESULTS : LINEAR EXTRAPO-
LATED DATA.

WITCH OF AGNESI BOTTOM

TECHNIQUE: SPATIAL FOURIER SERIES FIT WITH LANCZOS SMOOTHING   NO. OF ORIGINAL DATA POINTS: 11

RANGE (KM)	YB(EXACT) (M)	YB(FIT) (M)	% ERROR	YBDOT(EXACT)	YBDOT(FIT)	% ERROR	YBDOT2(EXACT) (1/M)	YBDOT2(FIT) (1/M)	% ERROR
0.00	50.00	49.87	-0.260	0.000E+00	0.219E-01	********	0.400E-03	0.125E-03	-68.698
0.05	50.50	51.08	1.164	0.196E-01	0.260E-01	32.861	0.377E-03	0.614E-04	-83.688
0.10	51.92	52.50	1.105	0.370E-01	0.317E-01	-14.372	0.313E-03	0.194E-03	-37.880
0.15	54.13	54.40	0.498	0.505E-01	0.455E-01	-9.893	0.225E-03	0.326E-03	44.383
0.20	56.90	57.05	0.269	0.595E-01	0.594E-01	-0.124	0.133E-03	0.187E-03	40.436
0.25	60.00	60.15	0.256	0.640E-01	0.630E-01	-1.583	0.512E-04	-0.222E-04	-143.319
0.30	63.24	63.25	0.024	0.649E-01	0.609E-01	-6.174	-0.127E-04	-0.275E-04	116.316
0.35	66.44	66.29	-0.226	0.631E-01	0.613E-01	-2.726	-0.568E-04	0.306E-04	-153.896
0.40	69.51	69.33	-0.197	0.595E-01	0.611E-01	2.786	-0.834E-04	-0.623E-04	-25.270
0.45	72.38	72.30	-0.106	0.549E-01	0.549E-01	-0.026	-0.965E-04	-0.165E-03	70.570
0.50	75.00	74.85	-0.193	0.500E-01	0.478E-01	-4.478	-0.100E-03	-0.980E-04	-1.903
0.55	77.38	77.16	-0.277	0.450E-01	0.453E-01	0.546	-0.975E-04	-0.219E-04	-77.546
0.60	79.51	79.38	-0.162	0.403E-01	0.428E-01	6.077	-0.914E-04	-0.991E-04	8.424
0.65	81.41	81.35	-0.072	0.359E-01	0.357E-01	-0.656	-0.836E-04	-0.158E-03	89.434
0.70	83.11	82.97	-0.165	0.320E-01	0.299E-01	-6.457	-0.753E-04	-0.549E-04	-26.996
0.75	84.62	84.44	-0.204	0.284E-01	0.296E-01	4.055	-0.670E-04	0.123E-04	-118.308
0.80	85.96	85.90	-0.060	0.252E-01	0.279E-01	10.639	-0.592E-04	-0.946E-04	59.657
0.85	87.15	87.14	-0.006	0.225E-01	0.212E-01	-5.734	-0.521E-04	-0.140E-03	169.507
0.90	88.21	88.08	-0.149	0.200E-01	0.175E-01	-12.607	-0.458E-04	0.110E-04	-124.080
0.95	89.15	89.02	-0.153	0.179E-01	0.207E-01	15.976	-0.401E-04	0.756E-04	-280.354
1.00	90.00	90.09	0.104	0.160E-01	0.209E-01	30.633	-0.352E-04	-0.864E-04	145.526

60

and

$$y_B(z_{(NZBPTS-1+i)}) = y_B(z_{(NZBPTS-1-i)}) \; , \; i = 1,2,...,SYNTHP. \tag{3.9}$$

Figure 35 illustrates this mirroring process.
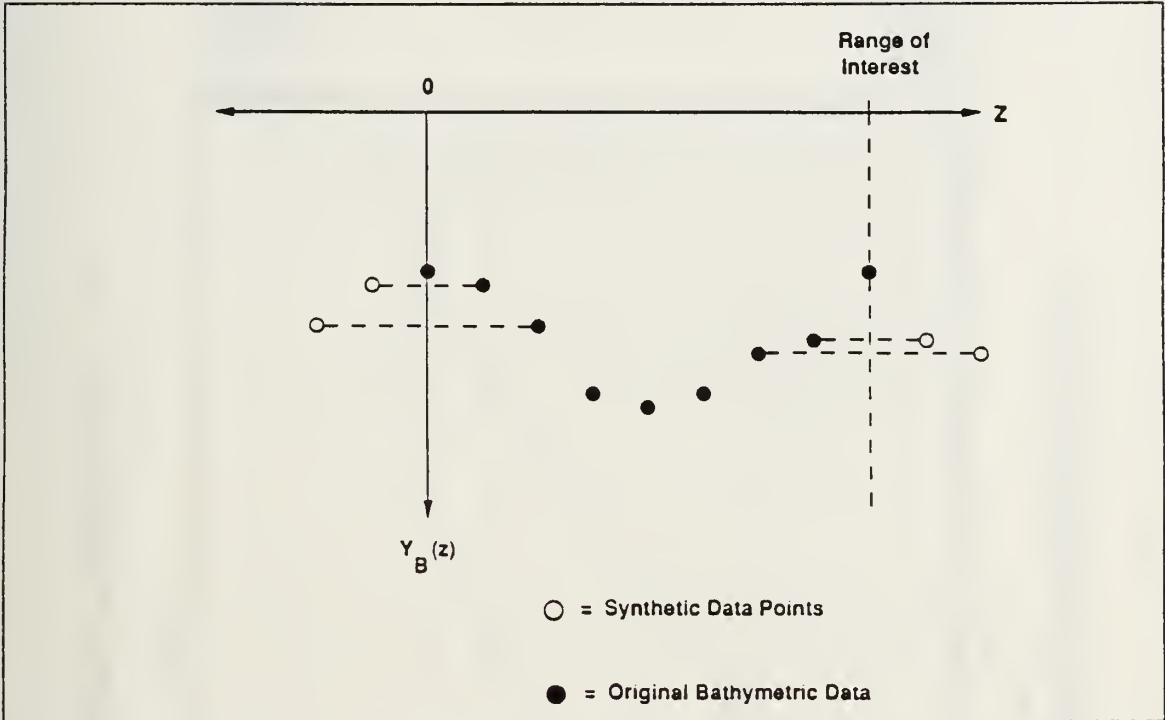
Figure 35.   Generation of Synthetic Data: Synthetic data is generated by mirror imaging the original data points.

Figures 36, 37 and 38 and Table 17 give the results for the SFS modeling of the modified Witch Of Agnesi contour using synthetic data points derived from the mirroring technique. Further improvement in the overall curve fit and accuracy of the first and second-order derivatives was observed. However, some leveling of the bottom contour curvature was still prevalent. The cause of this phenomenon was attributed to the apparent function discontinuity arising from the mirroring process. This problem is identified in Figure 35 where mirror imaging at the right contour boundary has created a spike in the data. In an effort to compensate for this, the SFS technique has smoothed this feature, thereby suppressing the true function curvature at the end points of the range of interest.

To resolve this problem of curvature suppression, the mirror imaging technique given by Equations (3.8) and (3.9) was altered as follows:
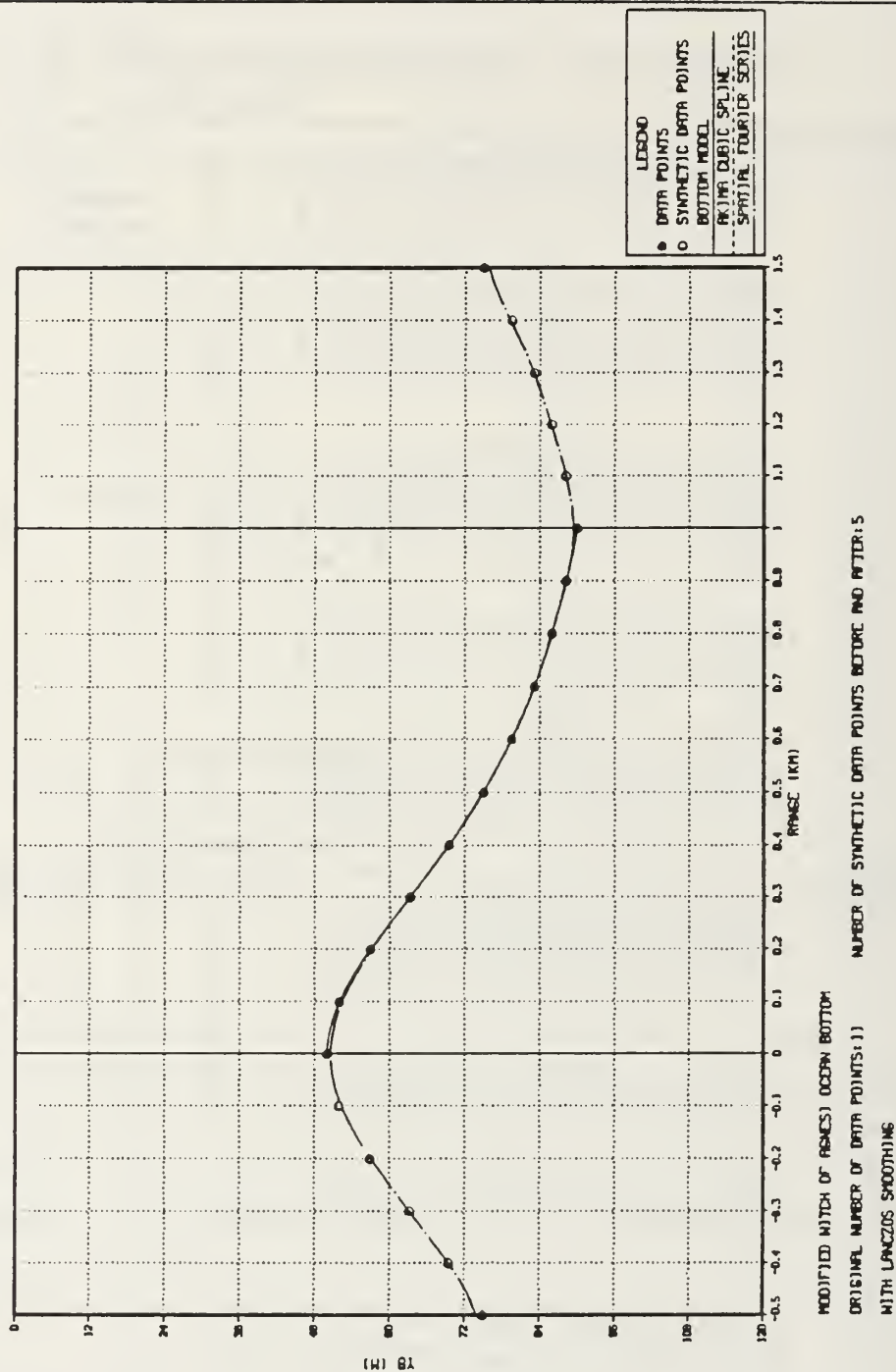
Figure 36.   Modified   Witch   Of   Agnesi   Ocean   Bottom   Contour
Reconstruction: Fourier Series reconstruction with Lanczos smooth-
ing and mirrored data.
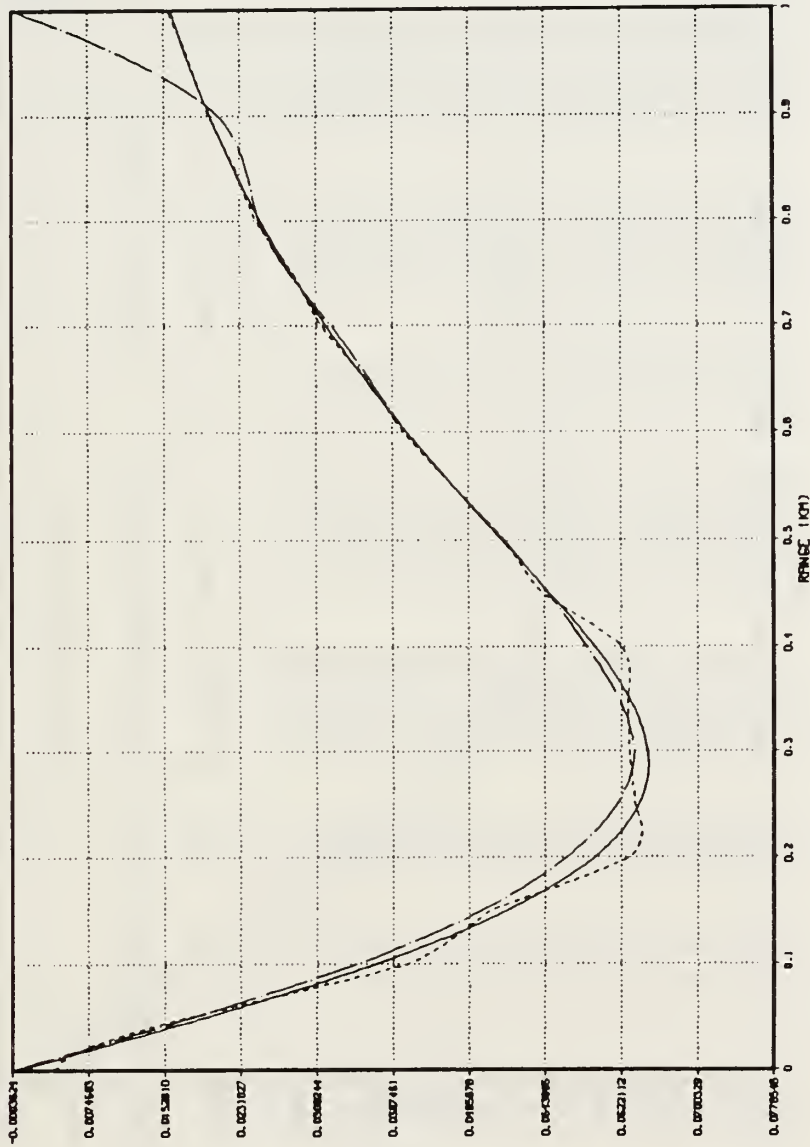
Figure 37. Modified Witch Of Agnesi Ocean Bottom First-Order Derivatives: Fourier Series reconstruction with Lanczos smoothing and mirrored data.
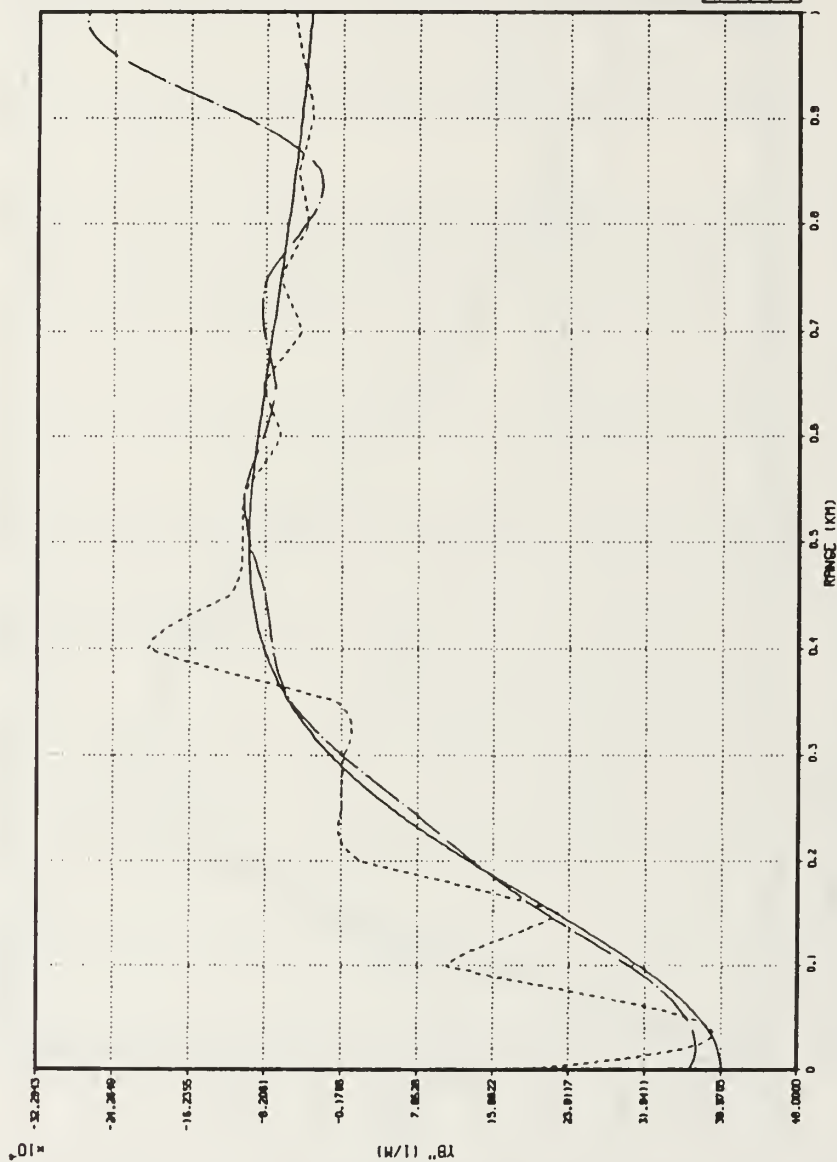
Figure 38. Modified Witch of Agnesi Ocean Bottom Second-Order Derivatives: Fourier Series reconstruction with Lanczos smoothing and mirrored data.

64

Table 17. FOURIER SERIES RESULTS : MIRROR IMAGED DATA.

WITCH OF AGNESI BOTTOM

TECHNIQUE: SPATIAL FOURIER SERIES FIT WITH LANCZOS SMOOTHING   NO. OF ORIGINAL DATA POINTS: 11

RANGE (KM)	YB(EXACT) (M)	YB(FIT) (M)	% ERROR	YBDOT(EXACT)	YBDOT(FIT)	% ERROR	YBDOT2(EXACT) (1/M)	YBDOT2(FIT) (1/M)	% ERROR
0.00	50.00	50.60	1.203	0.000E+00	-0.302E-03	********	0.400E-03	0.366E-03	-8.514
0.05	50.50	51.05	1.094	0.196E-01	0.181E-01	-7.579	0.377E-03	0.363E-03	-3.717
0.10	51.92	52.39	0.894	0.370E-01	0.350E-01	-5.442	0.313E-03	0.303E-03	-3.330
0.15	54.13	54.48	0.645	0.505E-01	0.479E-01	-5.195	0.225E-03	0.213E-03	-5.371
0.20	56.90	57.10	0.365	0.595E-01	0.566E-01	-4.879	0.133E-03	0.137E-03	2.769
0.25	60.00	60.08	0.125	0.640E-01	0.617E-01	-3.527	0.512E-04	0.703E-04	37.396
0.30	63.24	63.22	-0.023	0.649E-01	0.635E-01	-2.139	-0.127E-04	-0.374E-06	-97.061
0.35	66.44	66.37	-0.111	0.631E-01	0.620E-01	-1.714	-0.568E-04	-0.547E-04	-3.750
0.40	69.51	69.39	-0.178	0.595E-01	0.586E-01	-1.441	-0.834E-04	-0.743E-04	-10.967
0.45	72.38	72.22	-0.209	0.549E-01	0.547E-01	-0.356	-0.965E-04	-0.820E-04	-14.987
0.50	75.00	74.85	-0.196	0.500E-01	0.502E-01	0.493	-0.100E-03	-0.989E-04	-1.113
0.55	77.38	77.24	-0.180	0.450E-01	0.450E-01	0.011	-0.975E-04	-0.105E-03	7.341
0.60	79.51	79.36	-0.181	0.403E-01	0.402E-01	-0.184	-0.914E-04	-0.853E-04	-6.716
0.65	81.41	81.28	-0.166	0.359E-01	0.364E-01	1.319	-0.836E-04	-0.724E-04	-13.393
0.70	83.11	83.00	-0.126	0.320E-01	0.325E-01	1.800	-0.753E-04	-0.846E-04	12.396
0.75	84.62	84.52	-0.111	0.284E-01	0.282E-01	-0.689	-0.670E-04	-0.816E-04	21.840
0.80	85.96	85.84	-0.128	0.252E-01	0.251E-01	-0.711	-0.592E-04	-0.404E-04	-31.704
0.85	87.15	87.06	-0.098	0.225E-01	0.237E-01	5.602	-0.521E-04	-0.256E-04	-50.842
0.90	88.21	88.19	-0.017	0.200E-01	0.209E-01	4.230	-0.458E-04	-0.104E-03	127.414
0.95	89.15	89.05	-0.111	0.179E-01	0.126E-01	-29.664	-0.401E-04	-0.224E-03	459.221
1.00	90.00	89.37	-0.697	0.160E-01	-0.249E-03	-101.554	-0.352E-04	-0.269E-05	664.354

$$y_B(-z_i) = y_B(z_{(i-1)}), \quad i = 1,2,...,SYNTHP \tag{3.10}$$

and

$$y_B(z_{(NZBPTS-1+i)}) = y_B(z_{(NZBPTS-i)}), \quad i = 1,2,...,SYNTHP. \tag{3.11}$$

Figure 39 illustrates this modification.
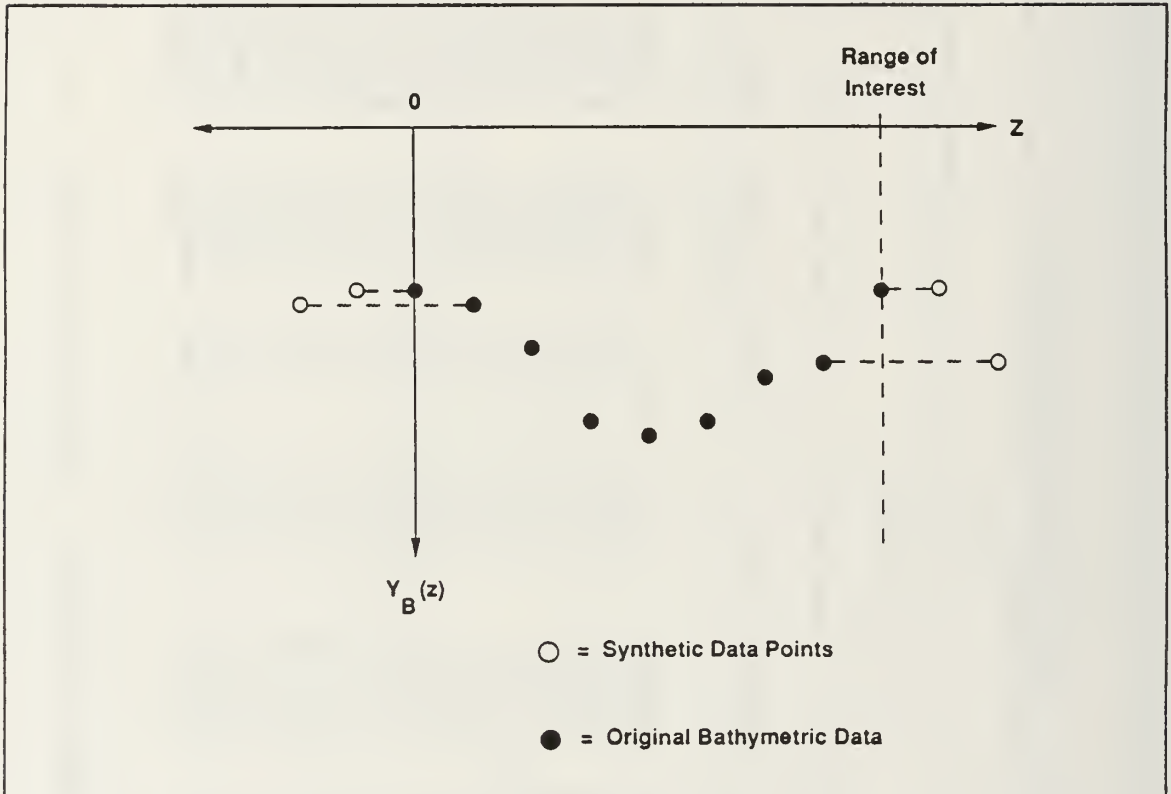
Figure 39.   Generation of Synthetic Data: Synthetic data is generated from a shifted mirror imaging of the original data.

Figures 40, 41 and 42 and Table 18 reflect only a marginal improvement in the modified Witch of Agnesi curve fit as a consequence of using the modified mirror imaging procedure. Additionally, for other exact mathematical models such as the one period cosine contour, this procedure proved detrimental, again because of curvature suppression.

An alternative means of eliminating function discontinuities created by mirror imaging was investigated. This problem was most pronounced when the slope between successive data points increased toward the end points of the contour. A new method
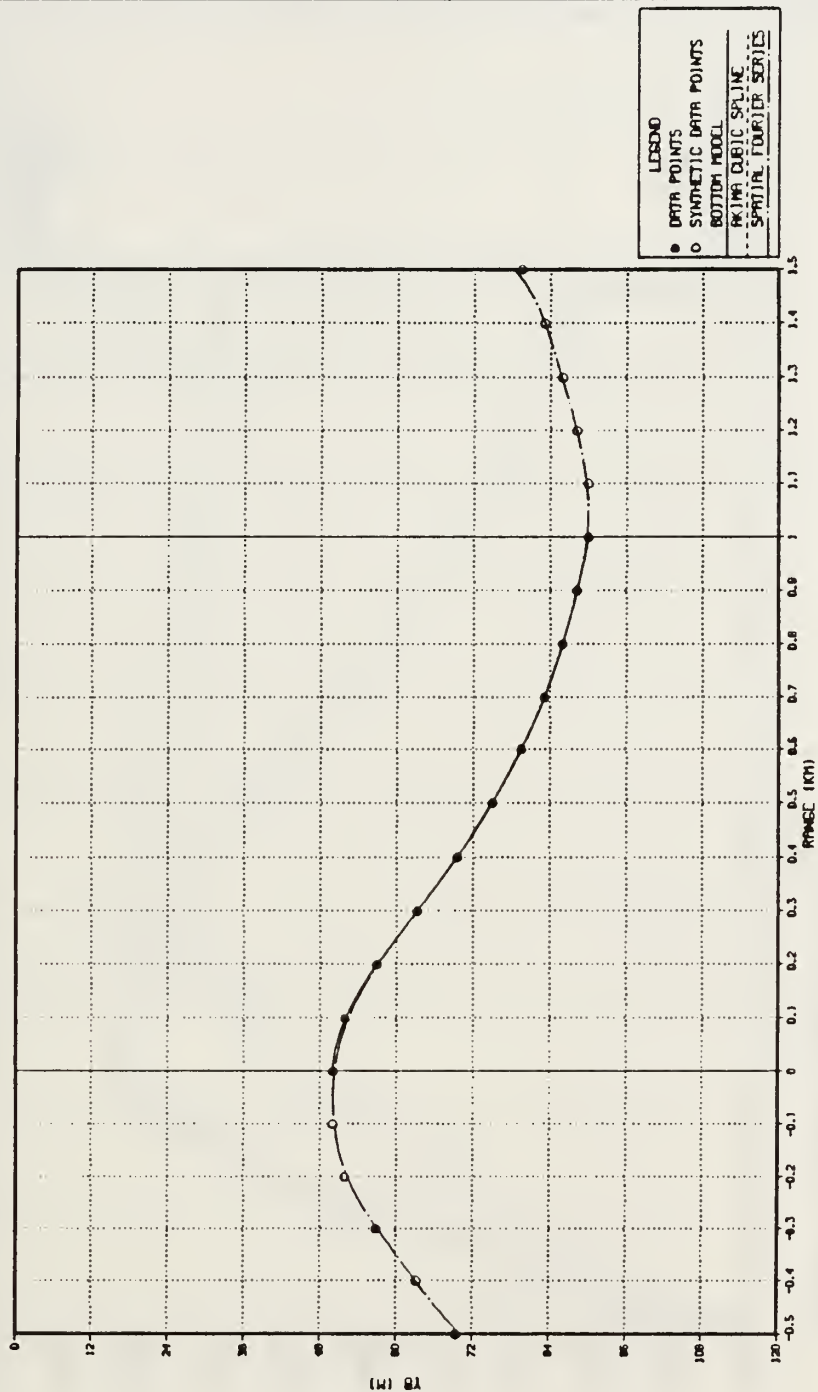
66

Figure 40.   Modified   Witch   of   Agnesi   Ocean   Bottom   Contour
Reconstruction: Fourier Series reconstruction with Lanczos smooth-
ing and shifted mirrored data.

67
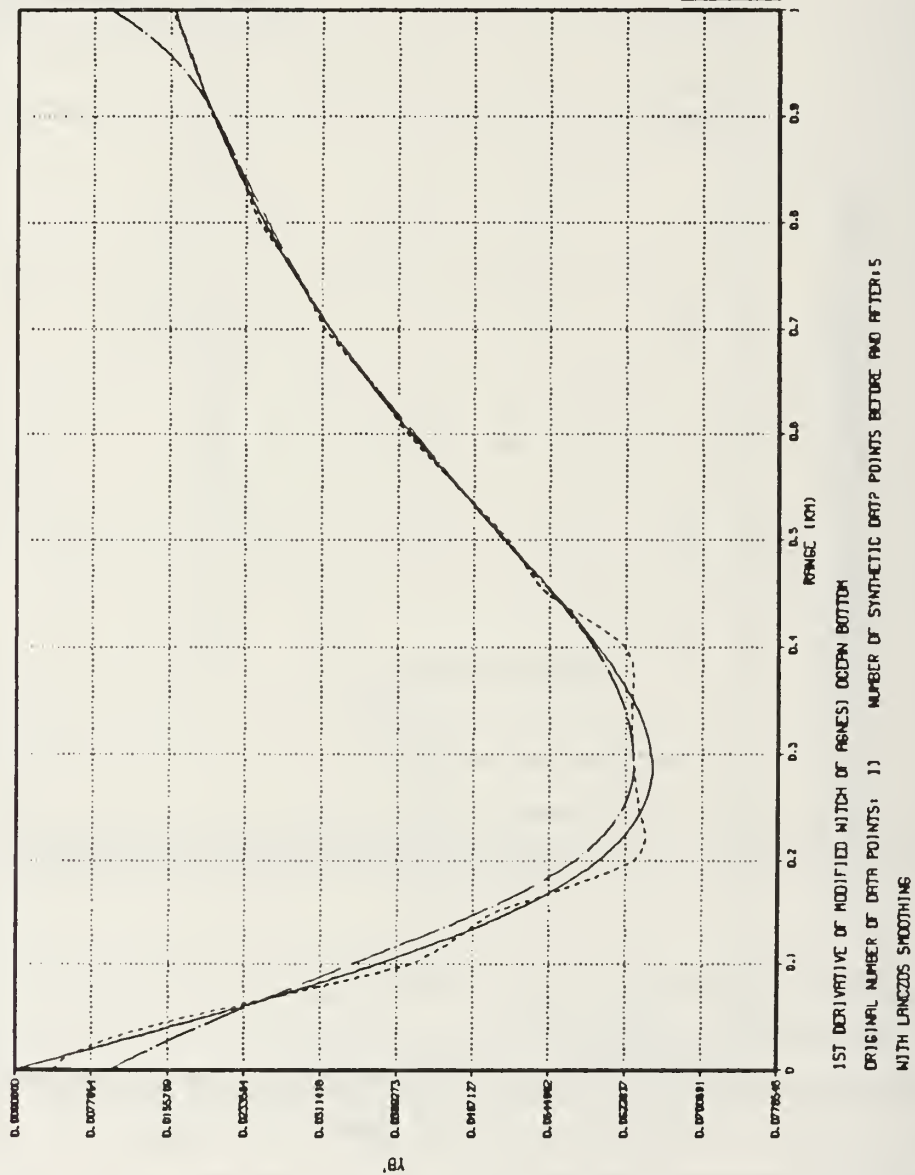
Figure 41.   Modified   Witch   Of   Agnesi   Ocean   Bottom   First-Order
Derivatives: Fourier Series reconstruction with Lanczos smoothing
and shifted mirrored data.

Figure 42.   Modified   Witch   of   Agnesi   Ocean   Bottom   Second-Order
Derivatives: Fourier Series reconstruction with Lanczos smoothing
and shifted mirrored data.

69

Table 18. FOURIER SERIES RESULTS : SHIFTED MIRROR IMAGED DATA.

WITCH OF AGNESI BOTTOM

TECHNIQUE: SPATIAL FOURIER SERIES FIT WITH LANCZOS SMOOTHING   NO. OF ORIGINAL DATA POINTS: 11

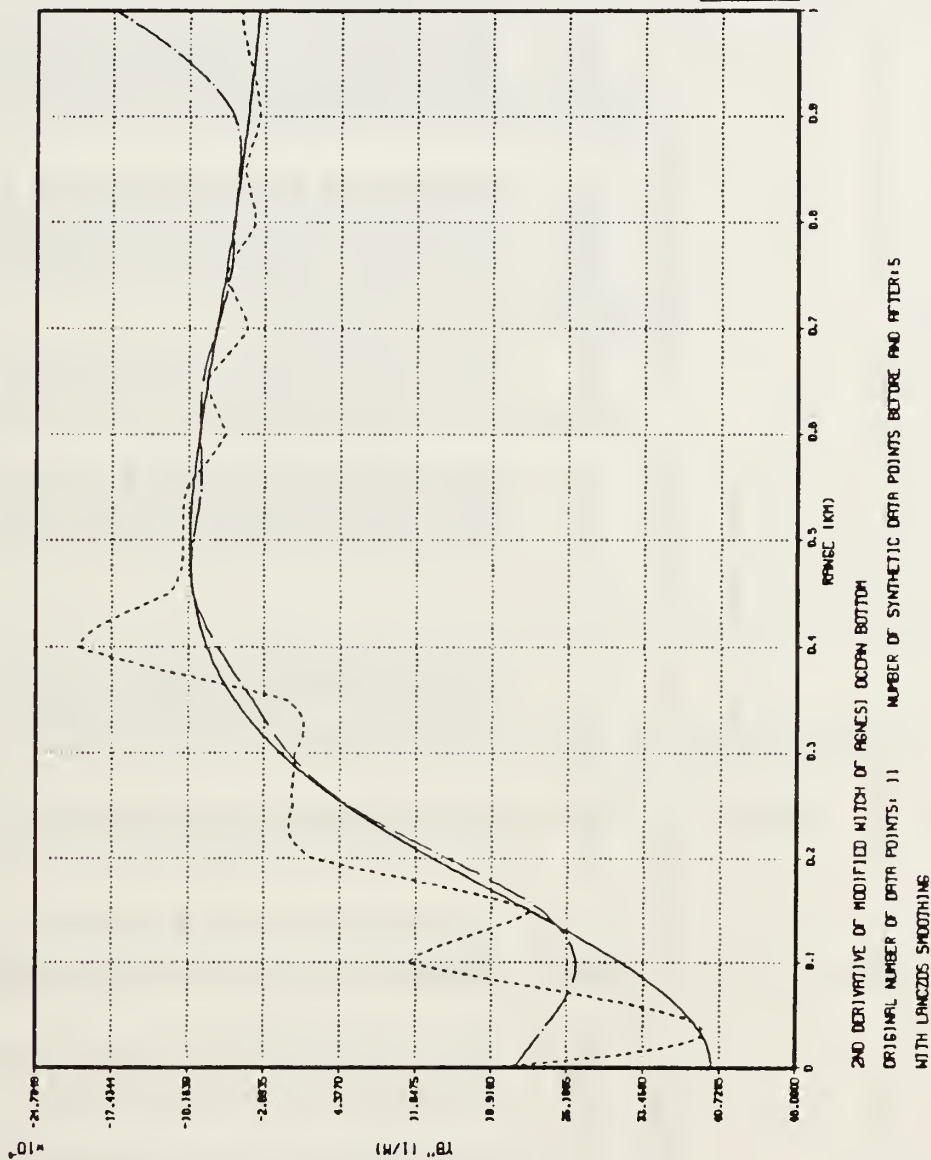| RANGE (KM)	YB(EXACT) (M)	YB(FIT) (M)	% ERROR	YBDOT(EXACT)	YBDOT(FIT)	% ERROR	YBDOT2(EXACT) (1/M)	YBDOT2(FIT) (1/M)	% ERROR
0.00	50.00	50.27	0.545	0.000E+00	0.964E-02	********	0.400E-03	0.212E-03	-46.919
0.05	50.50	51.04	1.070	0.196E-01	0.212E-01	7.986	0.377E-03	0.249E-03	-33.764
0.10	51.92	52.42	0.953	0.370E-01	0.343E-01	-7.189	0.313E-03	0.271E-03	-13.555
0.15	54.13	54.47	0.622	0.505E-01	0.473E-01	-6.360	0.225E-03	0.237E-03	5.101
0.20	56.90	57.09	0.345	0.595E-01	0.571E-01	-4.032	0.133E-03	0.148E-03	10.818
0.25	60.00	60.09	0.147	0.640E-01	0.620E-01	-3.155	0.512E-04	0.534E-04	4.314
0.30	63.24	63.23	-0.015	0.649E-01	0.630E-01	-2.847	-0.127E-04	-0.499E-05	-60.773
0.35	66.44	66.36	-0.131	0.631E-01	0.619E-01	-1.861	-0.568E-04	-0.395E-04	-30.556
0.40	69.51	69.39	-0.180	0.595E-01	0.591E-01	-0.696	-0.834E-04	-0.731E-04	-12.396
0.45	72.38	72.24	-0.191	0.549E-01	0.547E-01	-0.370	-0.965E-04	-0.968E-04	0.384
0.50	75.00	74.85	-0.199	0.500E-01	0.498E-01	-0.396	-0.100E-03	-0.972E-04	-2.757
0.55	77.33	77.22	-0.197	0.450E-01	0.452E-01	0.244	-0.975E-04	-0.894E-04	-8.259
0.60	79.51	79.37	-0.174	0.403E-01	0.407E-01	0.960	-0.914E-04	-0.901E-04	-1.484
0.65	81.41	81.29	-0.149	0.359E-01	0.362E-01	0.687	-0.836E-04	-0.889E-04	6.305
0.70	83.11	82.99	-0.138	0.320E-01	0.320E-01	0.238	-0.753E-04	-0.753E-04	0.066
0.75	84.62	84.51	-0.127	0.284E-01	0.286E-01	0.821	-0.670E-04	-0.622E-04	-7.234
0.80	85.96	85.86	-0.106	0.252E-01	0.256E-01	1.569	-0.592E-04	-0.584E-04	-1.390
0.85	87.15	87.07	-0.083	0.225E-01	0.228E-01	1.534	-0.521E-04	-0.544E-04	4.285
0.90	88.21	88.15	-0.068	0.200E-01	0.201E-01	0.345	-0.458E-04	-0.585E-04	27.756
0.95	89.15	89.07	-0.098	0.179E-01	0.163E-01	-8.926	-0.401E-04	-0.102E-03	153.830
1.00	90.00	89.72	-0.307	0.160E-01	0.940E-02	-41.239	-0.352E-04	-0.173E-03	391.454

70

for creating synthetic data was therefore developed to take advantage of this change in contour slope. Let

$$m_{10} = \frac{y_B(z_1) - y_B(z_0)}{\Delta z} \quad , \tag{3.12}$$

$$m_{21} = \frac{y_B(z_2) - y_B(z_1)}{\Delta z} \quad , \tag{3.13}$$

$$m_{E1} = \frac{y_B(z_{(NZBPTS-1)}) - y_B(z_{(NZBPTS-2)})}{\Delta z} \quad , \tag{3.14}$$

and

$$m_{E2} = \frac{y_B(z_{(NZBPTS-2)}) - y_B(z_{(NZBPTS-3)})}{\Delta z} \tag{3.15}$$

where again Δz is the distance between each data point. If

$$|m_{21}| < |m_{10}| \tag{3.16}$$

and, or

$$|m_{E2}| < |m_{E1}| \ , \tag{3.17}$$

then synthetic data is generated at the appropriate end of the profile as follows:

$$y_B(z_{-i}) = y_B(z_0) + (i\Delta z(m_{10} - i\Delta m)) \ , \quad i = 1,2,...,SYNTHP \tag{3.18}$$

and, or

$$y_B(z_{(NZBPTS-1+i)}) = y_B(z_{(NZBPTS-1)}) + (i\Delta z(m_{E1} - i\Delta m_E)) \ , \ i = 1,2,...,SYNTHP \tag{3.19}$$

where

$$\Delta m = m_{10} - m_{21} \tag{3.20}$$

and

$$\Delta m_E = m_{E1} - m_{E2}. \tag{3.21}$$

71

A comparison of the end points in Figures 35 and 43 demonstrate the utility of this new method in preserving curvature and eliminating apparent function discontinuities.
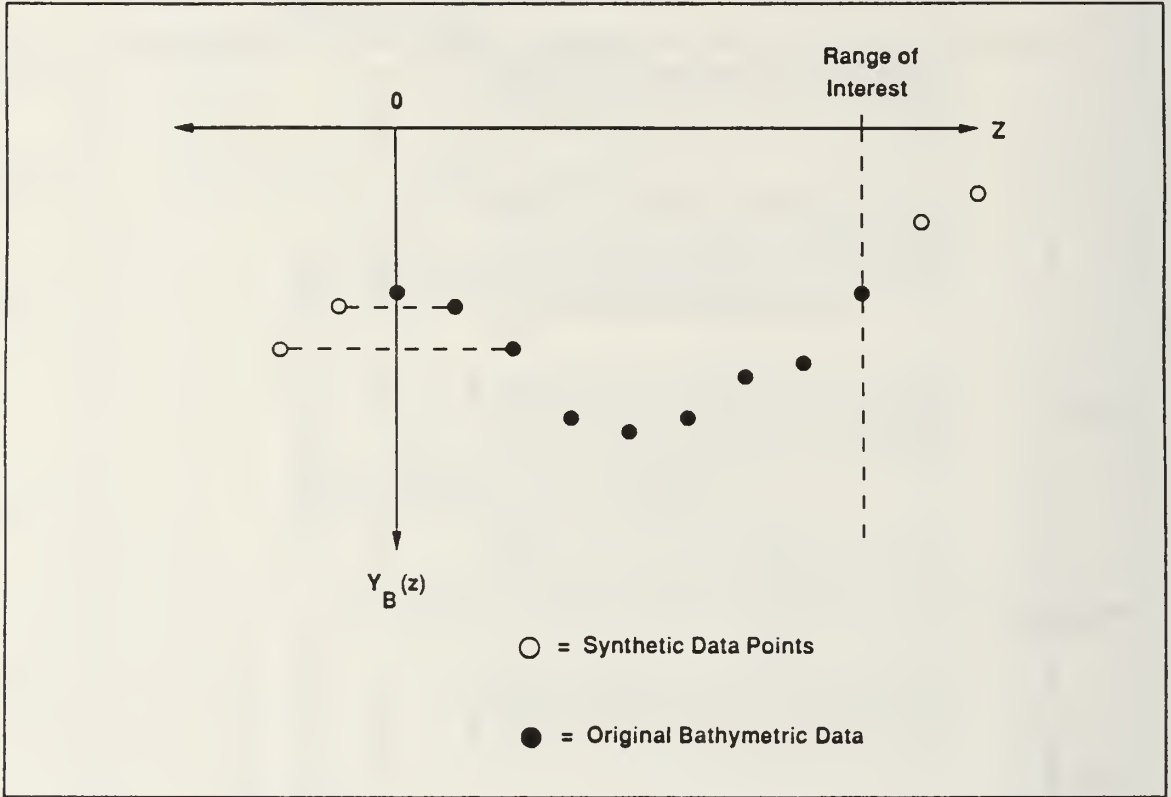
Figure 43.   Generation of Synthetic Data: Synthetic data is generated by reversing the rate of change of slope of the original boundary data.

Enhancing the original bathymetric data with synthetic points proved beneficial to the SFS modeling of the bottom contour, but no one procedure for creating this artificial data dominated. Each of the methods investigated showed merit under specific circumstances. Consequently, the SFS computer algorithm was modified to incorporate the three methods outlined previously. If

$$|\Delta m| = |m_{10} - m_{21}| < \varepsilon \tag{3.22}$$

and, or

$$|\Delta m_E| = |m_{E1} - m_{E2}| < \varepsilon , \tag{3.23}$$

where ε is some arbitrarily small number, then the synthetic data was constructed by linear extrapolation as given in Equations (3.5) and (3.7). However, if

72

$$|m_{10}| < |m_{21}| \qquad\qquad (3.24)$$

and, or

$$|m_{E1}| < |m_{E2}| \,, \qquad\qquad (3.25)$$

then mirror imaging as given by Equations (3.8) and (3.9) is used to generate the data. Finally, if the conditions given by Equations (3.16) or (3.17) hold then the method employing the reversal of the rate of change of slope is activated to simulate data at the appropriate end point.

C. SPATIAL FOURIER SERIES ANALYSIS OF THE AKIMA CUBIC SPLINE REPRESENTATION OF THE OCEAN BOTTOM CONTOUR.

Results from the SFS technique contained significant errors in the reconstruction of both the original contour and first and second-order derivatives despite Lanczos smoothing and the optimization of methods for generating synthetic data. However, for the more complex ocean bottom models such as the modified Witch of Agnesi and one period cosine functions, SFS methods yielded the more accurate derivative values.

The ACS method provided precise reproductions of the original test functions, but the subsequent first and second-order derivative values were reliable only for the flat, constant slope and parabolic ocean bottoms. Efforts were therefore made to incorporate the desired aspects of both methods.

The ACS representation of the ocean bottom model was discretized at ten times the sampling frequency used to generate the original bathymetric data. Synthetic data was then constructed as described in Section B of Chapter 3, with the exception that Δz was now based upon this new sampling frequency. For example, where previously 5 synthetic data points covered a 500 m range, now 50 synthetic points describe this same range. A SFS representation of the entire contour was then obtained. This approach was applied to each of the seven exact mathematical functions.

Figures 44, 45 and 46 and Table 19 provide results for the SFS representation of the flat ocean bottom generated by the ACS method. The original contour is replicated precisely and the small errors observed in both the first and second-order derivatives approach the limits of machine precision. However, while these errors are very small, they are actually larger than those generated by the fundamental SFS reconstruction of the flat bottom without Lanczos smoothing or synthetic data. Table 2 refers.

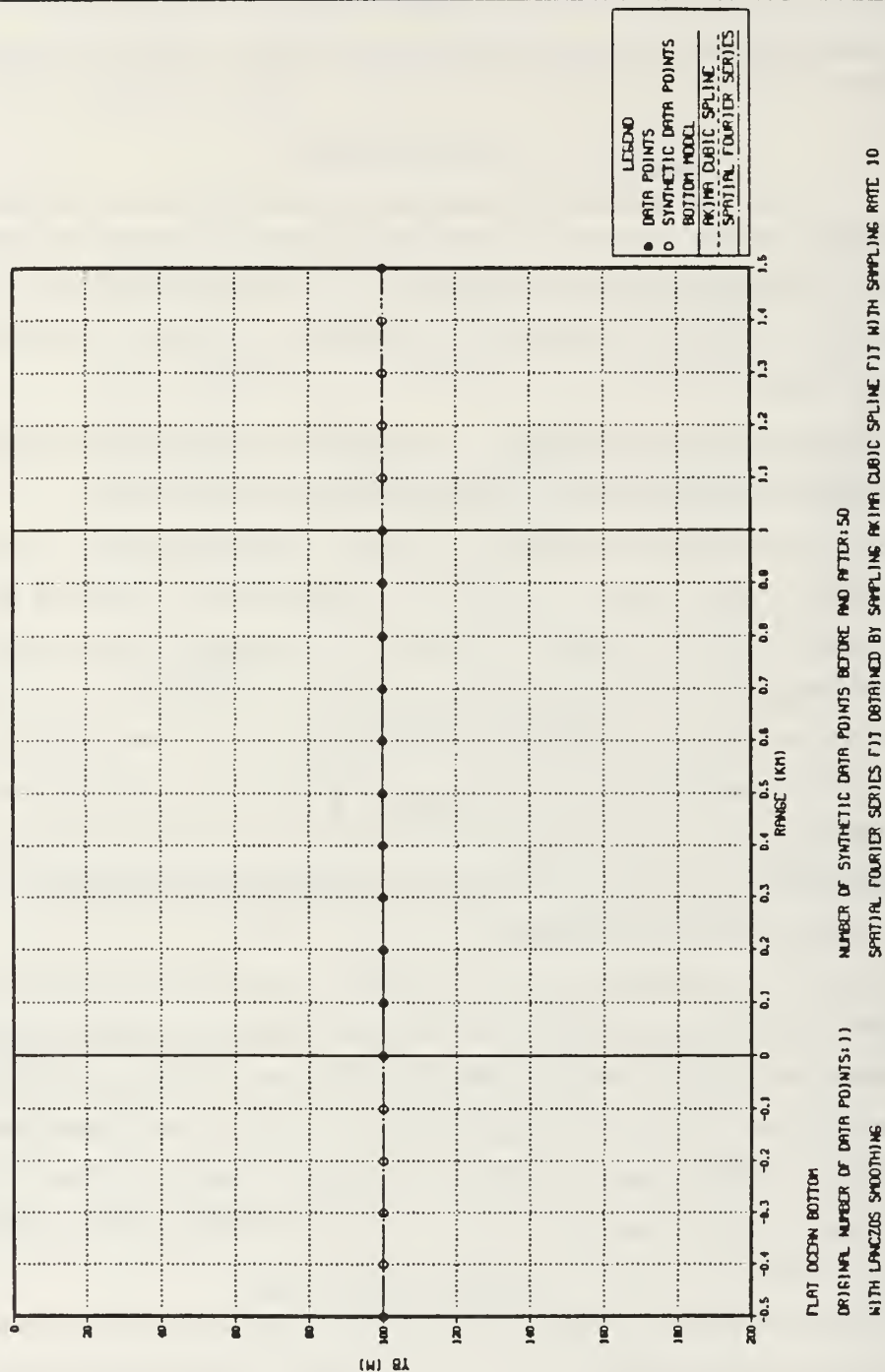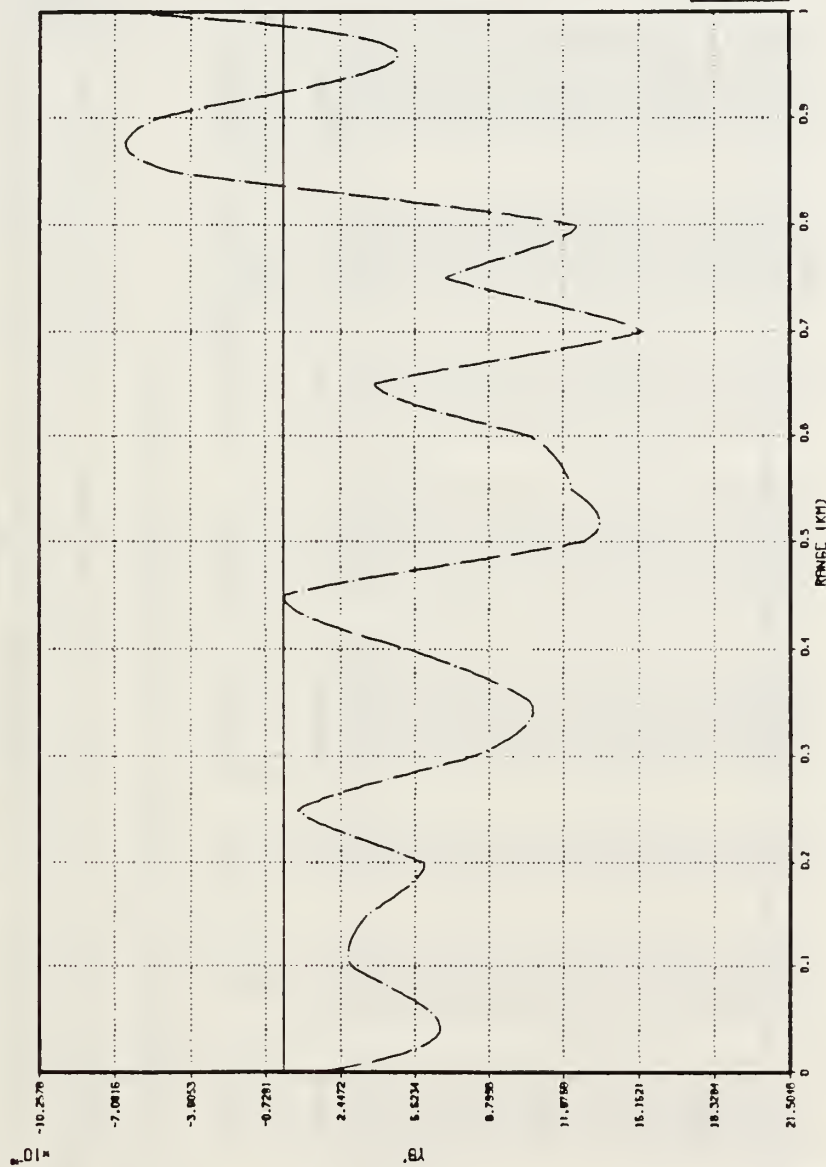Figure 44. Flat Ocean Bottom Contour Reconstruction: Spatial Fourier Series representation of the Akima Cubic Spline flat bottom model.

74

Figure 45. Flat Ocean Bottom First-Order Derivatives: Spatial Fourier Series representation of the Akima Cubic Spline flat bottom model.
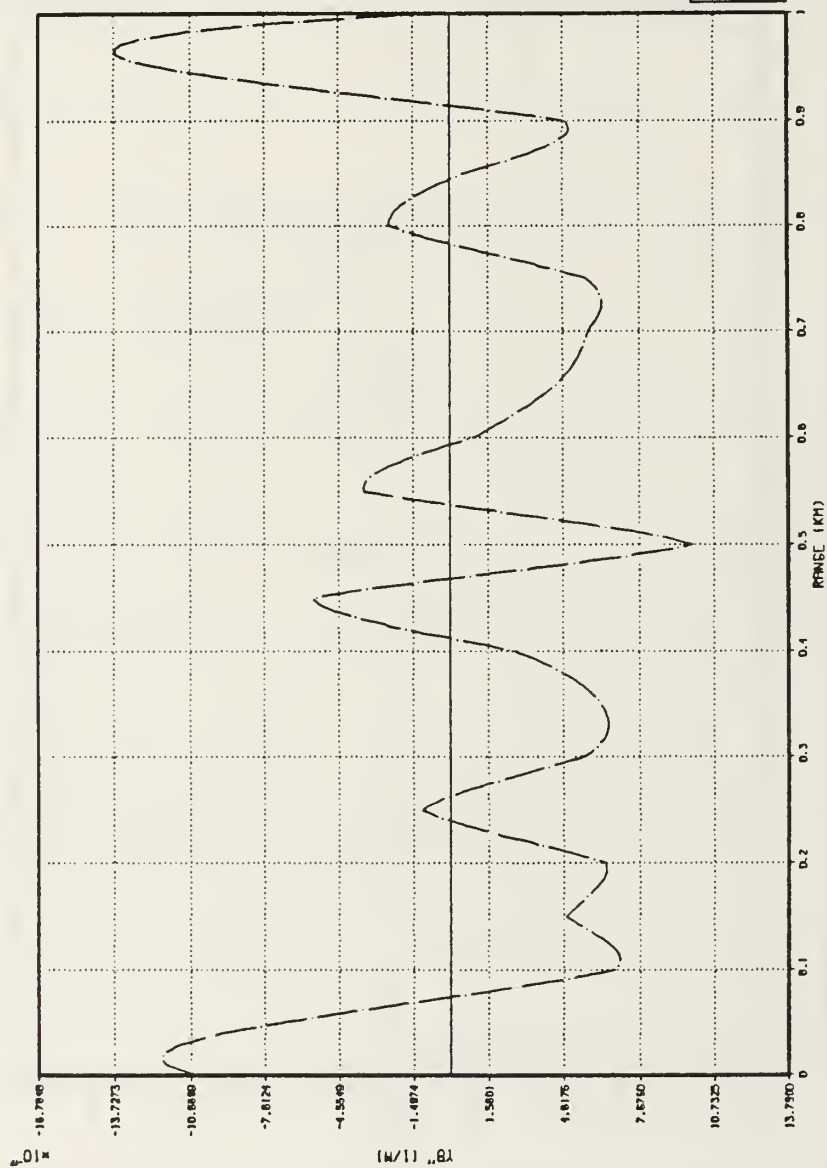
Figure 46. Flat Ocean Bottom Second-Order Derivatives: Spatial Fourier Series representation of the Akima Cubic Spline flat bottom model.

Table 19. FOURIER SERIES RESULTS : ACS FLAT OCEAN BOTTOM

FLAT BOTTOM

TECHNIQUE: SPATIAL FOURIER SERIES FIT WITH LANCZOS SMOOTHING   NO. OF ORIGINAL DATA POINTS: 11

SPATIAL FOURIER SERIES FIT OBTAINED BY SAMPLING AKIMA CUBIC SPLINE FIT

RANGE (KM)	YB(EXACT) (M)	YB(FIT) (M)	% ERROR	YBDOT(EXACT)	YBDOT(FIT)	% ERROR	YBDOT2(EXACT) (1/M)	YBDOT2(FIT) (1/M)	% ERROR
0.00	100.00	100.00	0.000	0.000E+00	0.162E-15	0.000	0.000E+00	-0.103E-15	0.000
0.05	100.00	100.00	0.000	0.000E+00	0.658E-15	0.000	0.000E+00	-0.690E-16	0.000
0.10	100.00	100.00	0.000	0.000E+00	0.289E-15	0.000	0.000E+00	0.662E-16	0.000
0.15	100.00	100.00	0.000	0.000E+00	0.364E-15	0.000	0.000E+00	0.471E-16	0.000
0.20	100.00	100.00	0.000	0.000E+00	0.603E-15	0.000	0.000E+00	0.628E-16	0.000
0.25	100.00	100.00	0.000	0.000E+00	0.533E-16	0.000	0.000E+00	-0.115E-16	0.000
0.30	100.00	100.00	0.000	0.000E+00	0.813E-15	0.000	0.000E+00	0.543E-16	0.000
0.35	100.00	100.00	0.000	0.000E+00	0.106E-14	0.000	0.000E+00	0.608E-16	0.000
0.40	100.00	100.00	0.000	0.000E+00	0.536E-15	0.000	0.000E+00	0.265E-16	0.000
0.45	100.00	100.00	0.000	0.000E+00	0.738E-17	0.000	0.000E+00	-0.563E-16	0.000
0.50	100.00	100.00	0.000	0.000E+00	0.128E-14	0.000	0.000E+00	0.985E-16	0.000
0.55	100.00	100.00	0.000	0.000E+00	0.123E-14	0.000	0.000E+00	-0.349E-16	0.000
0.60	100.00	100.00	0.000	0.000E+00	0.106E-14	0.000	0.000E+00	0.965E-17	0.000
0.65	100.00	100.00	0.000	0.000E+00	0.391E-15	0.000	0.000E+00	0.436E-16	0.000
0.70	100.00	100.00	0.000	0.000E+00	0.154E-14	0.000	0.000E+00	0.561E-16	0.000
0.75	100.00	100.00	0.000	0.000E+00	0.694E-15	0.000	0.000E+00	0.555E-16	0.000
0.80	100.00	100.00	0.000	0.000E+00	0.125E-14	0.000	0.000E+00	-0.243E-16	0.000
0.85	100.00	100.00	0.000	0.000E+00	-0.472E-15	0.000	0.000E+00	0.617E-17	0.000
0.90	100.00	100.00	0.000	0.000E+00	-0.517E-15	0.000	0.000E+00	0.467E-16	0.000
0.95	100.00	100.00	0.000	0.000E+00	0.454E-15	0.000	0.000E+00	-0.120E-15	0.000
1.00	100.00	100.00	0.000	0.000E+00	-0.732E-15	0.000	0.000E+00	-0.370E-17	0.000

Figures 47, 48 and 49 and Table 20 give the results for the SFS representation of the constant down-slope ocean bottom generated by the ACS technique. The percentage errors recorded for both the bottom contour and the first and second-order derivatives are two orders of magnitude lower than the initial results given at Table 4. This reduction, although significant, is not sufficient to eliminate residual errors likely to adversely impact on ray acoustic computations.

Figures 50, 51 and 52 and Table 21 provide results for the SFS representation of the constant up-slope ocean bottom model. The observations made for this case are identical to those recorded for the constant down-slope bottom.

Figures 53, 54 and 55 and Table 22 give results for the SFS representation of the one period cosine ocean bottom. The errors for both the contour reconstruction and its first and second-order derivatives were larger than those recorded in the earliest test provided in Table 8. Furthermore, the sampling of the ACS model for this bottom shape not only failed to assist SFS in more accurately reproducing the contour, but caused it to replicate anomolies in the ACS reconstruction of the first and second-order derivatives.

Figures 56, 57 and 58 and Table 23 provide results for the SFS representation of the modified Witch of Agnesi ocean bottom. This contour was used to demonstrate the development of successive numerical enhancements to the fundamental SFS technique, and therefore, gives the best opportunity for a complete comparative analysis. Significant improvement was observed in the modeling of this function with SFS methods employing Lanczos smoothing and synthetic data created by mirror imaging. A comparison of the results in Tables 17 and 23 show that further reductions in error were achieved by the SFS approach to modeling the ACS representation of the modified Witch of Agnesi bottom. However the recorded improvements in the first and second-order derivatives remain insufficient for the purposes of existing ray acoustics algorithms.

Figures 59, 60 and 61 and Table 24 give results for the SFS representation of the half catenary ocean bottom. Significant reductions in the percentage errors of the contour were achieved. For the first and second-order derivatives reductions in percentage error of three orders of magnitude were common. However, the residual errors remained sizeable and prohibited the use of these results in further computations.

Figures 62, 63 and 64 and Table 25 provide results for the SFS representation of the parabolic ocean bottom. The method of using the ACS model of the test function as input to the SFS procedure again proved beneficial with significant reductions in the magnitude of the percentage errors being observed for the contour. Reproductions of the
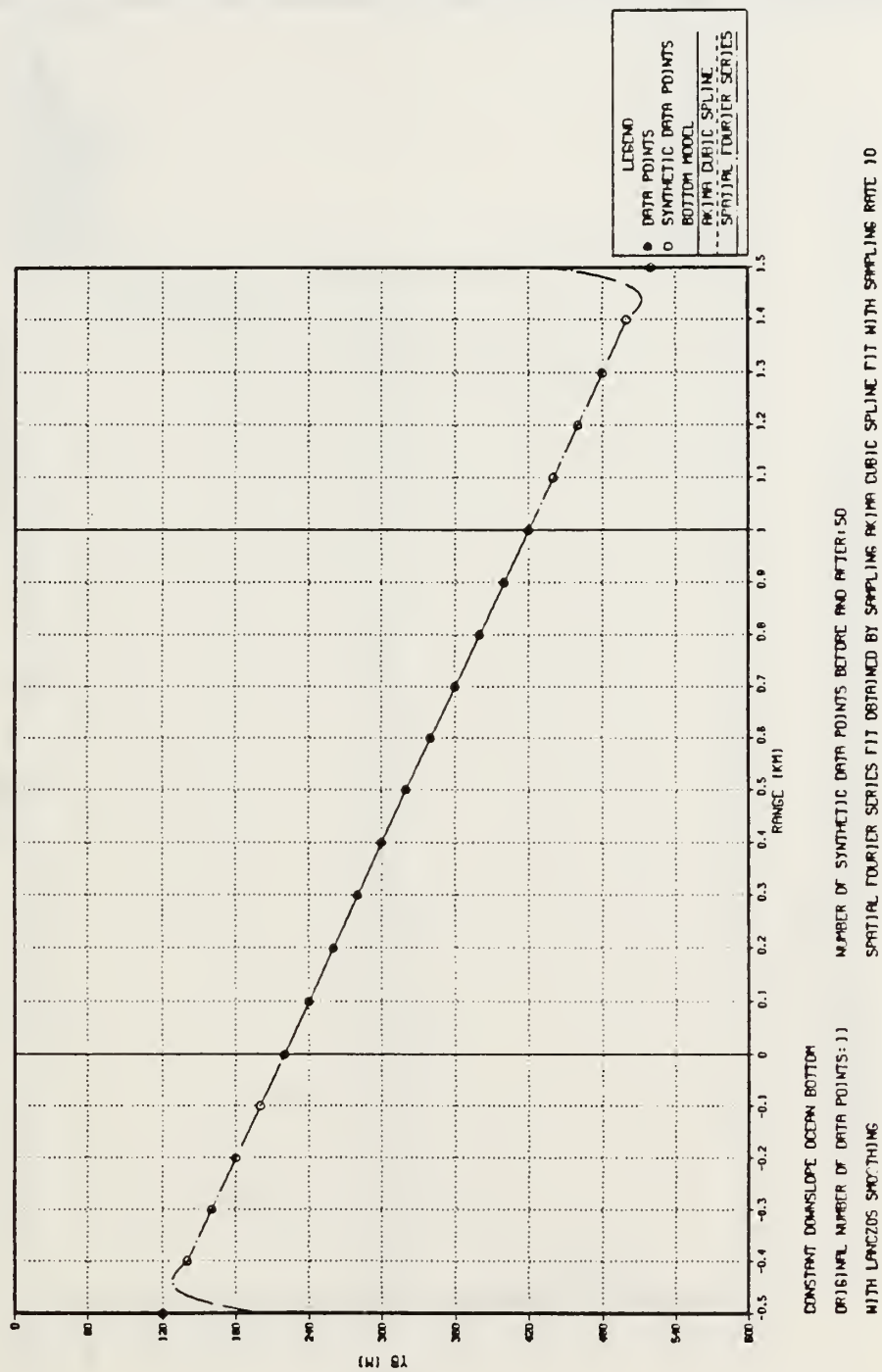
Figure 47. Down-Slope Ocean Bottom Contour Reconstruction: Spatial Fourier Series reconstruction of the Akima Cubic Spline down-slope bottom model.

79
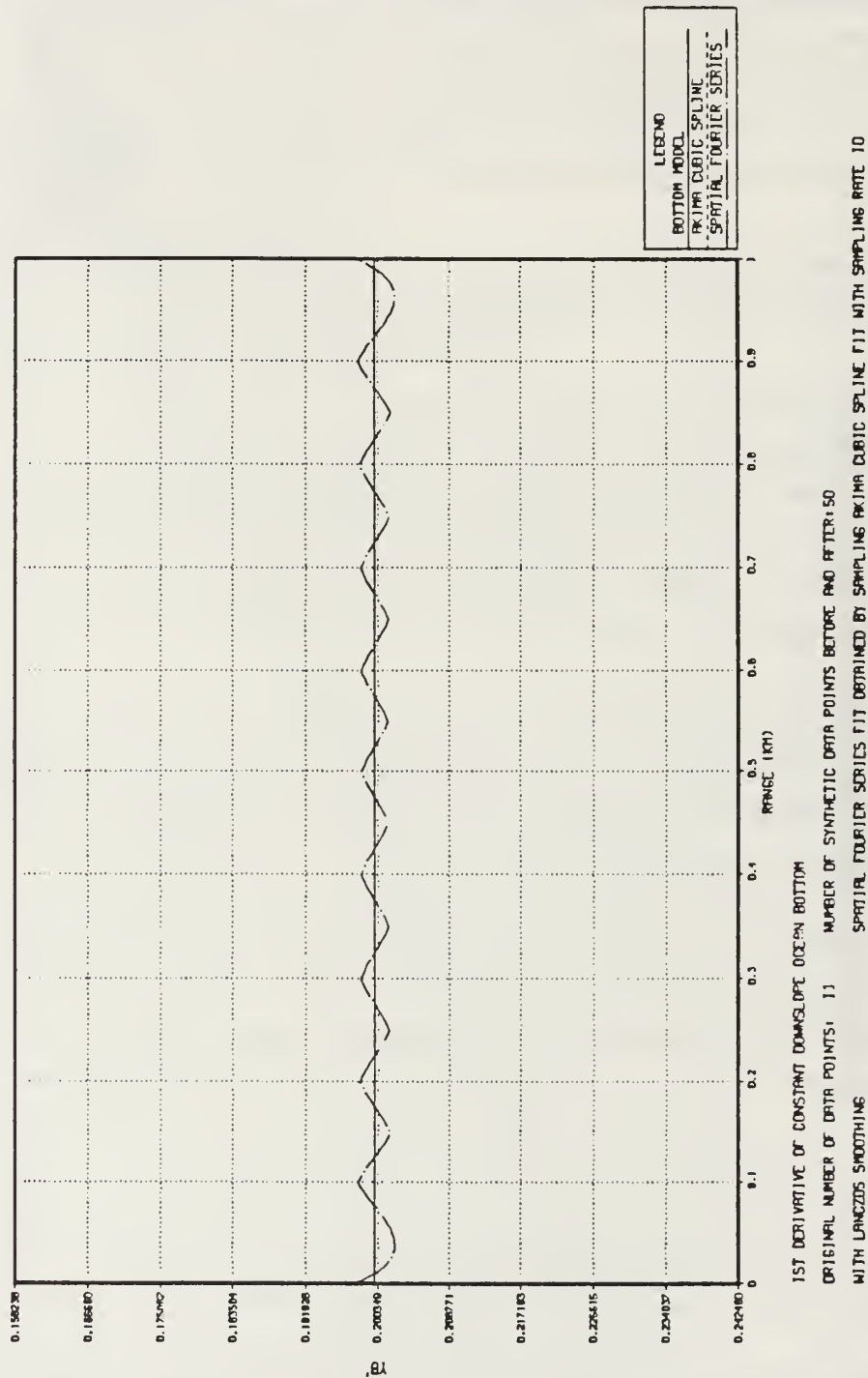
Figure 48.   Down-Slope Ocean Bottom First-Order Derivatives: Spatial Fourier
Series representation of the Akima Cubic Spline down-slope bottom
model.
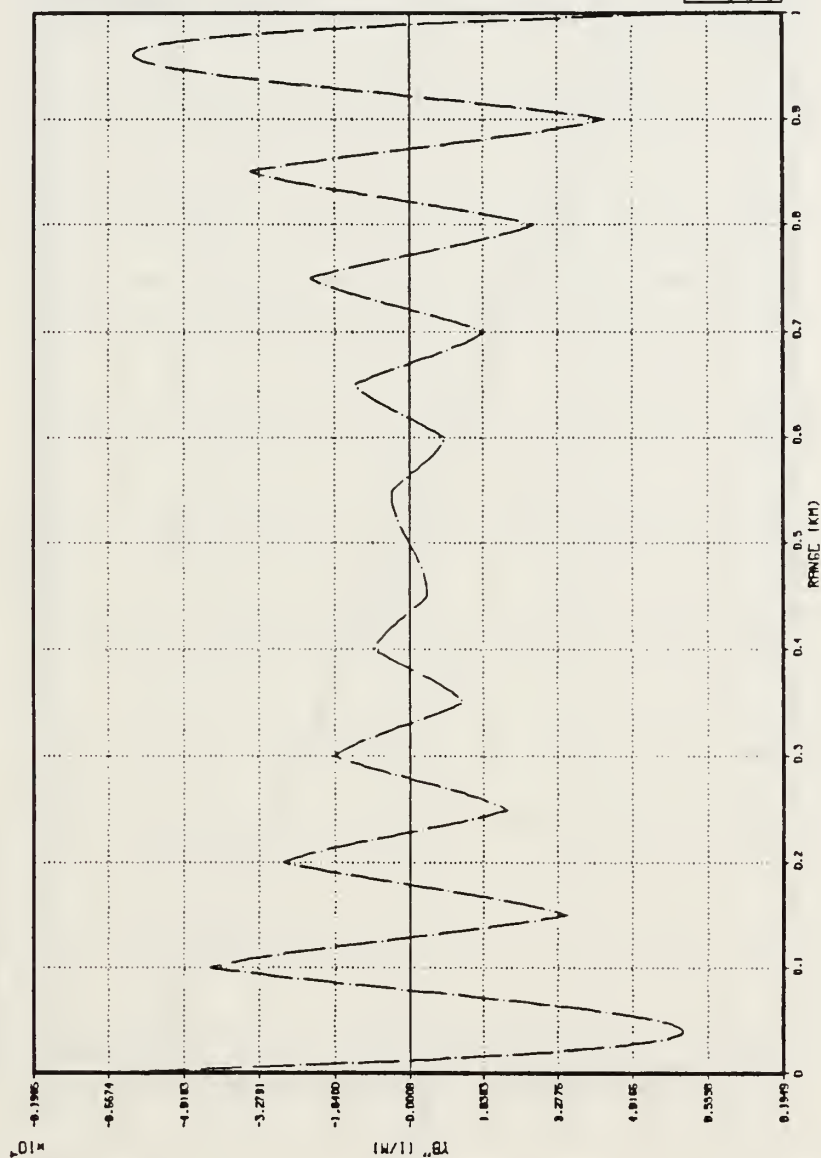
Figure 49. Down-Slope Ocean Bottom Second-Order Derivatives: Spatial Fourier Series representation of the Akima Cubic Spline down-slope bottom model.

81
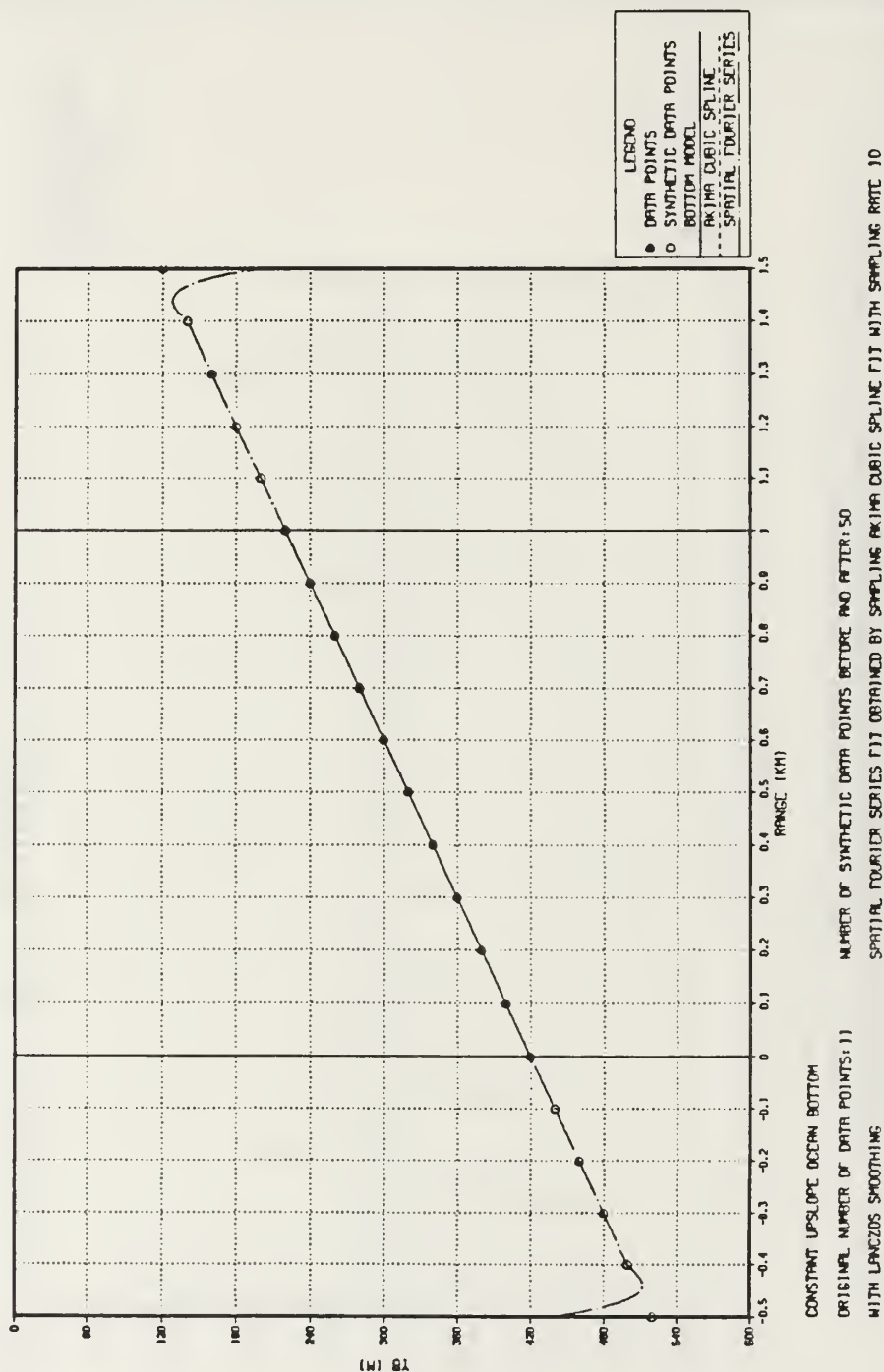
Figure 50.   Up-Slope Ocean Bottom Contour Reconstruction: Spatial Fourier Series representation of the Akima Cubic Spline up-slope bottom model.

82
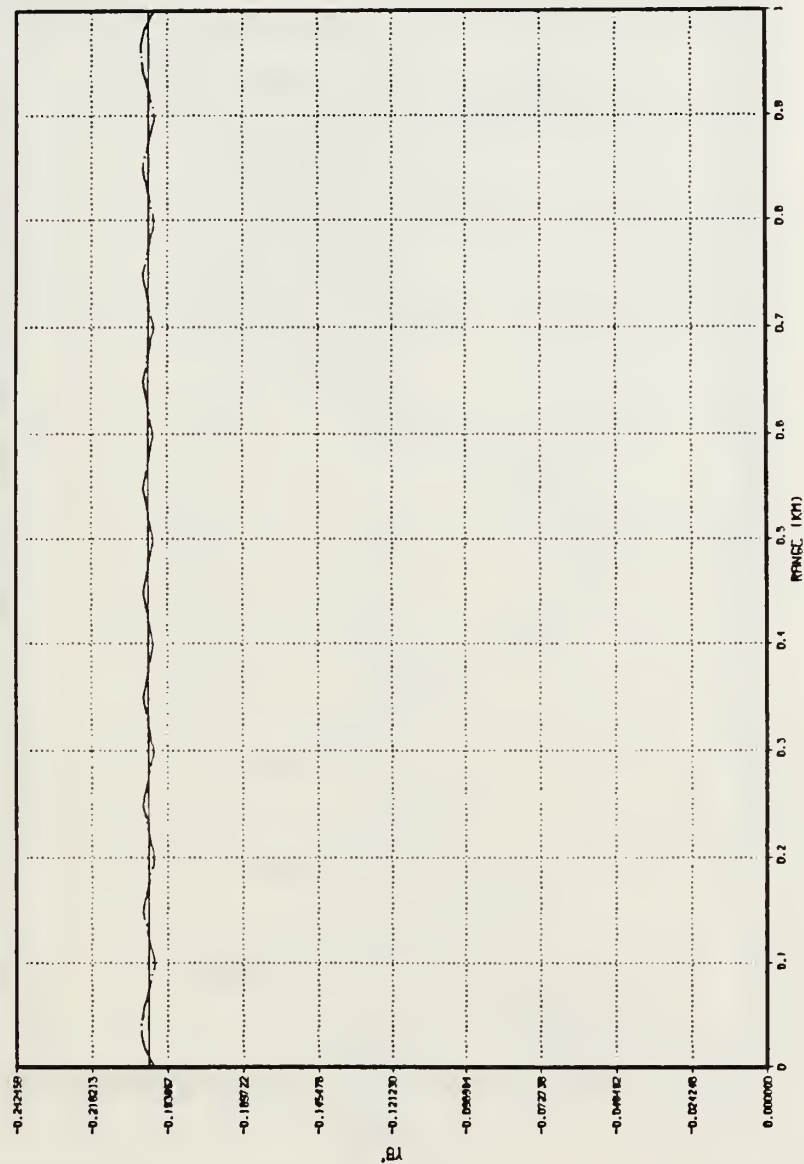
Figure 51. Up-Slope Ocean Bottom First-Order Derivatives: Spatial Fourier Series representation of the Akima Cubic Spline up-slope bottom model.

83
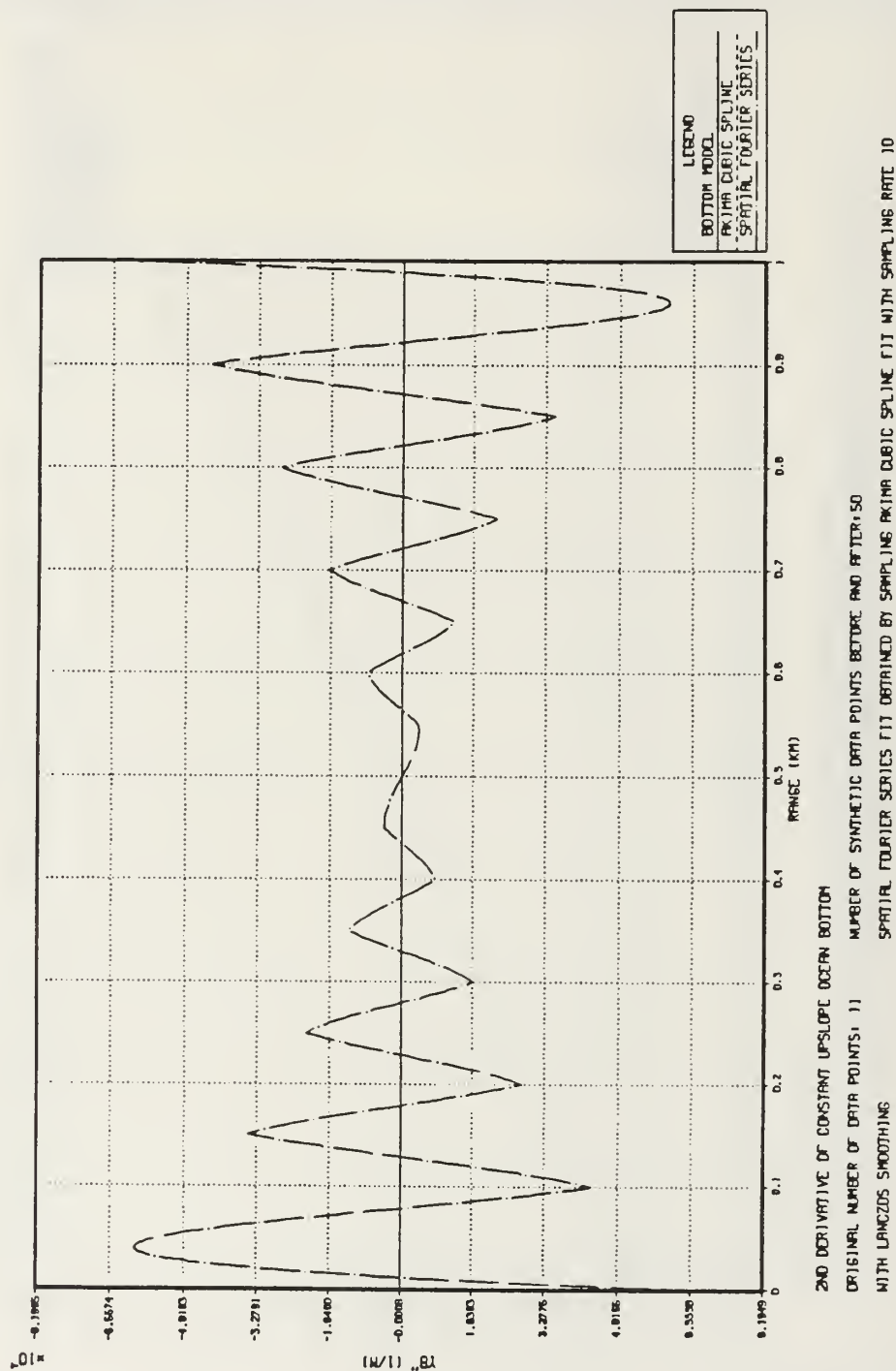
Figure 52. Up-Slope Ocean Bottom Second-Order Derivatives: Spatial Fourier Series representation of the Akima Cubic Spline up-slope bottom model.

84
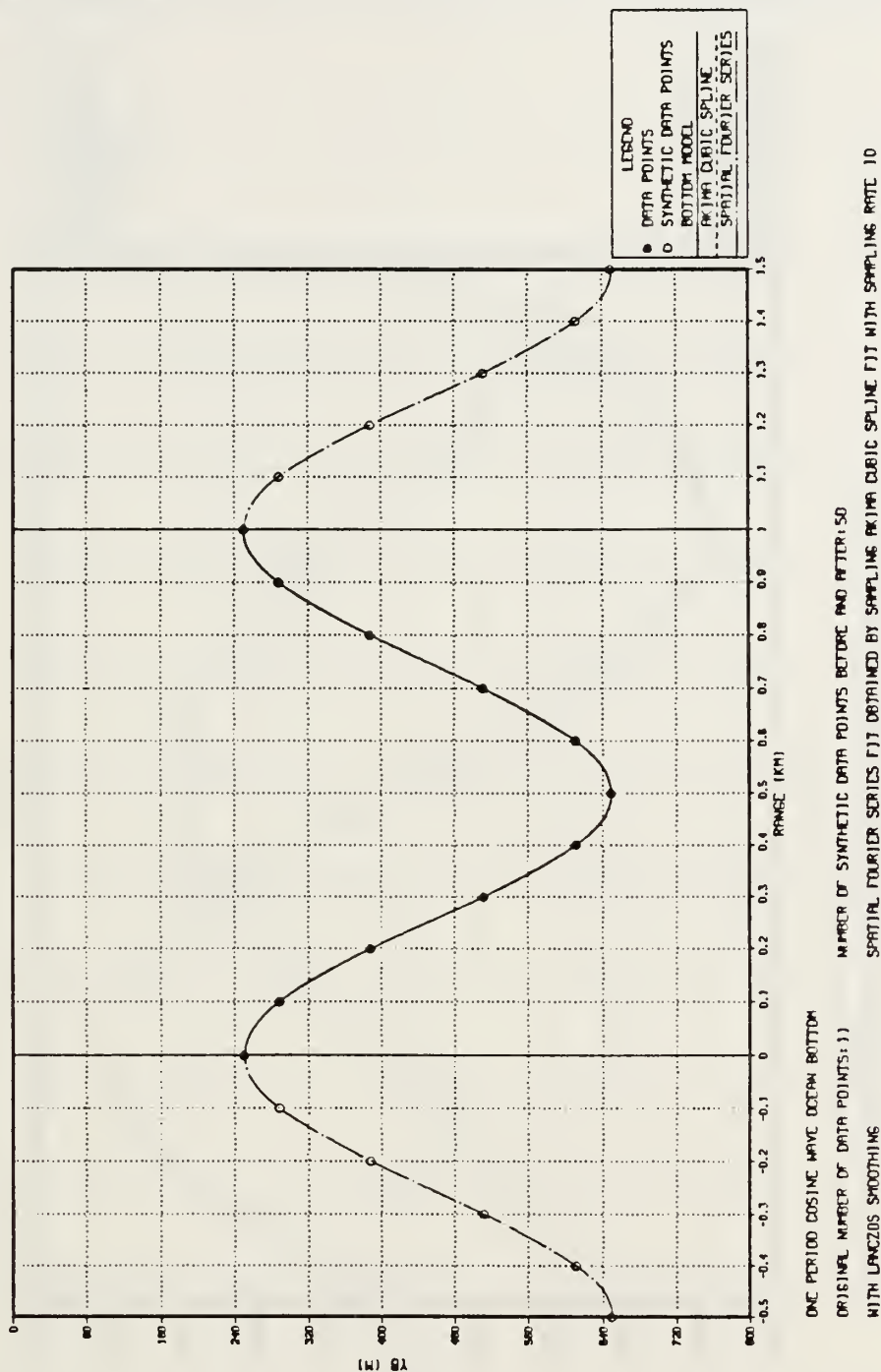
Figure 53.   One Period Cosine Ocean Bottom Contour Reconstruction: Spatial
Fourier Series representation of the Akima Cubic Spline cosine bottom
model.
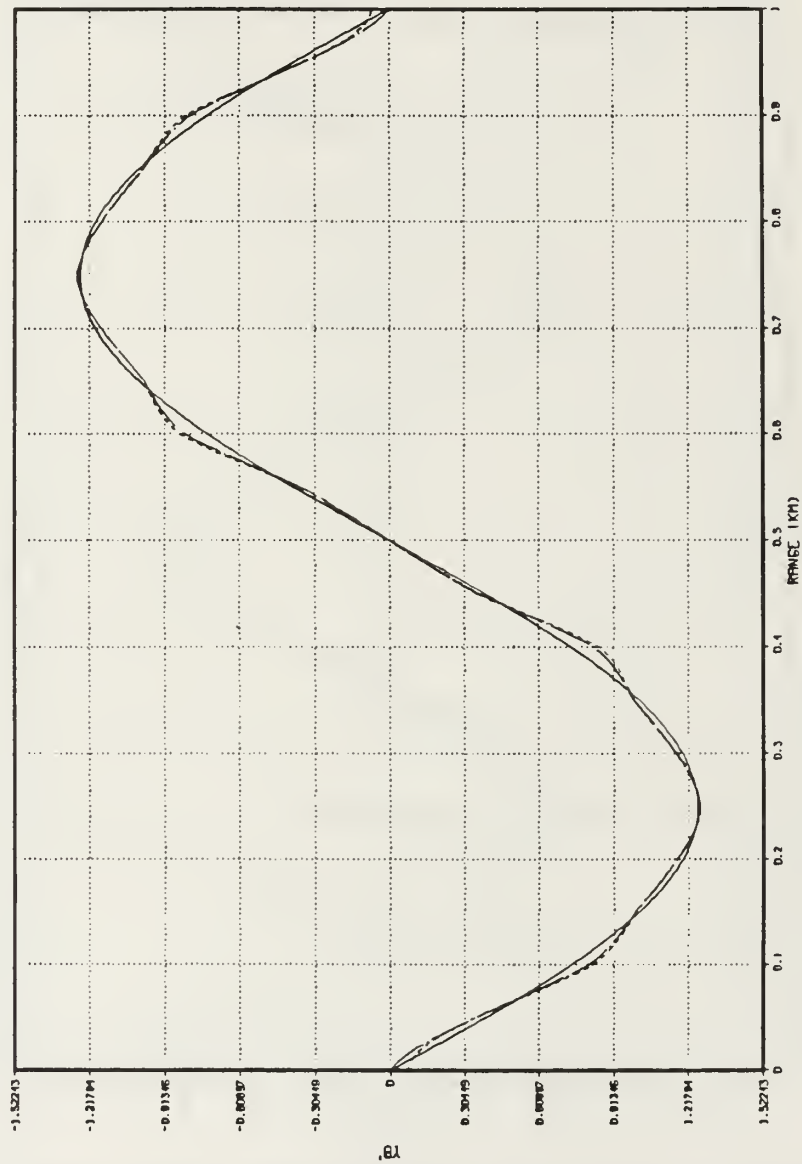
Figure 54. One Period Cosine Ocean Bottom First-Order Derivatives: Spatial Fourier Series representation of the Akima Cubic Spline cosine bottom model.

86
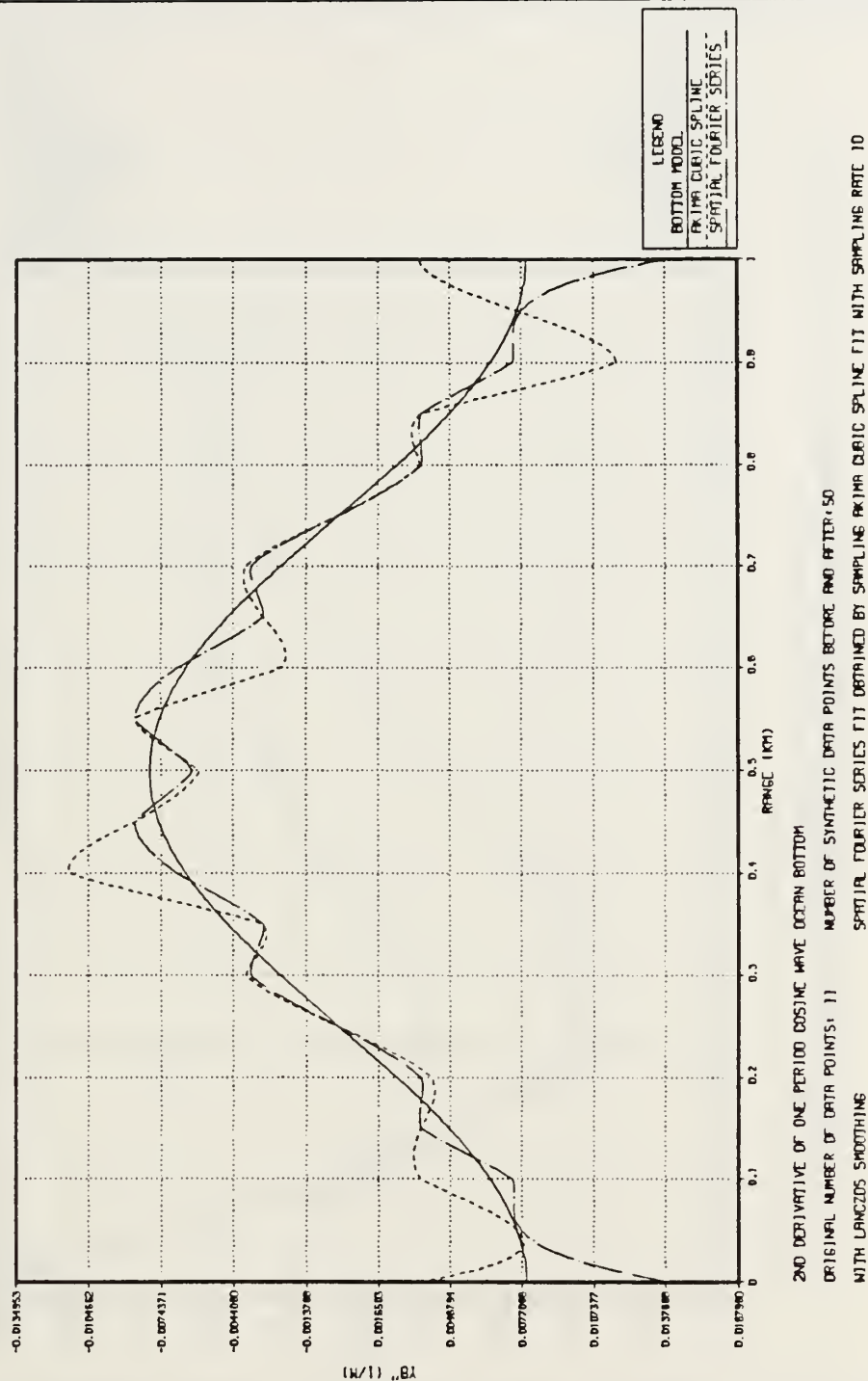
Figure 55. One Period Cosine Ocean Bottom Second-Order Derivatives: Spatial Fourier Series representation of the Akima Cubic Spline cosine bottom model.

87
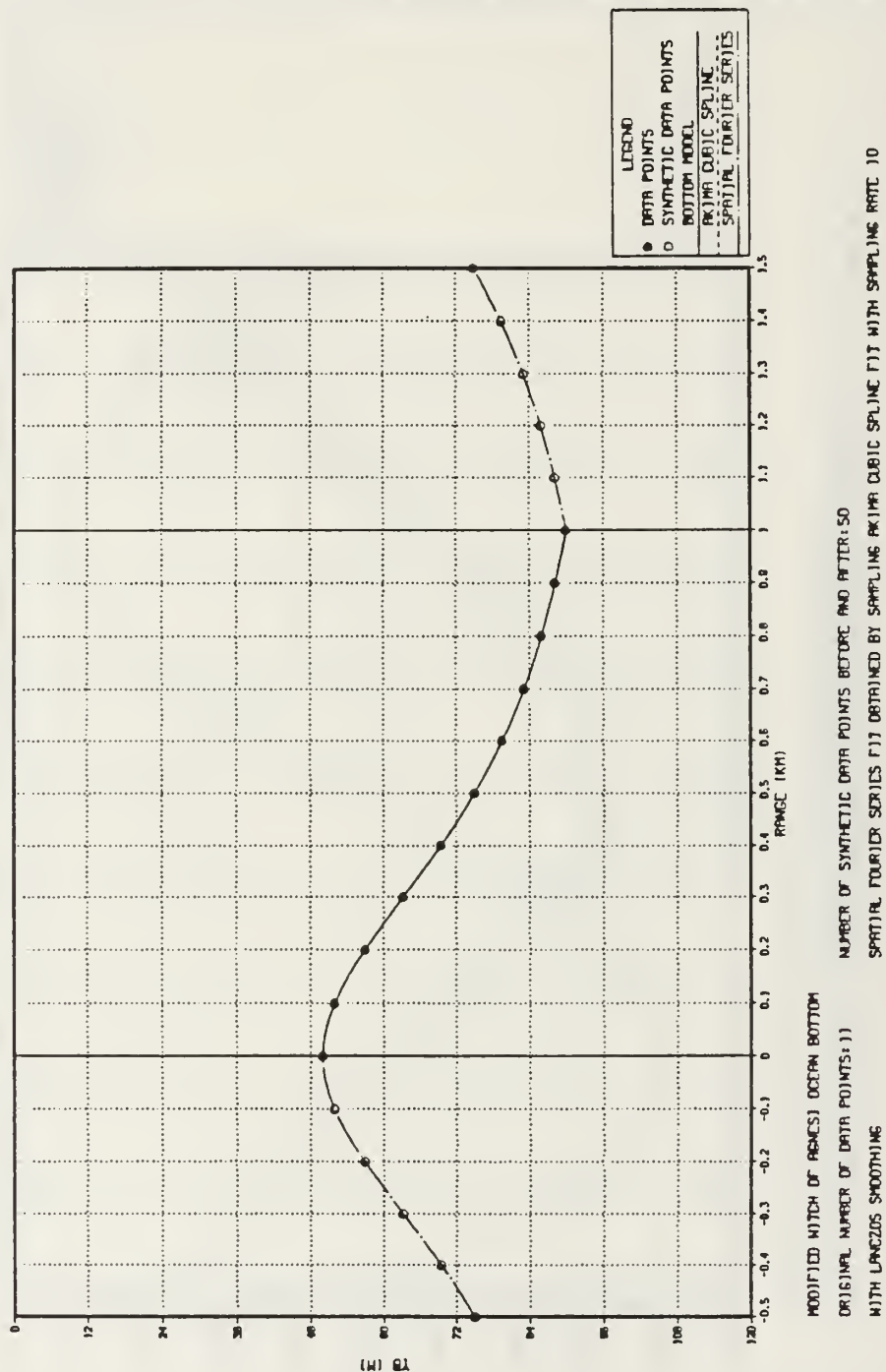
Figure 56. Modified Witch Of Agnesi Ocean Bottom Contour Reconstruction: Spatial Fourier Series representation of the Akima Cubic Spline Witch of Agnesi bottom model.
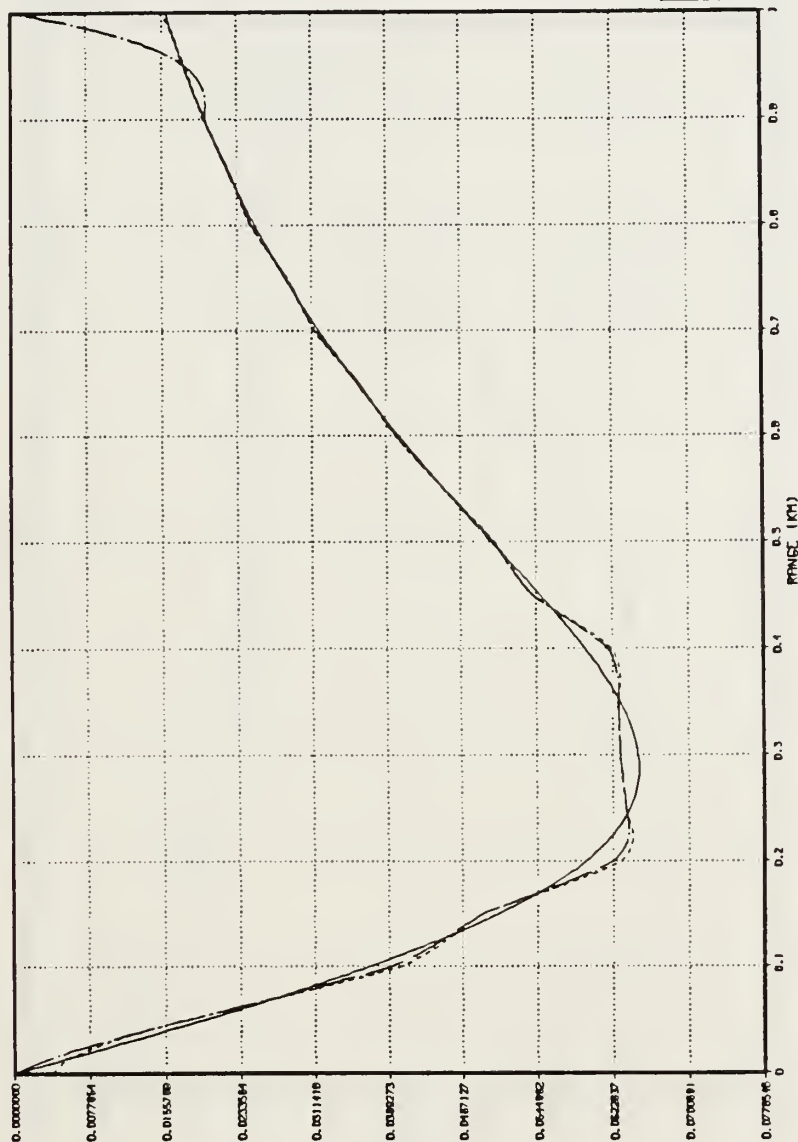
Figure 57. Modified Witch of Agnesi Ocean Bottom First-Order Derivatives: Spatial Fourier Series representation of the Akima Cubic Spline Witch of Agnesi bottom model.

89
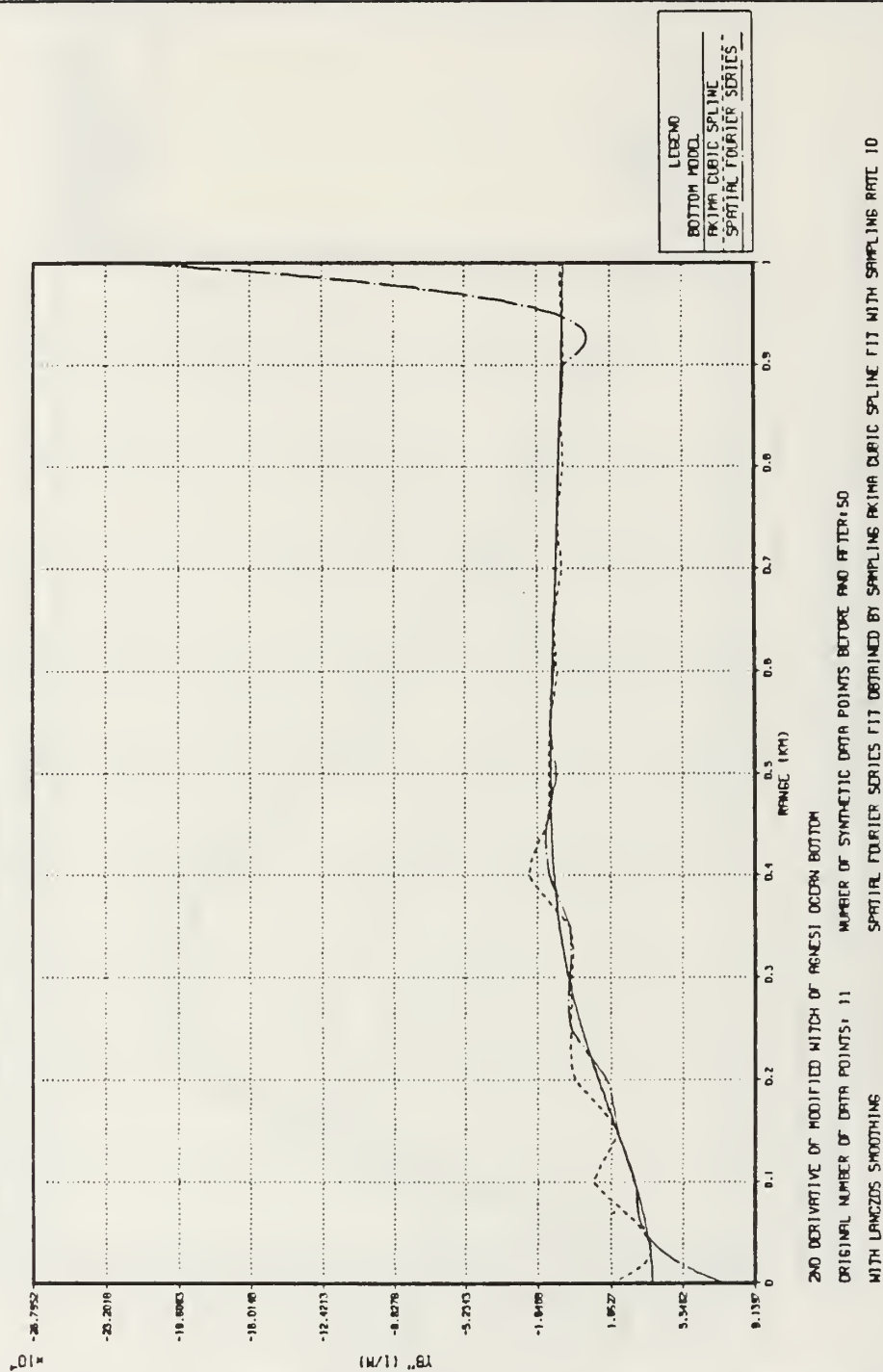
Figure 58. Modified Witch of Agnesi Ocean Bottom Second-Order Derivatives: Spatial Fourier Series representation of the Akima Cubic Spline Witch of Agnesi bottom model.

90
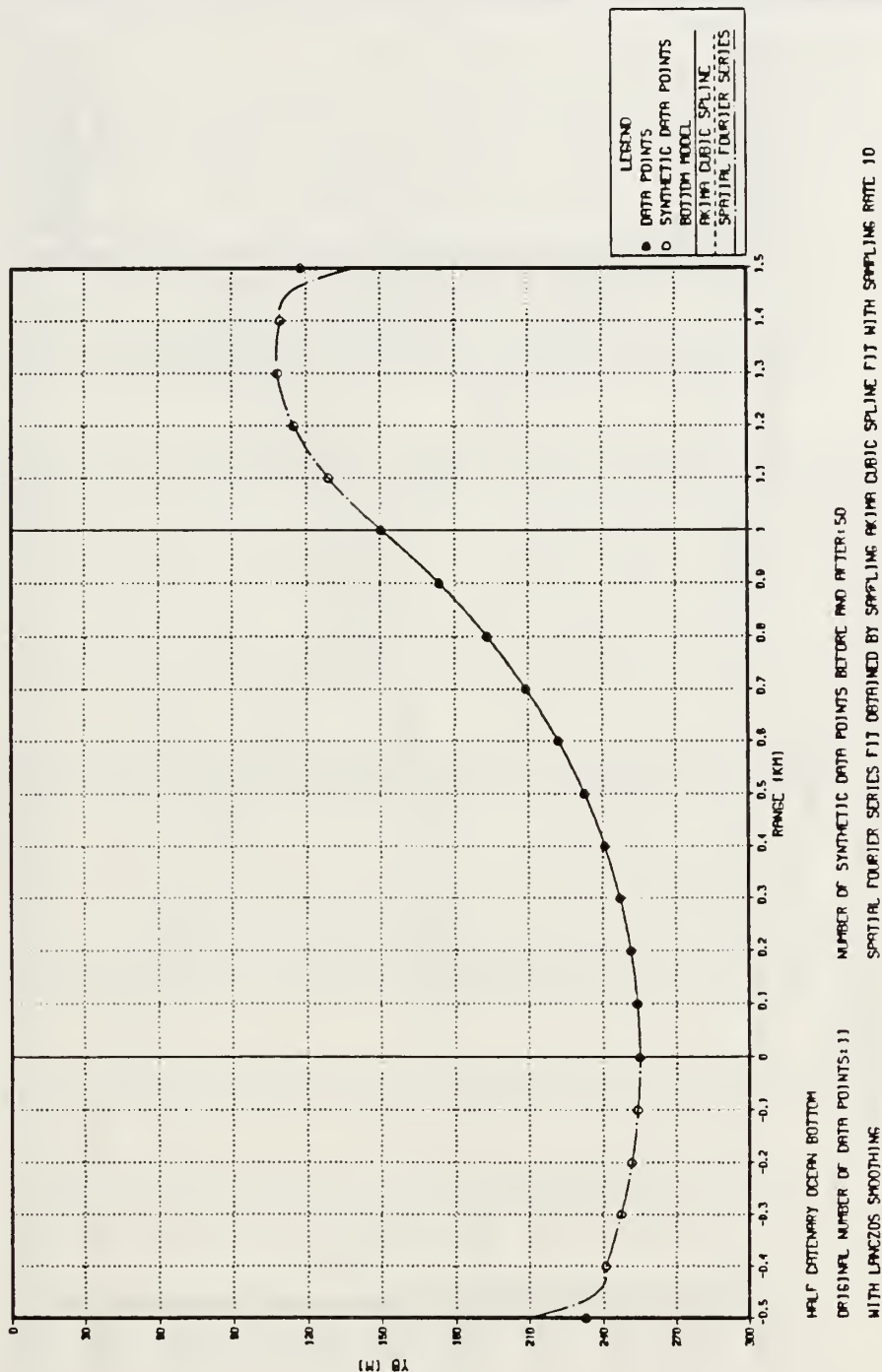
Figure 59. Half Catenary Ocean Bottom Contour Reconstruction: Spatial Fourier Series representation of the Akima Cubic Spline half catenary bottom.
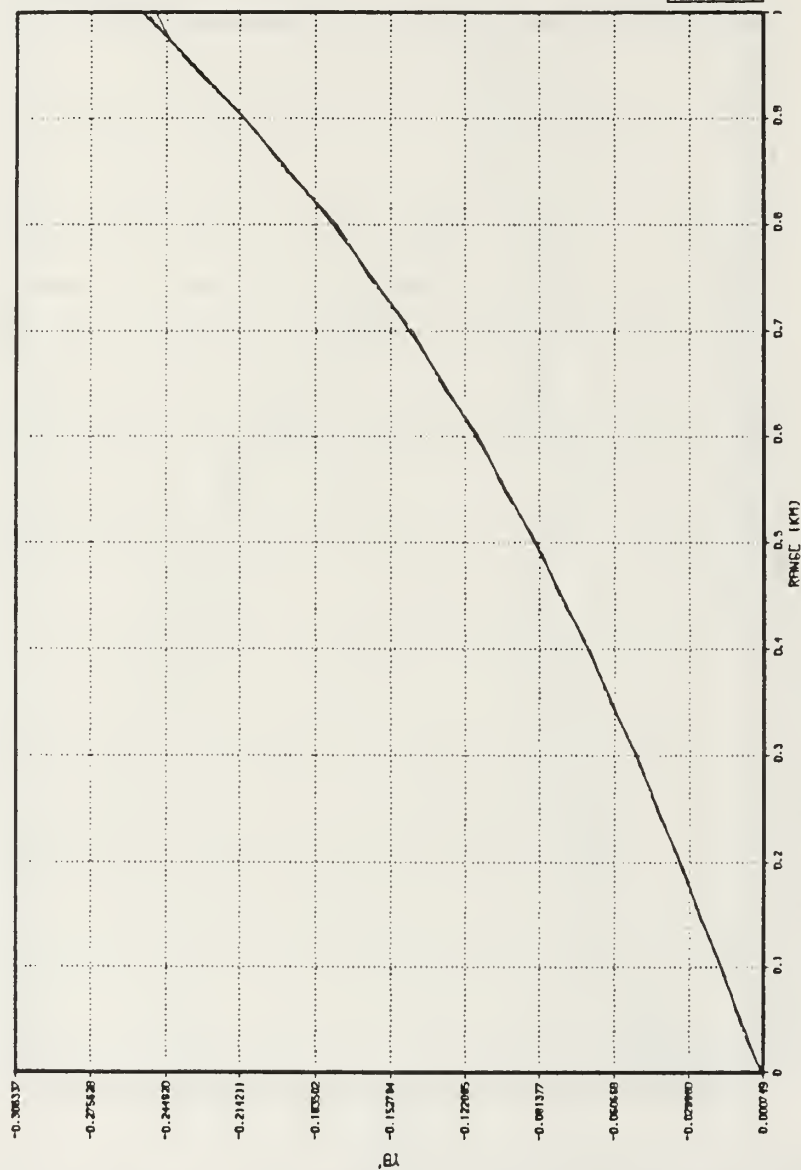
Figure 60. Half Catenary Ocean Bottom First-Order Derivatives: Spatial Fourier Series representation of the Akima Cubic Spline half catenary bottom.
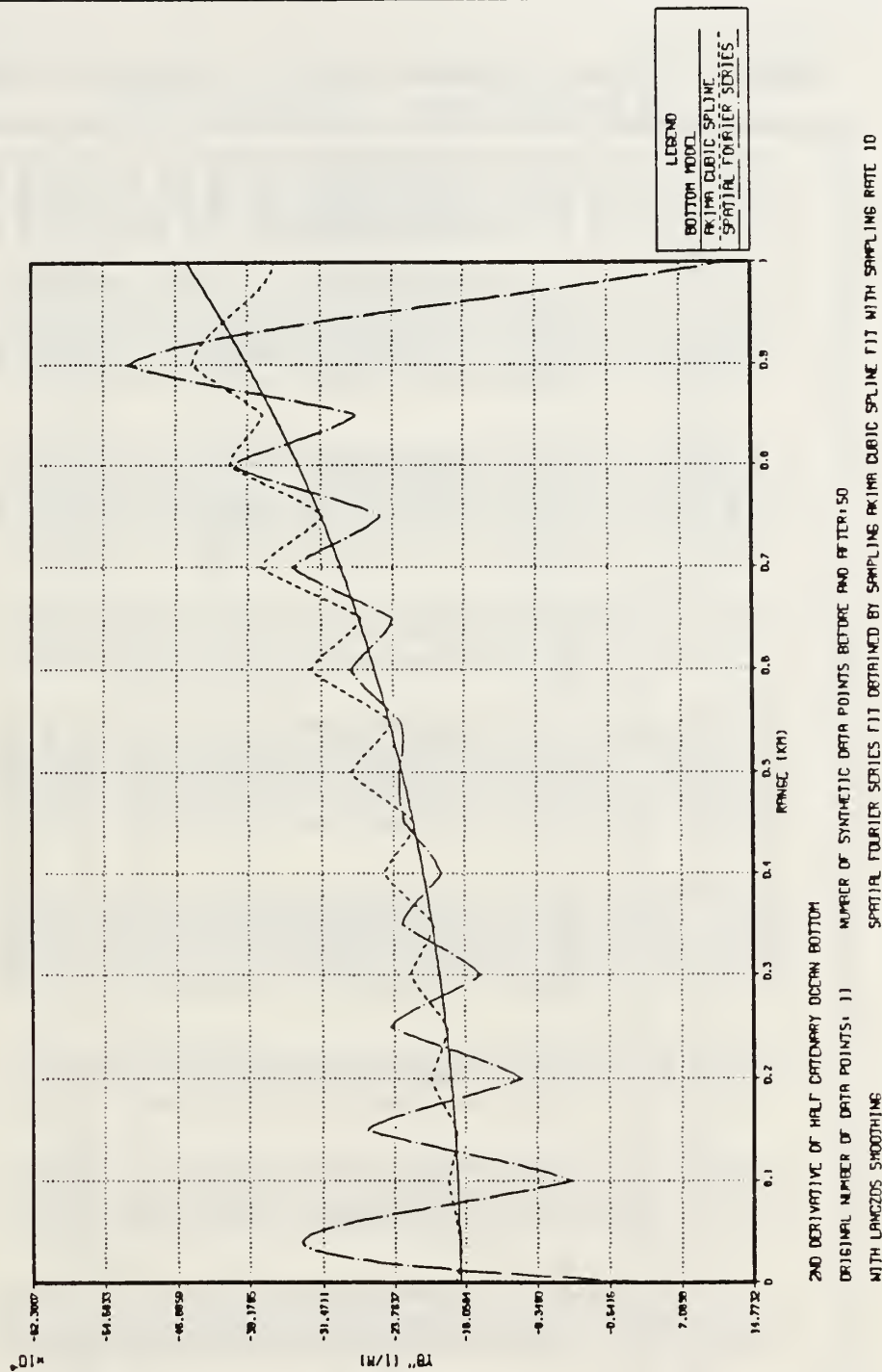
Figure 61. Half Catenary Ocean Bottom Second-Order Derivatives: Spatial Fourier Series representation of the Akima Cubic Spline half catenary bottom.

93

Table 20. FOURIER SERIES RESULTS : ACS DOWN-SLOPE OCEAN BOTTOM

CONSTANT DOWNSLOPE BOTTOM

TECHNIQUE: SPATIAL FOURIER SERIES FIT WITH LANCZOS SMOOTHING   NO. OF ORIGINAL DATA POINTS: 11

SPATIAL FOURIER SERIES FIT OBTAINED BY SAMPLING AKIMA CUBIC SPLINE FIT

RANGE (KM)	YB(EXACT) (M)	YB(FIT) (M)	% ERROR	YBDOT(EXACT)	YBDOT(FIT)	% ERROR	YBDOT2(EXACT) (1/M)	YBDOT2(FIT) (1/M)	% ERROR
0.00	220.00	220.01	0.003	0.200E+00	0.198E+00	-1.101	0.000E+00	-0.683E-03	********
0.05	230.00	229.99	-0.002	0.200E+00	0.202E+00	1.025	0.000E+00	0.543E-03	********
0.10	240.00	240.00	0.002	0.200E+00	0.198E+00	-0.964	0.000E+00	-0.435E-03	********
0.15	250.00	250.00	-0.001	0.200E+00	0.202E+00	0.915	0.000E+00	0.348E-03	********
0.20	260.00	260.00	0.001	0.200E+00	0.198E+00	-0.876	0.000E+00	-0.277E-03	********
0.25	270.00	270.00	-0.001	0.200E+00	0.202E+00	0.845	0.000E+00	0.218E-03	********
0.30	280.00	280.00	0.001	0.200E+00	0.198E+00	-0.821	0.000E+00	-0.166E-03	********
0.35	290.00	290.00	0.000	0.200E+00	0.202E+00	0.804	0.000E+00	0.120E-03	********
0.40	300.00	300.00	0.000	0.200E+00	0.198E+00	-0.791	0.000E+00	-0.779E-04	********
0.45	310.00	310.00	0.000	0.200E+00	0.202E+00	0.784	0.000E+00	0.384E-04	********
0.50	320.00	320.00	0.000	0.200E+00	0.198E+00	-0.782	0.000E+00	0.161E-14	0.000
0.55	330.00	330.00	0.000	0.200E+00	0.202E+00	0.784	0.000E+00	-0.384E-04	********
0.60	340.00	340.00	0.000	0.200E+00	0.198E+00	-0.791	0.000E+00	0.779E-04	********
0.65	350.00	350.00	0.000	0.200E+00	0.202E+00	0.804	0.000E+00	-0.120E-03	********
0.70	360.00	360.00	0.000	0.200E+00	0.198E+00	-0.821	0.000E+00	0.166E-03	********
0.75	370.00	370.00	0.001	0.200E+00	0.202E+00	0.845	0.000E+00	-0.218E-03	********
0.80	380.00	380.00	-0.001	0.200E+00	0.198E+00	-0.876	0.000E+00	0.277E-03	********
0.85	390.00	390.00	-0.001	0.200E+00	0.202E+00	0.915	0.000E+00	-0.348E-03	********
0.90	400.00	400.00	-0.001	0.200E+00	0.198E+00	-0.964	0.000E+00	0.435E-03	********
0.95	410.00	410.01	0.001	0.200E+00	0.202E+00	1.025	0.000E+00	-0.543E-03	********
1.00	420.00	419.99	-0.002	0.200E+00	0.198E+00	-1.101	0.000E+00	0.683E-03	********

Table 21. FOURIER SERIES RESULTS : ACS UP-SLOPE OCEAN BOTTOM

CONSTANT UPSLOPE BOTTOM

TECHNIQUE: SPATIAL FOURIER SERIES FIT WITH LANCZOS SMOOTHING   NO. OF ORIGINAL DATA POINTS: 11

SPATIAL FOURIER SERIES FIT OBTAINED BY SAMPLING AKIMA CUBIC SPLINE FIT

RANGE (KM)	YB(EXACT) (M)	YB(FIT) (M)	% ERROR	YBDOT(EXACT)	YBDOT(FIT)	% ERROR	YBDOT2(EXACT) (1/M)	YBDOT2(FIT) (1/M)	% ERROR
0.00	420.00	419.99	-0.002	-0.200E+00	-0.198E+00	-1.101	0.000E+00	0.683E-03	*********
0.05	410.00	410.01	0.001	-0.200E+00	-0.202E+00	1.025	0.000E+00	-0.543E-03	*********
0.10	400.00	400.00	-0.001	-0.200E+00	-0.198E+00	-0.964	0.000E+00	0.435E-03	*********
0.15	390.00	390.00	0.001	-0.200E+00	-0.202E+00	0.915	0.000E+00	-0.348E-03	*********
0.20	380.00	380.00	-0.001	-0.200E+00	-0.198E+00	-0.876	0.000E+00	0.277E-03	*********
0.25	370.00	370.00	0.001	-0.200E+00	-0.202E+00	0.845	0.000E+00	-0.218E-03	*********
0.30	360.00	360.00	0.000	-0.200E+00	-0.198E+00	-0.821	0.000E+00	0.166E-03	*********
0.35	350.00	350.00	0.000	-0.200E+00	-0.202E+00	0.804	0.000E+00	-0.120E-03	*********
0.40	340.00	340.00	0.000	-0.200E+00	-0.198E+00	-0.791	0.000E+00	0.779E-04	*********
0.45	330.00	330.00	0.000	-0.200E+00	-0.202E+00	0.784	0.000E+00	-0.384E-04	*********
0.50	320.00	320.00	0.000	-0.200E+00	-0.198E+00	-0.782	0.000E+00	-0.148E-14	0.000
0.55	310.00	310.00	0.000	-0.200E+00	-0.202E+00	0.784	0.000E+00	0.384E-04	*********
0.60	300.00	300.00	0.000	-0.200E+00	-0.198E+00	-0.791	0.000E+00	-0.779E-04	*********
0.65	290.00	290.00	0.000	-0.200E+00	-0.202E+00	0.804	0.000E+00	0.120E-03	*********
0.70	280.00	280.00	0.001	-0.200E+00	-0.198E+00	-0.821	0.000E+00	-0.166E-03	*********
0.75	270.00	270.00	-0.001	-0.200E+00	-0.202E+00	0.845	0.000E+00	0.218E-03	*********
0.80	260.00	260.00	0.001	-0.200E+00	-0.198E+00	-0.876	0.000E+00	-0.277E-03	*********
0.85	250.00	250.00	-0.001	-0.200E+00	-0.202E+00	0.915	0.000E+00	0.348E-03	*********
0.90	240.00	240.00	0.002	-0.200E+00	-0.198E+00	-0.964	0.000E+00	-0.435E-03	*********
0.95	230.00	229.99	-0.002	-0.200E+00	-0.202E+00	1.025	0.000E+00	0.543E-03	*********
1.00	220.00	220.01	0.003	-0.200E+00	-0.198E+00	-1.101	0.000E+00	-0.683E-03	*********

Table 22.   FOURIER SERIES RESULTS : ACS ONE PERIOD
COSINE OCEAN BOTTOM

ONE PERIOD COSINE WAVE BOTTOM

TECHNIQUE: SPATIAL FOURIER SERIES FIT WITH LANCZOS SMOOTHING   NO. OF ORIGINAL DATA POINTS: 11

SPATIAL FOURIER SERIES FIT OBTAINED BY SAMPLING AKIMA CUBIC SPLINE FIT

RANGE (KM)	YB(EXACT) (M)	YB(FIT) (M)	% ERROR	YBDOT(EXACT)	YBDOT(FIT)	% ERROR	YBDOT2(EXACT) (1/M)	YBDOT2(FIT) (1/M)	% ERROR
0.00	250.00	250.34	0.134	0.000E+00	0.284E-05	********	0.790E-02	0.140E-01	77.270
0.05	259.79	259.77	-0.008	0.388E+00	0.349E+00	-10.173	0.751E-02	0.770E-02	2.489
0.10	288.20	288.32	0.043	0.739E+00	0.809E+00	9.555	0.639E-02	0.733E-02	14.721
0.15	332.44	333.98	0.463	0.102E+01	0.100E+01	-1.636	0.464E-02	0.344E-02	-25.846
0.20	388.20	388.26	0.015	0.120E+01	0.117E+01	-1.985	0.244E-02	0.347E-02	42.151
0.25	450.00	450.00	0.000	0.126E+01	0.127E+01	0.857	0.224E-17	0.549E-05	********
0.30	511.80	511.74	-0.012	0.120E+01	0.117E+01	-2.078	-0.244E-02	-0.370E-02	51.453
0.35	567.56	565.71	-0.325	0.102E+01	0.994E+00	-2.225	-0.464E-02	-0.317E-02	-31.640
0.40	611.80	611.69	-0.018	0.739E+00	0.833E+00	12.735	-0.639E-02	-0.674E-02	5.550
0.45	640.21	641.44	0.191	0.388E+00	0.360E+00	-7.212	-0.751E-02	-0.853E-02	13.587
0.50	650.00	649.90	-0.015	0.154E-15	0.197E-14	0.000	-0.790E-02	-0.610E-02	-22.752
0.55	640.21	641.44	0.191	-0.388E+00	-0.360E+00	-7.212	-0.751E-02	-0.853E-02	13.587
0.60	611.80	611.69	-0.018	-0.739E+00	-0.833E+00	12.735	-0.639E-02	-0.674E-02	5.550
0.65	557.56	565.71	-0.325	-0.102E+01	-0.994E+00	-2.225	-0.464E-02	-0.317E-02	-31.640
0.70	511.80	511.74	-0.012	-0.120E+01	-0.117E+01	-2.078	-0.244E-02	-0.370E-02	51.453
0.75	450.00	450.00	0.000	-0.126E+01	-0.127E+01	0.857	-0.145E-17	0.549E-05	********
0.80	388.20	388.26	0.015	-0.120E+01	-0.117E+01	-1.985	0.244E-02	0.347E-02	42.151
0.85	332.44	333.98	0.463	-0.102E+01	-0.100E+01	-1.636	0.464E-02	0.344E-02	-25.846
0.90	288.20	288.32	0.043	-0.739E+00	-0.809E+00	9.555	0.639E-02	0.733E-02	14.721

96

Table 23. FOURIER SERIES RESULTS : ACS WITCH OF AGNESI OCEAN BOTTOM

WITCH OF AGNESI BOTTOM

TECHNIQUE: SPATIAL FOURIER SERIES FIT WITH LANCZOS SMOOTHING   NO. OF ORIGINAL DATA POINTS: 11

SPATIAL FOURIER SERIES FIT OBTAINED BY SAMPLING AKIMA CUBIC SPLINE FIT

RANGE (KM)	YB(EXACT) (M)	YB(FIT) (M)	% ERROR	YBDOT(EXACT)	YBDOT(FIT)	% ERROR	YBDOT2(EXACT) (1/M)	YBDOT2(FIT) (1/M)	% ERROR
0.00	50.00	50.02	0.037	0.000E+00	0.215E-05	*********	0.400E-03	0.762E-03	90.410
0.05	50.50	50.51	0.036	0.196E-01	0.178E-01	-9.041	0.377E-03	0.370E-03	-1.792
0.10	51.92	51.93	0.010	0.370E-01	0.393E-01	6.231	0.313E-03	0.320E-03	2.175
0.15	54.13	54.13	0.000	0.505E-01	0.488E-01	-3.397	0.225E-03	0.229E-03	1.394
0.20	56.90	56.90	0.005	0.595E-01	0.623E-01	4.818	0.133E-03	0.176E-03	32.014
0.25	60.00	60.07	0.112	0.640E-01	0.635E-01	-0.710	0.512E-04	-0.913E-06	-101.782
0.30	63.24	63.24	0.000	0.649E-01	0.630E-01	-2.826	-0.127E-04	-0.971E-05	-23.694
0.35	66.44	66.38	-0.091	0.631E-01	0.628E-01	-0.371	-0.568E-04	-0.728E-05	-87.186
0.40	69.51	69.51	-0.003	0.595E-01	0.618E-01	3.949	-0.834E-04	-0.105E-03	26.326
0.45	72.38	72.40	0.039	0.549E-01	0.542E-01	-1.374	-0.965E-04	-0.120E-03	24.222
0.50	75.00	75.00	-0.002	0.500E-01	0.502E-01	0.314	-0.100E-03	-0.741E-04	-25.868
0.55	77.38	77.38	0.008	0.450E-01	0.451E-01	0.025	-0.975E-04	-0.104E-03	6.600
0.60	79.51	79.51	-0.002	0.403E-01	0.400E-01	-0.702	-0.914E-04	-0.845E-04	-7.609
0.65	81.41	81.41	0.000	0.359E-01	0.361E-01	0.591	-0.836E-04	-0.854E-04	2.066
0.70	83.11	83.11	-0.001	0.320E-01	0.316E-01	-1.163	-0.753E-04	-0.738E-04	-1.968
0.75	84.62	84.61	-0.002	0.284E-01	0.286E-01	0.836	-0.670E-04	-0.676E-04	0.907
0.80	85.96	85.95	-0.001	0.252E-01	0.249E-01	-1.391	-0.592E-04	-0.611E-04	3.152
0.85	87.15	87.14	-0.006	0.225E-01	0.226E-01	0.614	-0.521E-04	-0.515E-04	-1.243
0.90	88.21	88.21	-0.001	0.200E-01	0.200E-01	-0.187	-0.458E-04	-0.392E-04	-14.251
0.95	89.15	89.16	0.004	0.179E-01	0.180E-01	0.670	-0.401E-04	-0.729E-04	81.575
1.00	90.00	89.94	-0.066	0.160E-01	0.260E-05	-99.984	-0.352E-04	-0.223E-02	6242.727

Table 24. FOURIER SERIES RESULTS : ACS HALF CATENARY OCEAN BOTTOM

HALF CATENARY BOTTOM

TECHNIQUE: SPATIAL FOURIER SERIES FIT WITH LANCZOS SMOOTHING   NO. OF ORIGINAL DATA POINTS: 11

SPATIAL FOURIER SERIES FIT OBTAINED BY SAMPLING AKIMA CUBIC SPLINE FIT

RANGE (KM)	YB(EXACT) (M)	YB(FIT) (M)	% ERROR	YBDOT(EXACT)	YBDOT(FIT)	% ERROR	YBDOT2(EXACT) (1/M)	YBDOT2(FIT) (1/M)	% ERROR
0.00	255.00	255.00	-0.002	0.000E+00	0.624E-03	********	-0.167E-03	0.374E-04	-122.434
0.05	254.79	254.79	0.000	-0.834E-02	-0.897E-02	7.572	-0.167E-03	-0.321E-03	92.154
0.10	254.16	254.16	-0.002	-0.167E-01	-0.161E-01	-3.603	-0.169E-03	-0.472E-04	-72.062
0.15	253.12	253.11	-0.002	-0.253E-01	-0.259E-01	2.443	-0.172E-03	-0.269E-03	56.284
0.20	251.64	251.63	-0.001	-0.340E-01	-0.332E-01	-2.125	-0.176E-03	-0.100E-03	-42.955
0.25	249.72	249.71	-0.002	-0.429E-01	-0.436E-01	1.563	-0.181E-03	-0.242E-03	33.216
0.30	247.34	247.34	-0.001	-0.521E-01	-0.513E-01	-1.548	-0.188E-03	-0.144E-03	-23.600
0.35	244.50	244.49	-0.002	-0.617E-01	-0.624E-01	1.184	-0.196E-03	-0.228E-03	16.567
0.40	241.17	241.16	-0.002	-0.717E-01	-0.708E-01	-1.280	-0.205E-03	-0.186E-03	-9.350
0.45	237.32	237.31	-0.002	-0.822E-01	-0.830E-01	0.986	-0.216E-03	-0.225E-03	4.248
0.50	232.93	232.93	-0.003	-0.933E-01	-0.923E-01	-1.129	-0.228E-03	-0.231E-03	1.418
0.55	227.98	227.97	-0.002	-0.105E+00	-0.106E+00	0.869	-0.242E-03	-0.229E-03	-5.291
0.60	222.42	222.41	-0.004	-0.118E+00	-0.116E+00	-1.036	-0.257E-03	-0.283E-03	10.008
0.65	216.21	216.20	-0.002	-0.131E+00	-0.132E+00	0.794	-0.274E-03	-0.238E-03	-13.185
0.70	209.32	209.32	-0.005	-0.145E+00	-0.144E+00	-0.976	-0.294E-03	-0.345E-03	17.447
0.75	201.69	201.69	-0.002	-0.160E+00	-0.161E+00	0.745	-0.315E-03	-0.250E-03	-20.415
0.80	193.28	193.28	0.004	-0.177E+00	-0.175E+00	-0.974	-0.338E-03	-0.409E-03	20.941
0.85	184.02	184.03	-0.003	-0.194E+00	-0.195E+00	0.529	-0.364E-03	-0.277E-03	-23.929
0.90	173.86	173.85	-0.017	-0.213E+00	-0.212E+00	-0.352	-0.392E-03	-0.519E-03	32.408
0.95	162.71	162.68	0.006	-0.233E+00	-0.234E+00	0.514	-0.423E-03	-0.251E-03	-40.743
1.00	150.50	150.51		-0.255E+00	-0.249E+00	-2.498	-0.457E-03	0.123E-03	-126.943

first and second-order derivatives were very accurate over the major portion of the range of interest, but were characterized by large errors at the outer end points of this region, as illustrated in Figure 64. This phenomenon is attributed to the reversal of slope method for generating synthetic data.

D.   ALTERNATIVE INTERIM MODELING TECHNIQUES

Efforts to model arbitrarily shaped ocean bottom contours by SFS methods yielded unsatisfactory results in every case studied despite three numerical modifications designed to enhance the performance of this technique. ACS results for the contours were accurate, but the subsequent derivative calculations were erroneous. The need for a program which could accurately model both the bottom and its derivatives remained paramount. Without this, the precise calculation of reflection angles for acoustic rays impinging an undulating sea floor could not be realized.

Motivated by the above requirements, attempts were made to salvage the ACS technique by utilizing its accurate contour reproduction and applying alternate numerical methods to obtain reliable values for the first and second-order derivatives. The following central differencing algorithms, extracted from [Ref. 7], were utilized:

$$y'_B(z_0) = \frac{-y_B(z_0 + 2h) + 8y_B(z_0 + h) - 8y_B(z_0 - h) + y_B(z_0 - 2h)}{12h} \qquad (3.26)$$

and

$$y''_B(z_0) = \frac{-y_B(z_0 + 2h) + 16y_B(z_0 + h) - 30y_B(z_0) + 16y_B(z_0 - h) - y_B(z_0 - 2h)}{12h^2} \qquad (3.27)$$

where h is some arbitrarily small number, nominally $1/100$ of the average spacing between each original data point.

The accuracy of Equations (3.26) and (3.27) was verified in separate tests using several mathematical functions. These relationships were then applied to the ACS reconstructions of the seven exact mathematical ocean bottom models listed in Section 1 of this chapter. The resultant first and second-order derivatives were an improvement on previous methods, but below the precision expected. These poor results are attributed to the nature of the ACS program and the manner in which the interpolating splines between each data point are generated.

Having abandoned both the SFS and ACS methods for modeling the ocean bottom, attention was focused upon a computer routine which provided a divided differences

Figure 62. Parabolic Ocean Bottom Contour Reconstruction: Spatial Fourier Series representation of the Akima Cubic Spline parabolic bottom.

Figure 63. Parabolic Ocean Bottom First-Order Derivatives: Spatial Fourier Series representation of the Akima Cubic Spline parabolic bottom.
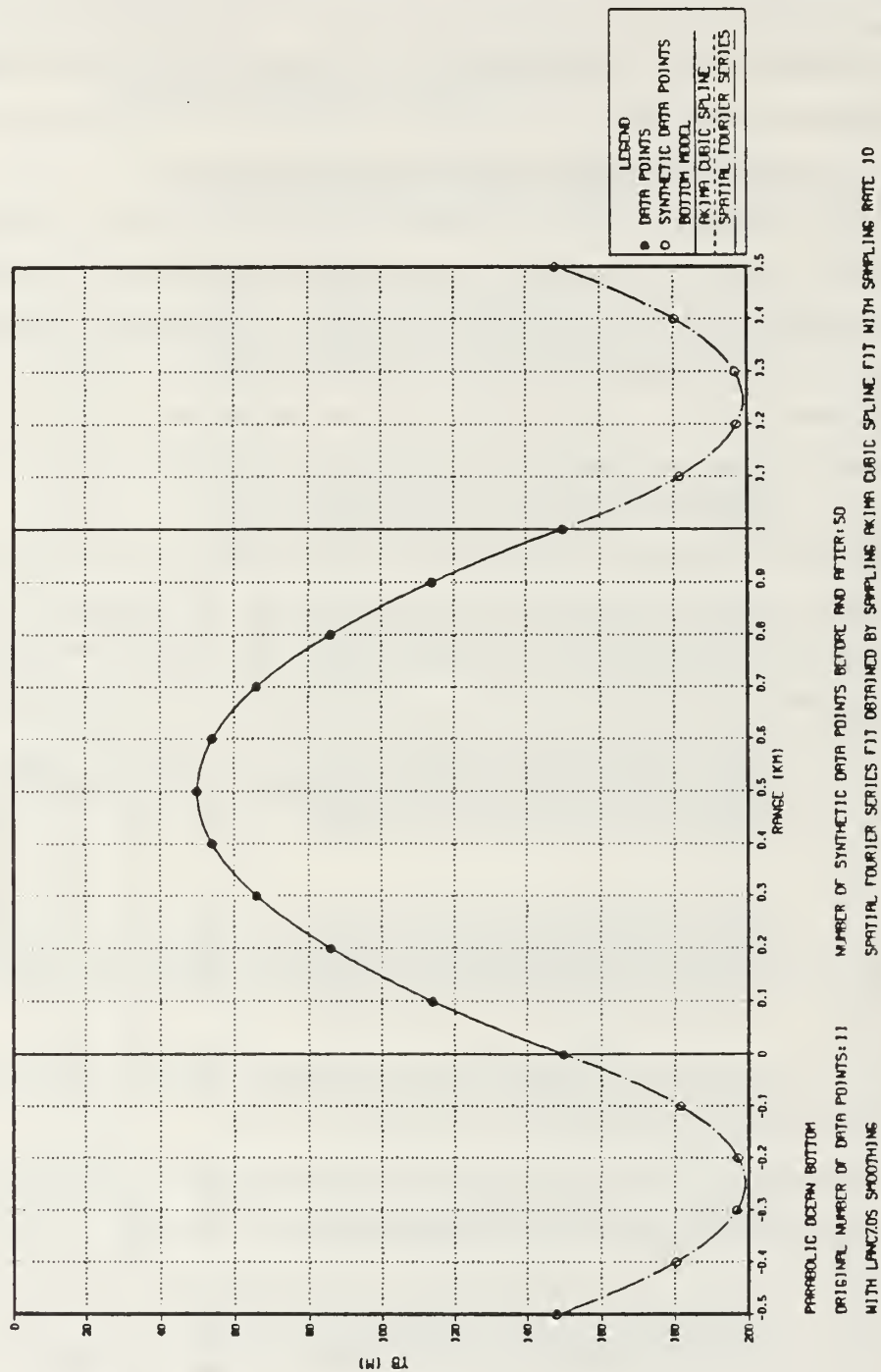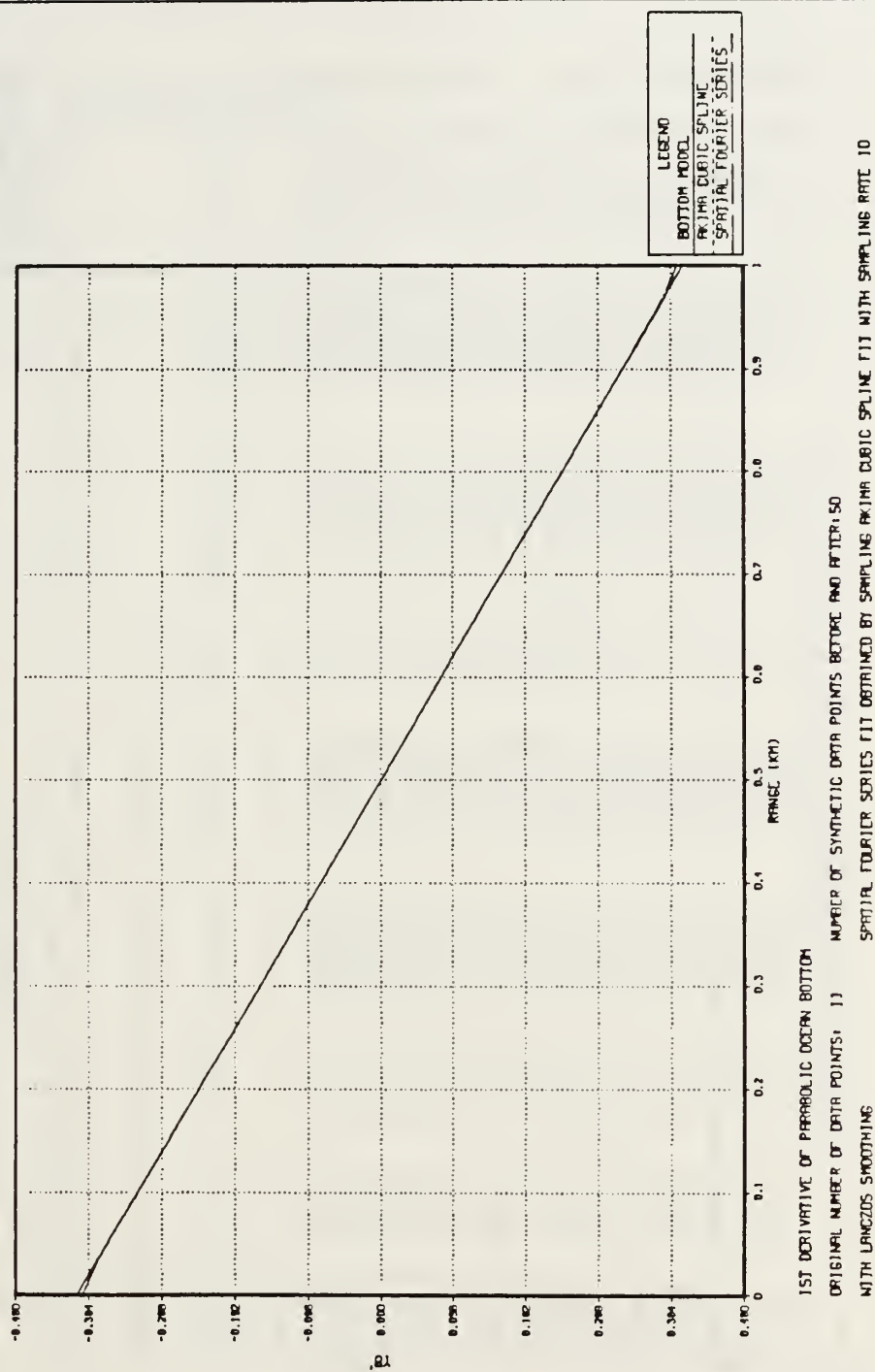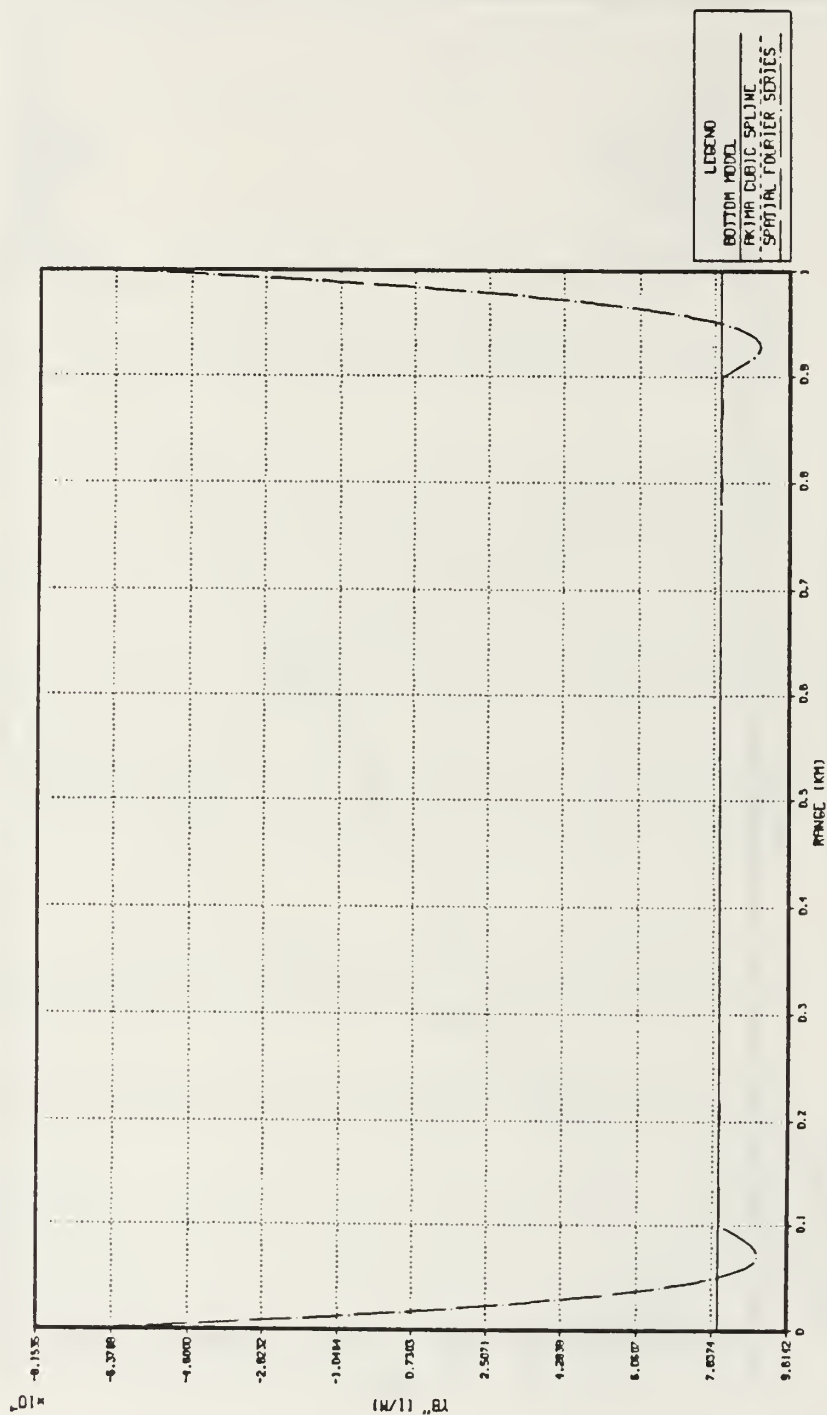
Figure 64. Parabolic Ocean Bottom Second-Order Derivatives: Spatial Fourier Series representation of the Akima Cubic Spline parabolic bottom.

Table 25. FOURIER SERIES RESULTS : ACS PARABOLIC OCEAN BOTTOM

PARABOLIC BOTTOM

TECHNIQUE: SPATIAL FOURIER SERIES FIT WITH LANCZOS SMOOTHING   NO. OF ORIGINAL DATA POINTS: 11

SPATIAL FOURIER SERIES FIT OBTAINED BY SAMPLING AKIMA CUBIC SPLINE FIT

RANGE (KM)	YB(EXACT) (M)	YB(FIT) (M)	% ERROR	YBDOT(EXACT)	YBDOT(FIT)	% ERROR	YBDOT2(EXACT) (1/M)	YBDOT2(FIT) (1/M)	% ERROR
0.00	150.00	149.99	-0.009	-0.400E+00	-0.392E+00	-1.993	0.800E-03	-0.679E-03	-184.914
0.05	131.00	131.01	0.010	-0.360E+00	-0.360E+00	0.000	0.800E-03	0.794E-03	-0.749
0.10	114.00	114.01	0.012	-0.320E+00	-0.320E+00	0.000	0.800E-03	0.801E-03	0.148
0.15	99.00	99.01	0.013	-0.280E+00	-0.280E+00	0.000	0.800E-03	0.800E-03	-0.056
0.20	86.00	86.01	0.015	-0.240E+00	-0.240E+00	0.000	0.800E-03	0.800E-03	0.028
0.25	75.00	75.01	0.018	-0.200E+00	-0.200E+00	0.000	0.800E-03	0.800E-03	-0.016
0.30	66.00	66.01	0.020	-0.160E+00	-0.160E+00	0.000	0.800E-03	0.800E-03	0.010
0.35	59.00	59.01	0.022	-0.120E+00	-0.120E+00	0.000	0.800E-03	0.800E-03	-0.007
0.40	54.00	54.01	0.024	-0.800E-01	-0.800E-01	0.000	0.800E-03	0.800E-03	0.006
0.45	51.00	51.01	0.026	-0.400E-01	-0.400E-01	0.000	0.800E-03	0.800E-03	-0.005
0.50	50.00	50.01	0.026	0.000E+00	-0.161E-16	0.000	0.800E-03	0.800E-03	0.004
0.55	51.00	51.01	0.026	0.400E-01	0.400E-01	0.000	0.800E-03	0.800E-03	-0.005
0.60	54.00	54.01	0.024	0.800E-01	0.800E-01	0.000	0.800E-03	0.800E-03	0.006
0.65	59.00	59.01	0.022	0.120E+00	0.120E+00	0.000	0.800E-03	0.800E-03	-0.007
0.70	66.00	66.01	0.020	0.160E+00	0.160E+00	0.000	0.800E-03	0.800E-03	0.010
0.75	75.00	75.01	0.018	0.200E+00	0.200E+00	0.000	0.800E-03	0.800E-03	-0.016
0.80	86.00	86.01	0.015	0.240E+00	0.240E+00	0.000	0.800E-03	0.800E-03	0.028
0.85	99.00	99.01	0.013	0.280E+00	0.280E+00	0.000	0.800E-03	0.800E-03	-0.056
0.90	114.00	114.01	0.012	0.320E+00	0.320E+00	0.000	0.800E-03	0.801E-03	0.148
0.95	131.00	131.01	0.010	0.360E+00	0.360E+00	0.000	0.800E-03	0.794E-03	-0.749
1.00	150.00	149.99	-0.009	0.400E+00	0.392E+00	-1.993	0.800E-03	-0.679E-03	-184.914

interpolating polynomial fit to unordered, randomly spaced data. This program , written by Gerald and Wheatley [Ref. 7], was tested on the seven exact mathematical bottom models. Accurate curve fits were achieved; however, more care was required in sampling each contour to avoid artificial curvatures in the fit which are often characteristic of this numerical technique. The subsequent first and second-order derivatives generated by applying Equations (3.26) and (3.27) to the polynomial fit were precise. Therefore, these equations and the polynomial coefficients program formed the basis of an interim modeling technique which would enable verification of the reflection angle algorithm for an arbitrarily shaped ocean bottom.

IV. ACOUSTIC RAY REFLECTIONS FROM ARBITRARILY SHAPED BOTTOM CONTOURS

The reflection angle algorithms given by Equations (2.13), (2.14), (2.15) and (2.35) were incorporated into an existing acoustic ray trace program. This Fortran program had previously been limited to the flat bottom case. Seven exact mathematical functions where then used to model ocean bathymetry. One acoustic ray was launched for each bottom contour and the computer generated angles of reflection and bottom slope compared with the corresponding theoretical values. An isospeed ocean was assumed in each case in order to interpret the results easily.

The seven exact mathematical functions employed were:

- Flat Bottom ($y_B(z) = 1000$ m)
- Constant down-slope bottom ($y_B(z) = 600.0 + 0.04z$ m)
- Constant up-slope bottom ($y_B(z) = 1000.0 - 0.04z$ m)
- One period cosine bottom ($y_B(z) = 250.0 - 50.0\cos(0.0002\pi z)$ m)
- Modified Witch of Agnesi bottom ($y_B(z) = 200.0 - \dfrac{125000.0}{0.0001z^2 + 2500.0}$ m)
- Half catenary bottom ($y_B(z) = 315.0 - 30.0(e^{z/6000.0} + e^{-z/6000.0})$ m)
- Parabolic bottom ($y_B(z) = 250.0 + \dfrac{(z - 5000.0)^2}{75000.0}$ m).

Figures 65 through 78 illustrate the ocean bottom models and the propagated acoustic ray for each of the test cases. A comparison between theory and the computer generated results for each model are given in Tables 26 through 32 inclusively. For each table, the terms $\gamma°$ and $\zeta°$ represent the exact values for the angle of bottom slope and acoustic ray reflection angle, respectively. The terms $\hat{\gamma}°$ and $\hat{\zeta}°$ represent the estimates generated by the ray trace program and reflection angle algorithm for these same parameters. The bottom and surface bounces are denoted by BB and SB, respectively.

These results were uniformly accurate with almost all of the recorded errors for the computed reflection angles, $\hat{\zeta}°$, below 0.1%. Errors in the estimated bottom slope, $\hat{\gamma}°$, were also reasonably small thus verifying the central differencing methods for determining the first-order derivatives. The parabolic ocean bottom model yielded the worst results with errors in the reflection angle, $\zeta°$, averaging 0.08%. The modified Witch of Agnesi and half catenary models generated the largest errors in angle of slope, $\gamma°$, but

105

the magnitudes of these angles were sufficiently small such that little impact on the computed angles of reflection resulted.

Arithmetic confirmation of the reflection angle algorithm is not readily determined for a ray launched in an ocean medium with speed of sound varying as a function of depth and for an arbitrarily shaped ocean bottom. However, two such cases were investigated as a means of visual verification of the effects of a ray incident upon an arbitrarily shaped ocean bottom. The one period cosine and modified Witch of Agnesi models were utilized after slight modification to limit the range of depth. Figures 79 and 80 refer. The sound-speed profile is given by Table 33.

RECONSTRUCTED OCEAN BOTTOM BATHYMETRY

NZBPTS: 11
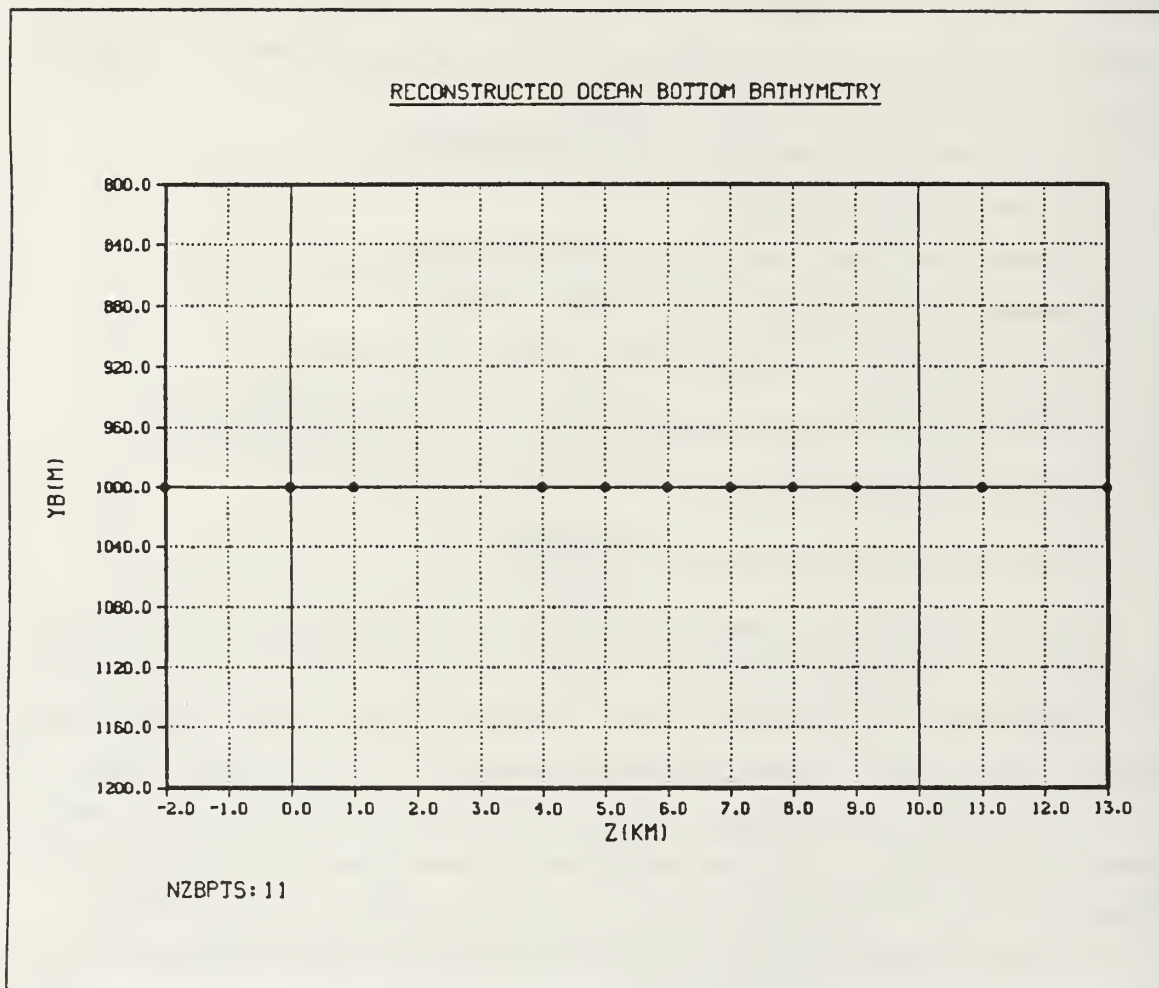
Figure 65.   Flat Ocean Bottom: This profile was used to test the reflection angle algorithm for an isospeed ocean.
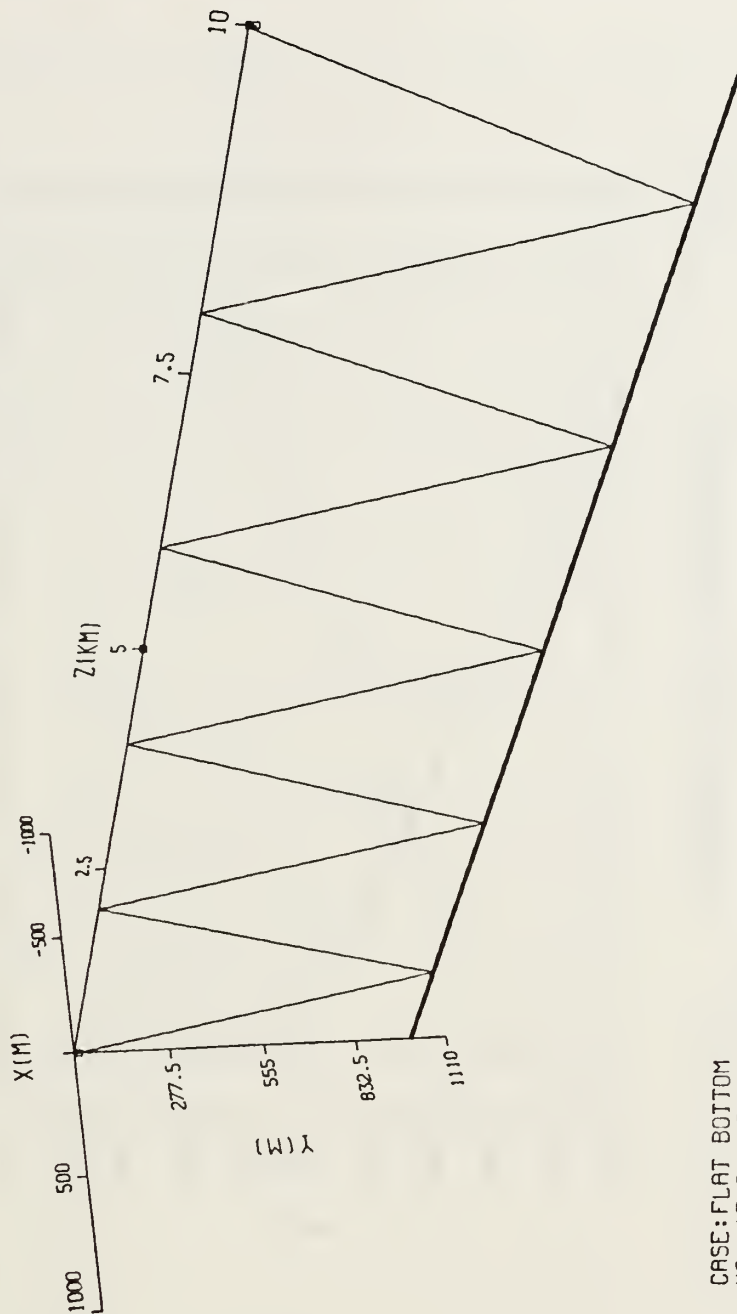
Figure 66. Acoustic Ray Impinging a Flat Bottom: This figure shows an acoustic ray launched at depth 15 m with initial angle $\beta_0 = 45°$ and propagating in an isospeed ocean with a flat bottom.
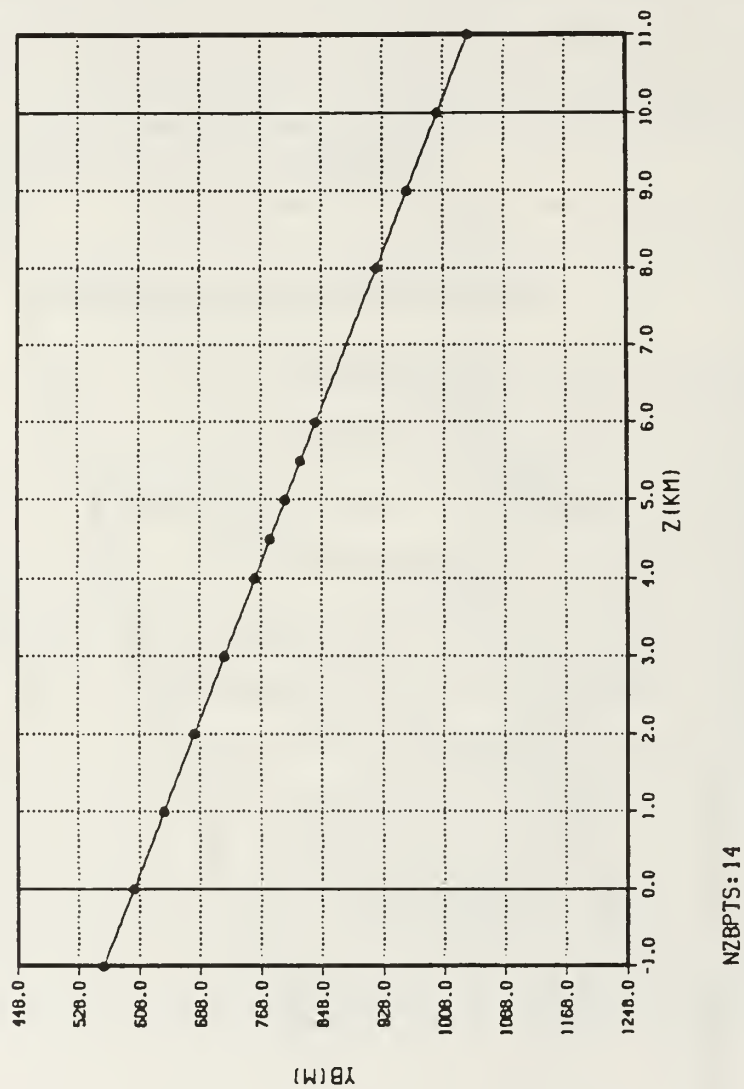
Figure 67. Constant Down-Slope Bottom: This profile was used to test the re-
flection angle algorithm for an isospeed ocean.
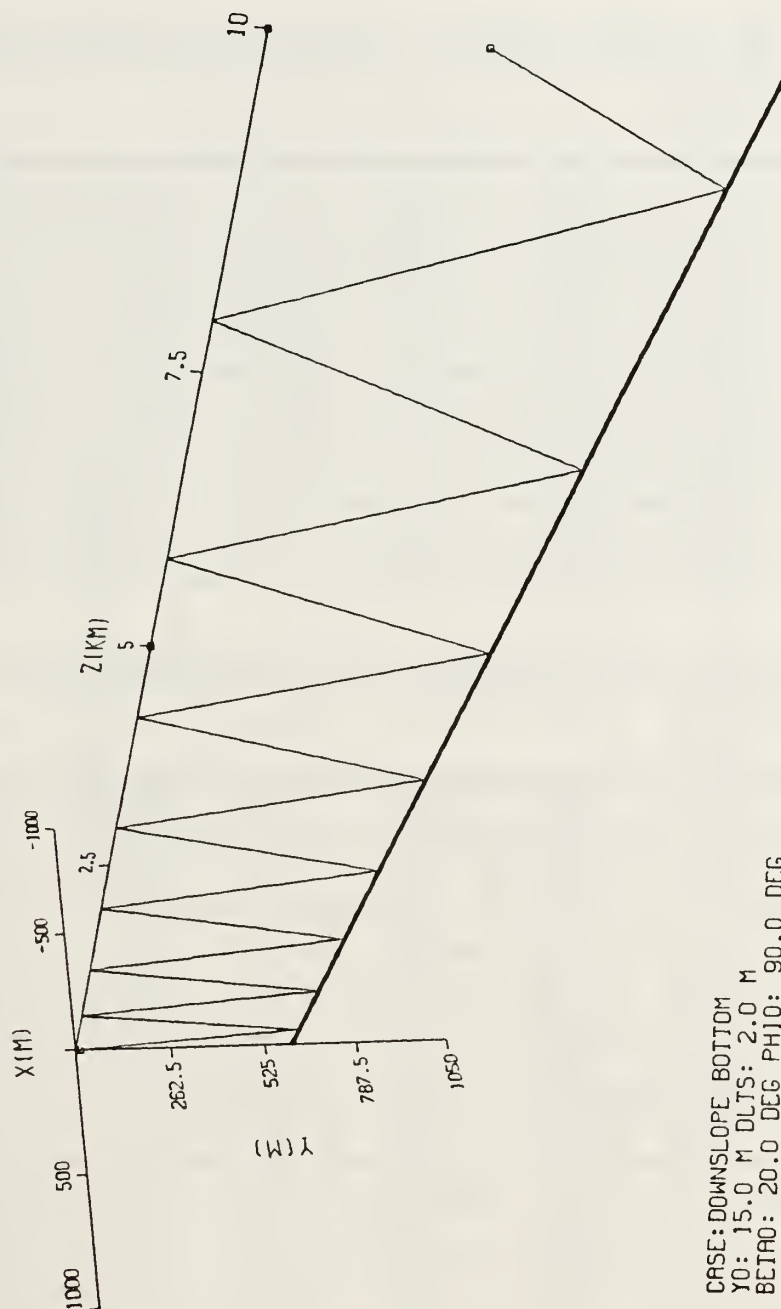
Figure 68. Acoustic Ray Impinging a Constant Down-Slope Bottom: This figure shows an acoustic ray launched at depth 15 m with initial angle $\beta_0 = 20°$ and propagating in an isospeed ocean with a constant down-slope bottom.

Table 26.   REFLECTION ANGLES : FLAT BOTTOM WITH $\beta_0 = 45°$

BOUNCE	Range (km)	$|\gamma°|$	$|\hat{\gamma}°|$	% Error	$\zeta°$	$\hat{\zeta}°$	% Error
1 BB	0.985	0.000	0.000	0.00	45.000	45.000	0.00
1 SB	1.985	0.000	0.000	0.00	45.000	45.000	0.00
2 BB	2.985	0.000	0.000	0.00	45.000	45.000	0.00
2 SB	3.985	0.000	0.000	0.00	45.000	45.000	0.00
3 BB	4.985	0.000	0.000	0.00	45.000	45.000	0.00
3 SB	5.985	0.000	0.000	0.00	45.000	45.000	0.00
4 BB	6.985	0.000	0.000	0.00	45.000	45.000	0.00
4 SB	7.985	0.000	0.000	0.00	45.000	45.000	0.00
5 BB	8.985	0.000	0.000	0.00	45.000	45.000	0.00
5 SB	9.985	0.000	0.000	0.00	45.000	45.000	0.00

Table 27.   REFLECTION ANGLES : DOWN-SLOPE BOTTOM WITH $\beta_0 = 20°$

| BOUNCE	Range (km)	$|\gamma°|$	$|\hat{\gamma}°|$	% Error	$\zeta°$	$\hat{\zeta}°$	% Error
1 BB	0.216	2.291	2.291	0.00	22.291	22.291	0.00
1 SB	0.494	0.000	0.000	0.00	24.581	24.581	0.00
2 BB	0.783	2.291	2.291	0.00	26.872	26.872	0.00
2 SB	1.136	0.000	0.000	0.00	29.162	29.162	0.00
3 BB	1.504	2.291	2.291	0.00	31.453	31.453	0.00
3 SB	1.945	0.000	0.000	0.00	33.744	33.744	0.00
4 BB	2.410	2.291	2.291	0.00	36.034	33.034	0.00
4 SB	2.961	0.000	0.000	0.00	38.325	38.325	0.00
5 BB	3.547	2.291	2.291	0.00	40.615	40.615	0.00
5 SB	4.237	0.000	0.000	0.00	42.906	42.906	0.00
6 BB	4.979	2.291	2.291	0.00	45.197	45.197	0.00
6 SB	5.851	0.000	0.000	0.00	47.487	47.487	0.00
7 BB	6.803	2.291	2.291	0.00	49.778	49.778	0.00
7 SB	7.922	0.000	0.000	0.00	52.069	52.069	0.00
8 BB	9.162	2.291	2.291	0.00	54.359	54.395	0.00
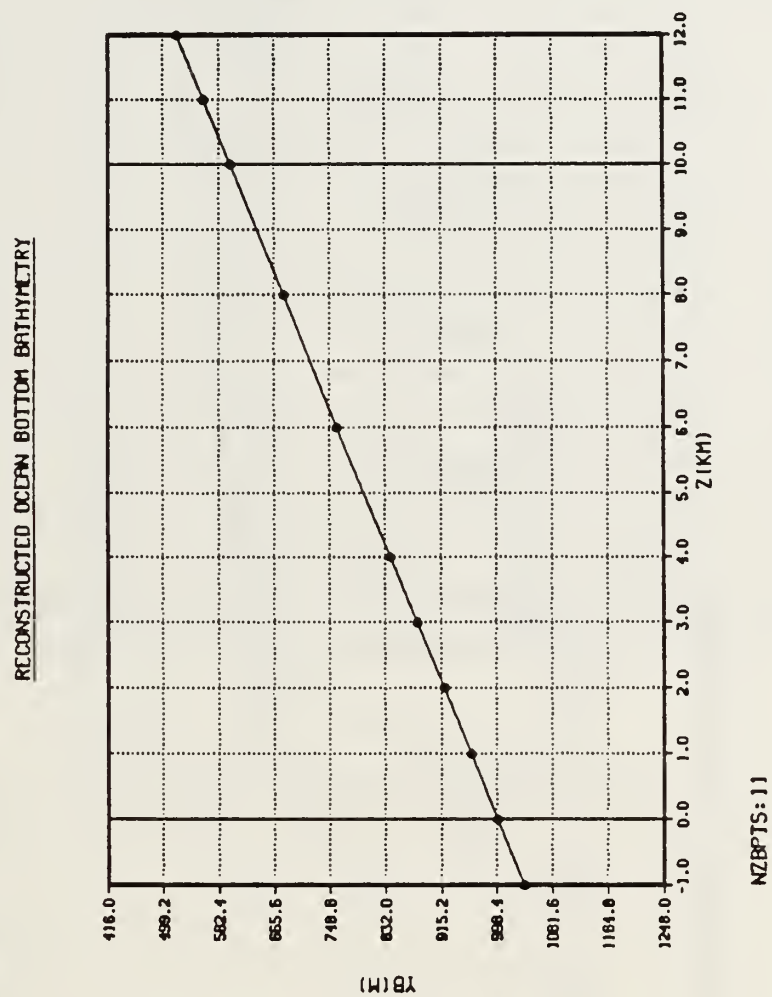
Figure 69. Constant Up-Slope Bottom: This profile was used to test the reflection angle algorithm for an isospeed ocean.

111

RECURSIVE RAY ACOUSTICS
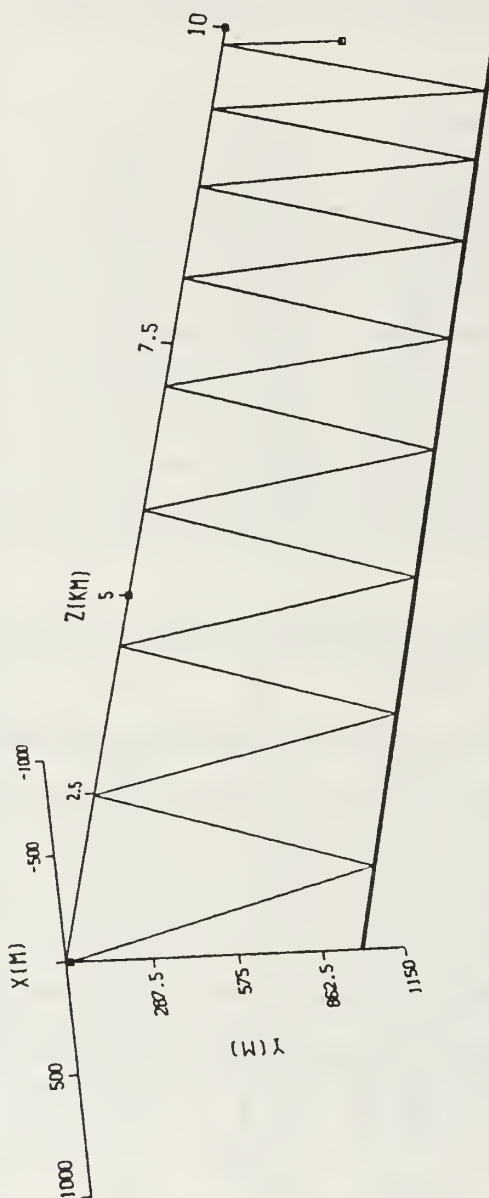
CASE:UPSLOPE BOTTOM
YO: 15.0 M DLTS: 2.0 M
BETAO: 55.0 DEG PHIO: 90.0 DEG

Figure 70.   Acoustic Ray Impinging a Constant Up-Slope Bottom: This figure
             shows an acoustic ray launched at depth 15 m with initial angle
             $\beta_0 = 55°$ and propagating in an isospeed ocean with a constant up-slope
             bottom.

112

Table 28. REFLECTION ANGLES : UP-SLOPE BOTTOM WITH $\beta_0 = 55°$

BOUNCE	Range (km)	$|\gamma°|$	$|\hat{\gamma}°|$	% Error	$\zeta°$	$\hat{\zeta}°$	% Error
1 BB	0.947	2.291	2.291	0.00	52.709	52.709	0.00
1 SB	2.476	0.000	0.000	0.00	50.419	50.419	0.00
2 BB	3.515	2.291	2.291	0.00	48.128	48.128	0.00
2 SB	4.400	0.000	0.000	0.00	45.838	45.838	0.00
3 BB	5.215	2.291	2.291	0.00	43.547	43.547	0.00
3 SB	5.909	0.000	0.000	0.00	41.256	41.256	0.00
4 BB	6.557	2.291	2.291	0.00	38.966	38.966	0.00
4 SB	7.106	0.000	0.000	0.00	36.675	36.675	0.00
5 BB	7.624	2.291	2.291	0.00	34.385	34.385	0.00
5 SB	8.059	0.000	0.000	0.00	32.094	32.094	0.00
6 BB	8.474	2.291	2.291	0.00	29.803	29.803	0.00
6 SB	8.818	0.000	0.000	0.00	27.513	27.513	0.00
7 BB	9.149	2.291	2.291	0.00	25.222	25.222	0.00
7 SB	9.417	0.000	0.000	0.00	22.931	22.931	0.00
8 BB	9,676	2.291	2.291	0.00	20.641	20.641	0.00
8 SB	9.879	0.000	0.000	0.00	18.350	18.350	0.00
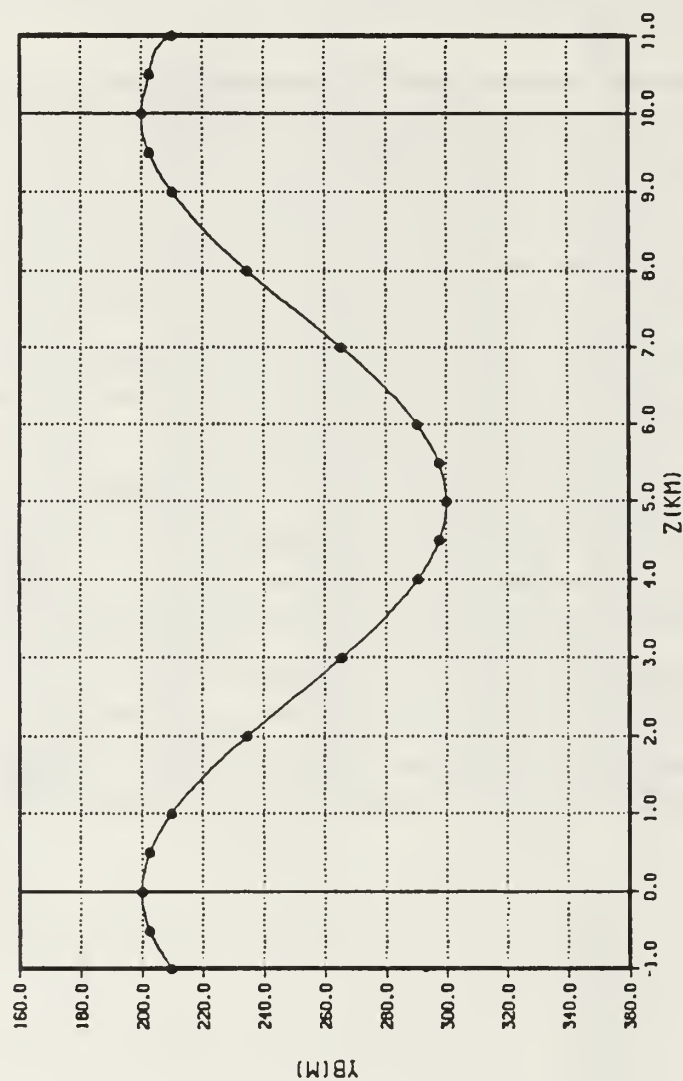
Figure 71. One Period Cosine Ocean Bottom: This profile was used to test the reflection angle algorithm for an isospeed ocean.

114
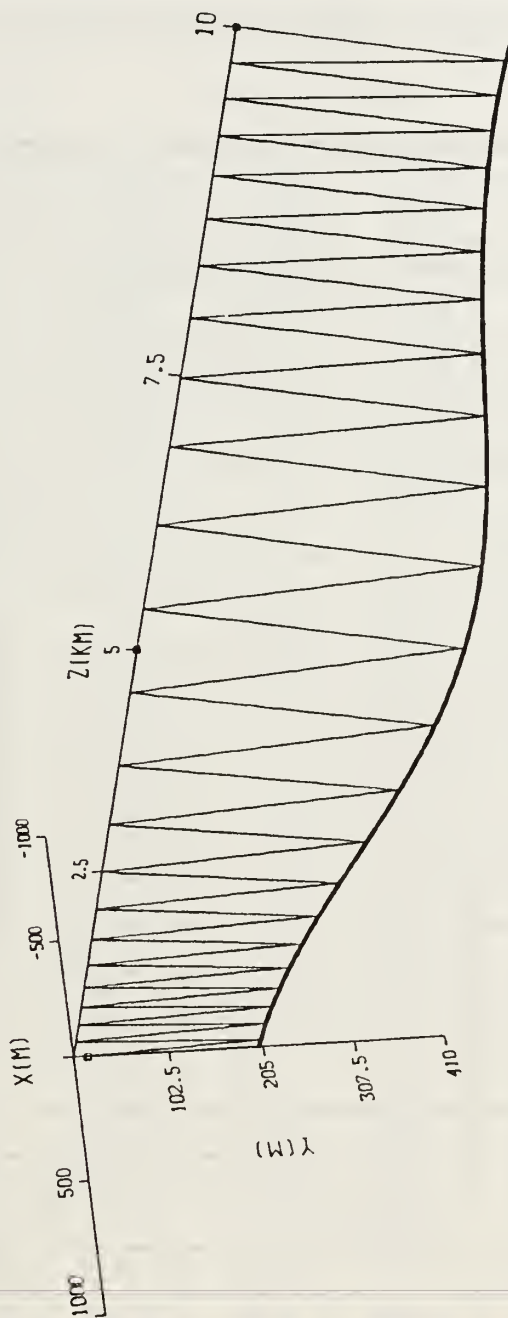
Figure 72.   Acoustic Ray Impinging a Cosine Bottom: This figure shows an
acoustic ray launched at depth 15 m with initial angle $\beta_0 = 30°$ and
propagating in an isospeed ocean.

115

Table 29. REFLECTION ANGLES : COSINE BOTTOM WITH $\beta_0 = 30°$

| BOUNCE	Range (km)	$\|\gamma°\|$	$\|\hat{\gamma}°\|$	% Error	$\zeta°$	$\hat{\zeta}°$	% Error
1 BB	0.107	0.121	0.124	2.48	30.121	30.124	0.010
1 SB	0.224	0.000	0.000	0.00	30.242	30.248	-0.019
2 BB	0.341	0.383	0.381	-0.52	30.624	30.628	0.013
2 SB	0.462	0.000	0.000	0.00	31.007	31.009	0.006
3 BB	0.584	0.646	0.644	-0.31	31.652	31.653	0.003
3 SB	0.713	0.000	0.000	0.00	32.298	32.297	-0.003
4 BB	0.843	0.910	0.910	0.00	33.208	33.207	-0.003
4 SB	0.983	0.000	0.000	0.00	34.118	34.118	0.000
5 BB	1.127	1.171	1.173	0.17	35.288	35.290	0.006
5 SB	1.284	0.000	0.000	0.00	36.456	36.463	0.019
6 BB	1.446	1.419	1.420	0.07	37.878	37.883	0.013
6 SB	1.625	0.000	0.000	0.00	39.297	39.302	0.013
7 BB	1.813	1.634	1.632	-1.22	40.931	40.935	0.009
7 SB	2.023	0.000	0.000	0.00	42.566	42.567	0.002
8 BB	2.245	1.777	1.775	-0.11	44.342	44.342	0.000
8 SB	2.497	0.000	0.000	0.00	46.118	46.117	-0.002
9 BB	2.766	1.774	1.776	0.11	47.893	47.893	0.000
9 SB	3.070	0.000	0.000	0.00	49.667	49.668	0.002
10 BB	3.396	1.522	1.522	0.00	51.189	51.190	0.002
10 SB	3.759	0.000	0.000	0.00	52.711	52.713	0.004
11 BB	4.144	0.922	0.922	0.00	53.633	53.634	0.002
11 SB	4.555	0.000	0.000	0.00	54.555	54.556	0.002
12 BB	4.977	0.026	0.026	0.00	54.581	54.582	0.002
12 SB	5.399	0.000	0.000	0.00	54.608	54.608	0.000
13 BB	5.812	0.879	0.879	0.00	53.728	53.729	0.002
13 SB	6.200	0.000	0.000	0.00	52.849	52.850	0.002
14 BB	6.566	1.499	1.498	-0.07	51.350	51.352	0.004
14 SB	6.896	0.000	0.000	0.00	49.851	49.854	0.006
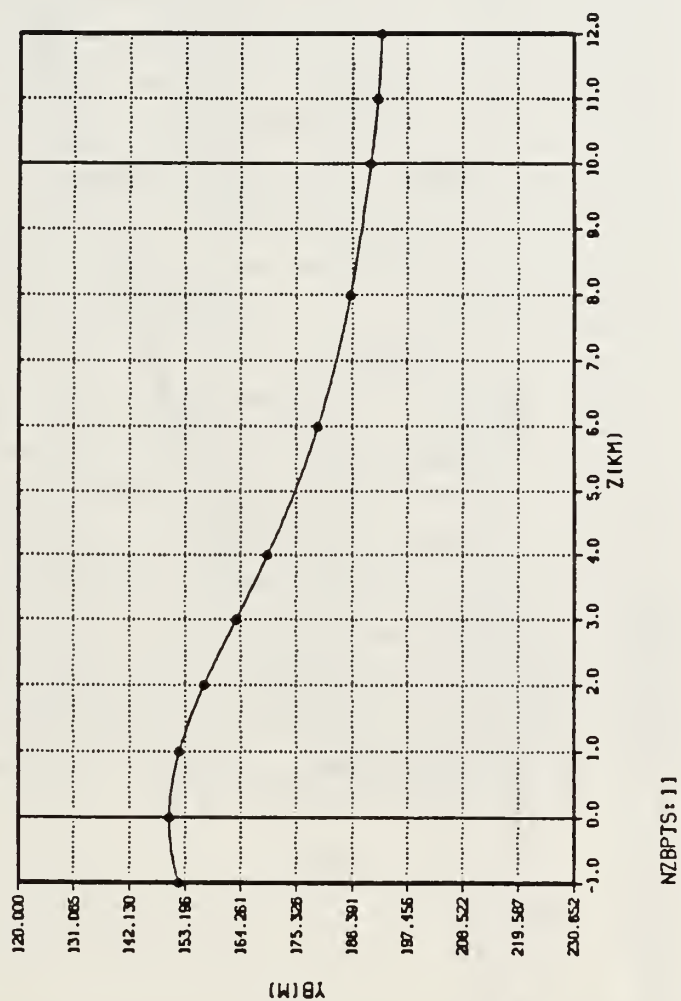
Figure 73.   Modified Witch Of Agnesi Ocean Bottom: This profile was used to test the reflection angle algorithm for an isospeed ocean.
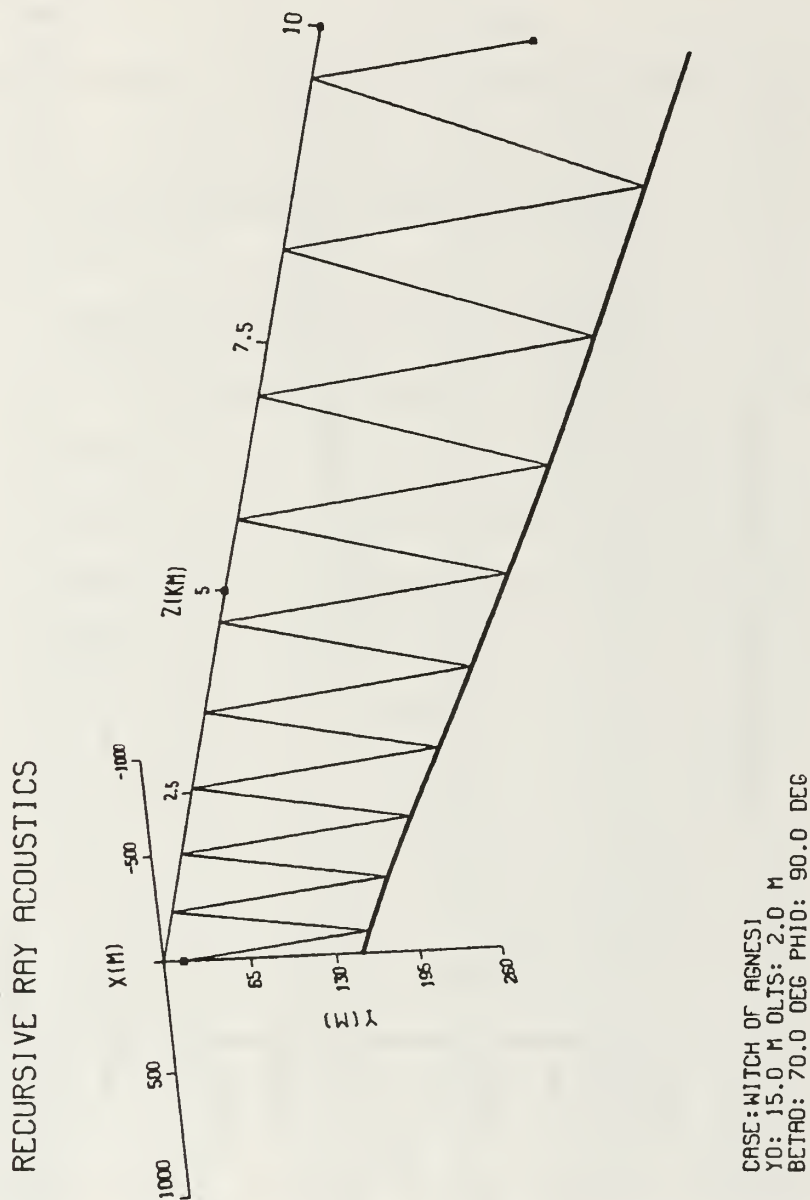
117

Figure 74. Acoustic Ray Impinging a Modified Witch Of Agnesi Bottom: This figure shows an acoustic ray launched at depth 15 m with initial angle $\beta_0 = 70°$ and propagating in an isospeed ocean with a Witch of Agnesi bottom.

118

Table 30. REFLECTION ANGLES : WITCH OF AGNESI BOTTOM WITH $\beta_0 = 70°$

BOUNCE	Range (km)	$|\gamma°|$	$|\hat{\gamma}°|$	% Error	$\zeta°$	$\hat{\zeta}°$	% Error
1 BB	0.372	0.084	0.084	0.00	70.084	70.084	0.000
1 SB	0.788	0.000	0.000	0.00	70.168	70.168	0.000
2 BB	1.212	0.248	0.247	-0.40	70.416	70.416	0.000
2 SB	1.647	0.000	0.000	0.00	70.644	70.663	0.027
3 BB	2.096	0.348	0.348	0.00	71.012	71.011	-0.001
3 SB	2.563	0.000	0.000	0.00	71.359	71.359	0.000
4 BB	3.048	0.371	0.372	0.27	71.730	71.731	0.001
4 SB	3.554	0.000	0.000	0.00	72.102	72.102	0.000
5 BB	4.080	0.337	0.336	-0.30	72.439	72.438	-0.001
5 SB	4.629	0.000	0.000	0.00	72.776	72.774	-0.003
6 BB	5.196	0.275	0.276	0.36	73.051	73.049	-0.003
6 SB	5.784	0.000	0.000	0.00	73.326	73.325	-0.001
7 BB	6.388	0.211	0.213	0.95	73.537	73.538	0.001
7 SB	7.009	0.000	0.000	0.00	73.749	73.752	0.004
8 BB	7.644	0.157	0.155	-1.27	73.906	73.907	0.001
8 SB	8.292	0.000	0.000	0.00	74.063	74.062	-0.001
9 BB	8.950	0.116	0.115	-0.86	74.179	74.177	-0.003
9 SB	9.619	0.000	0.000	0.00	74.295	74.291	-0.005
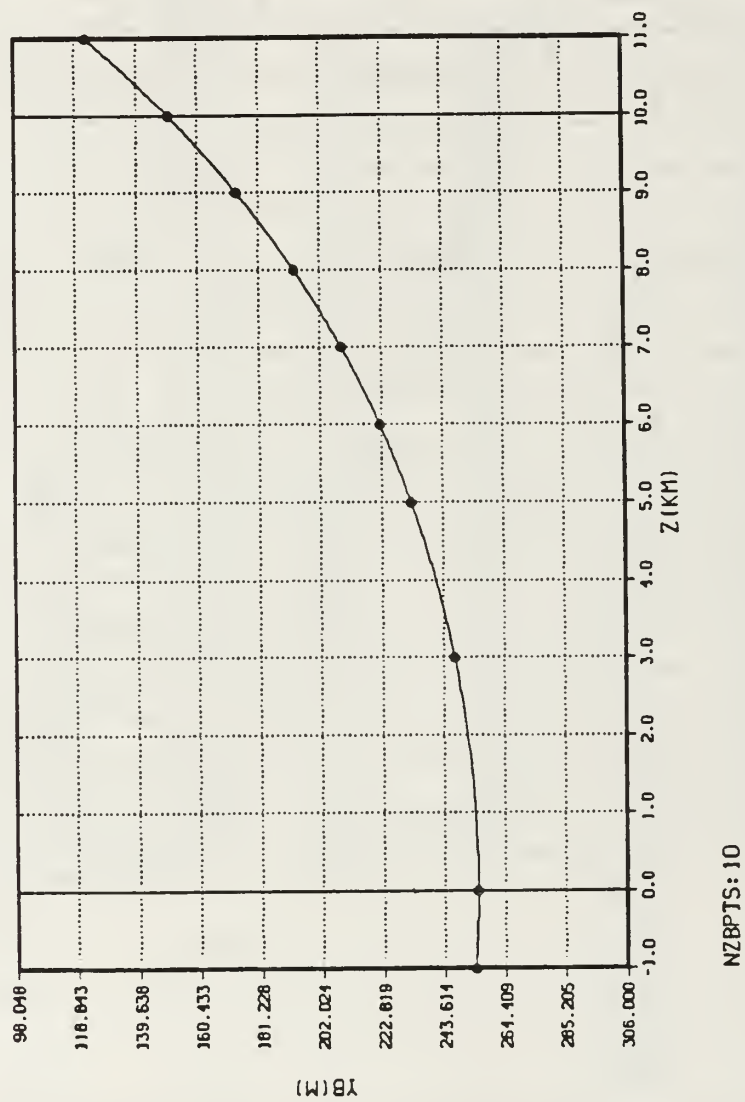
Figure 75.   Half Catenary Ocean Bottom: This profile was used to test the re-
flection angle algorithm for an isospeed ocean.

RECURSIVE RAY ACOUSTICS

CASE: HALF CATENARY
YO: 15.0 M DLTS: 2.0 M
BETAO: 60.0 DEG PHIO: 90.0 DEG

Figure 76.   Acoustic Ray Impinging a Half Catenary Bottom: This figure shows
an acoustic ray launched at depth 15 m with initial angle $\beta_0 = 60°$ and
propagating in an isospeed ocean with a half catenary bottom.

121

Table 31. REFLECTION ANGLES : HALF CATENARY BOTTOM WITH $\beta_0 = 60°$

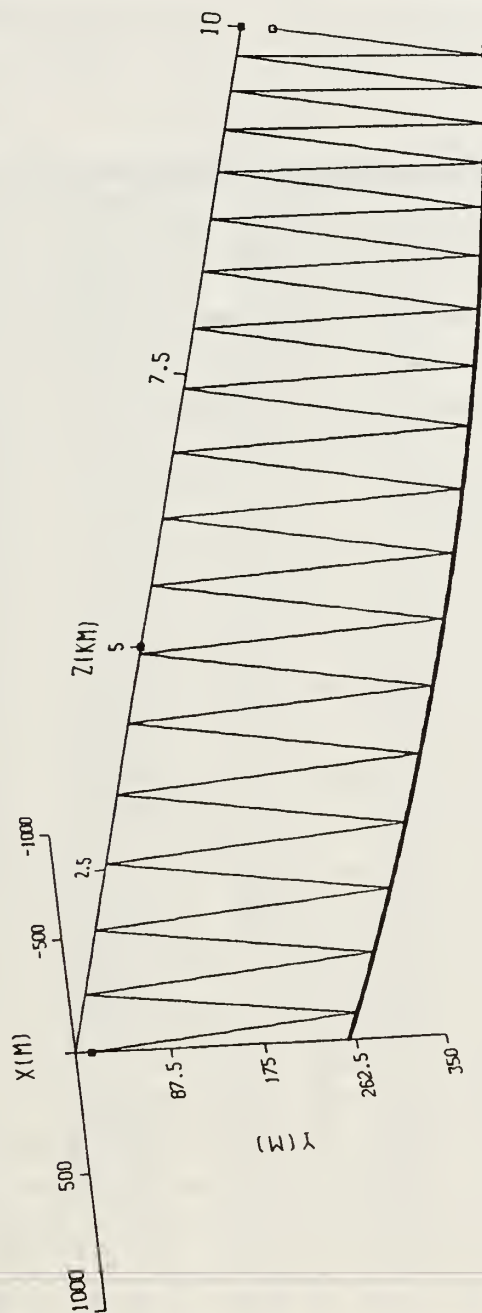| BOUNCE	Range (km)	$\lvert\gamma°\rvert$	$\lvert\hat{\gamma}°\rvert$	% Error	$\zeta°$	$\hat{\zeta}°$	% Error
1 BB	0.416	0.039	0.035	-10.25	59.960	59.965	0.008
1 SB	0.856	0.000	0.000	0.00	59.921	59.931	0.017
2 BB	1.294	0.125	0.125	0.00	59.800	59.805	0.008
2 SB	1.728	0.000	0.000	0.00	59.671	59.680	0.015
3 BB	2.157	0.210	0.214	1.90	59.461	59.466	0.008
3 SB	2.579	0.000	0.000	0.00	59.251	59.253	0.003
4 BB	2.995	0.298	0.300	0.67	58.953	58.953	0.000
4 SB	3.401	0.000	0.000	0.00	58.654	58.653	-0.002
5 BB	3.799	0.388	0.388	0.00	58.267	58.265	-0.003
5 SB	4.186	0.000	0.000	0.00	57.879	57.877	-0.003
6 BB	4.563	0.479	0.478	-0.21	57.400	57.399	-0.002
6 SB	4.926	0.000	0.000	0.00	56.922	56.921	-0.002
7 BB	5.280	0.572	0.571	-0.17	56.350	56.350	0.000
7 SB	5.618	0.000	0.000	0.00	56.922	56.921	-0.002
8 BB	5.946	0.665	0.665	0.00	55.113	55.114	0.002
8 SB	6.258	0.000	0.000	0.00	54.447	54.448	0.002
9 BB	6.560	0.756	0.759	0.39	53.688	53.689	0.002
9 SB	6.845	0.000	0.000	0.00	52.929	52.930	0.002
10 BB	7.120	0.851	0.851	0.00	52.078	52.078	0.000
10 SB	7.378	0.000	0.000	0.00	51.227	51.227	0.000
11 BB	7.627	0.941	0.941	0.00	50.287	50.286	-0.002
11 SB	7.859	0.000	0.000	0.00	49.346	49.345	-0.002
12 BB	8.083	1.027	1.027	0.00	48.319	41.318	-0.002
12 SB	8.290	0.000	0.000	0.00	47.291	47.291	0.000
13 BB	8.490	1.110	1.109	0.09	46.182	46.182	0.000
13 SB	8.675	0.000	0.000	0.00	45.072	45.073	0.002
14 BB	8.852	1.187	1.187	0.00	43.885	43.887	0.005
14 SB	9.015	0.000	0.000	0.00	42.698	42.700	0.005

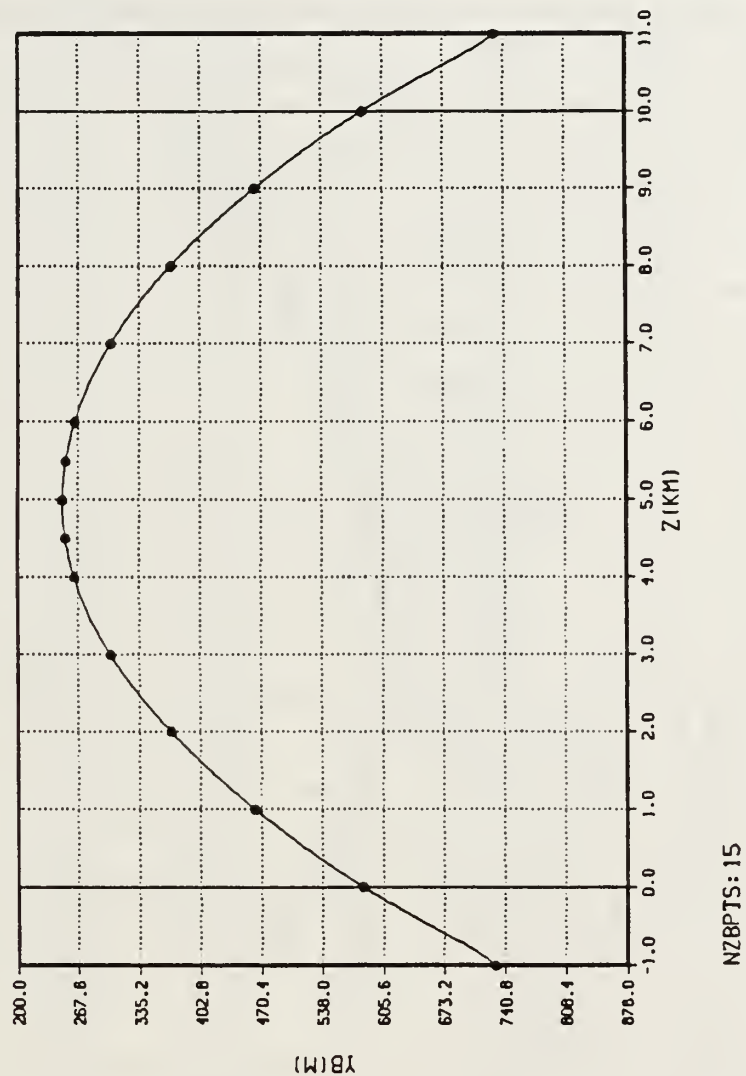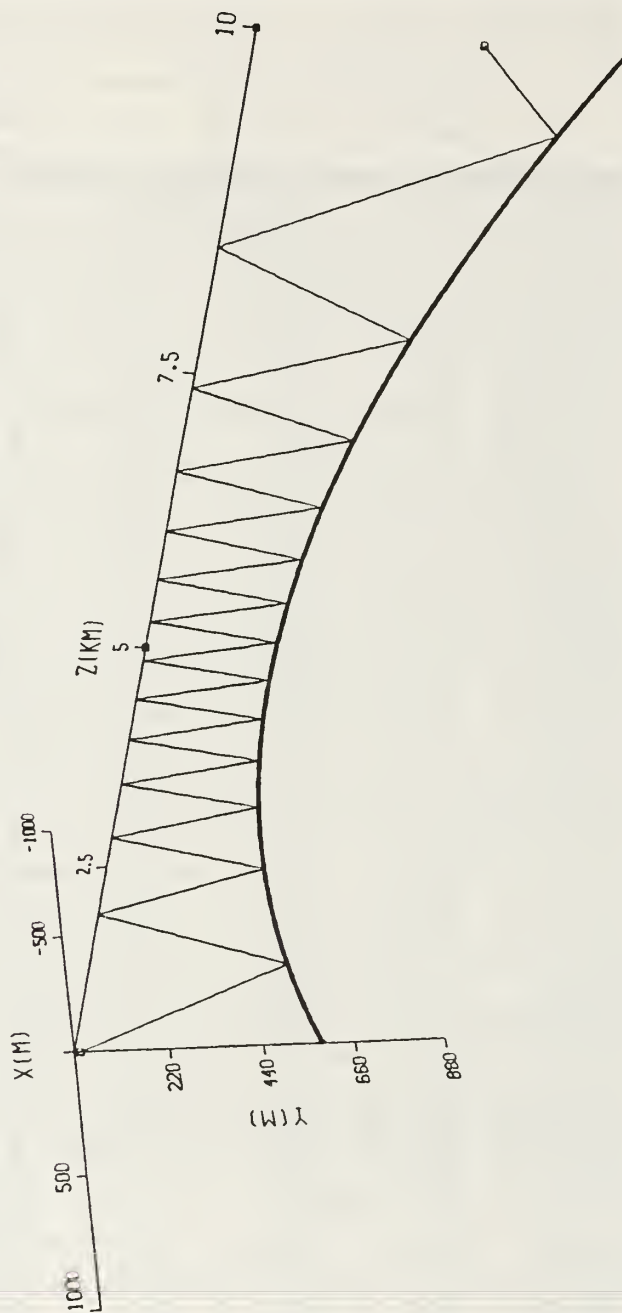Figure 77.   Parabolic Ocean Bottom: This profile was used to test the reflection angle algorithm for an isospeed ocean.

123

Figure 78. Acoustic Ray Impinging a Parabolic Bottom: This figure shows an acoustic ray launched at depth 15 m with initial angle $\beta_0 = 70°$ and propagating in an isospeed ocean with a parabolic bottom.

Table 32. REFLECTION ANGLES : PARABOLIC BOTTOM WITH $\beta_0 = 70°$

| BOUNCE	Range (km)	$|\gamma°|$	$|\hat{\gamma}°|$	% Error	$\zeta°$	$\hat{\zeta}°$	% Error
1 BB	1.180	5.816	5.798	0.31	64.184	64.202	-0.028
1 SB	1.903	0.000	0.000	0.00	58.368	58.405	0.063
2 BB	2.451	3.889	3.888	-0.03	54.479	54.517	0.069
2 SB	2.861	0.000	0.000	0.00	50.590	50.628	0.075
3 BB	3.217	2.722	2.721	-0.04	47.868	47.907	0.081
3 SB	3.511	0.000	0.000	0.00	45.145	45.186	0.091
4 BB	3.783	1.859	1.860	0.05	43.287	43.326	0.09
4 SB	4.021	0.000	0.000	0.00	41.428	41.467	0.094
5 BB	4.249	1.148	1.147	-0.09	40.280	40.319	0.097
5 SB	4.459	0.000	0.000	0.00	39.133	39.172	0.099
6 BB	4.664	0.514	0.513	-0.19	38.619	38.658	0.101
6 SB	4.861	0.000	0.000	0.00	38.104	38.145	0.108
7 BB	5.057	0.088	0.088	0.00	38.192	38.232	0.105
7 SB	5.255	0.000	0.000	0.00	38.280	38.320	0.104
8 BB	5.454	0.695	0.694	-0.14	38.975	39.014	0.100
8 SB	5.665	0.000	0.000	0.00	39.670	39.709	0.098
9 BB	5.881	1.346	1.346	0.00	41.016	41.055	0.095
9 SB	6.118	0.000	0.000	0.00	42.362	42.401	0.092
10 BB	6.370	2.092	2.093	0.05	44.454	44.494	0.090
10 SB	6.661	0.000	0.000	0.00	46.546	46.587	0.088
11 BB	6.980	3.022	3.020	-0.07	49.568	49.607	0.078
11 SB	7.376	0.000	0.000	0.00	52.591	52.627	0.068
12 BB	7.844	4.337	4.343	0.14	56.928	56.970	0.073
12 SB	8.498	0.000	0.000	0.00	61.265	61.313	0.078
13 BB	9.433	6.742	6.669	-1.08	68.007	67.982	-0.037
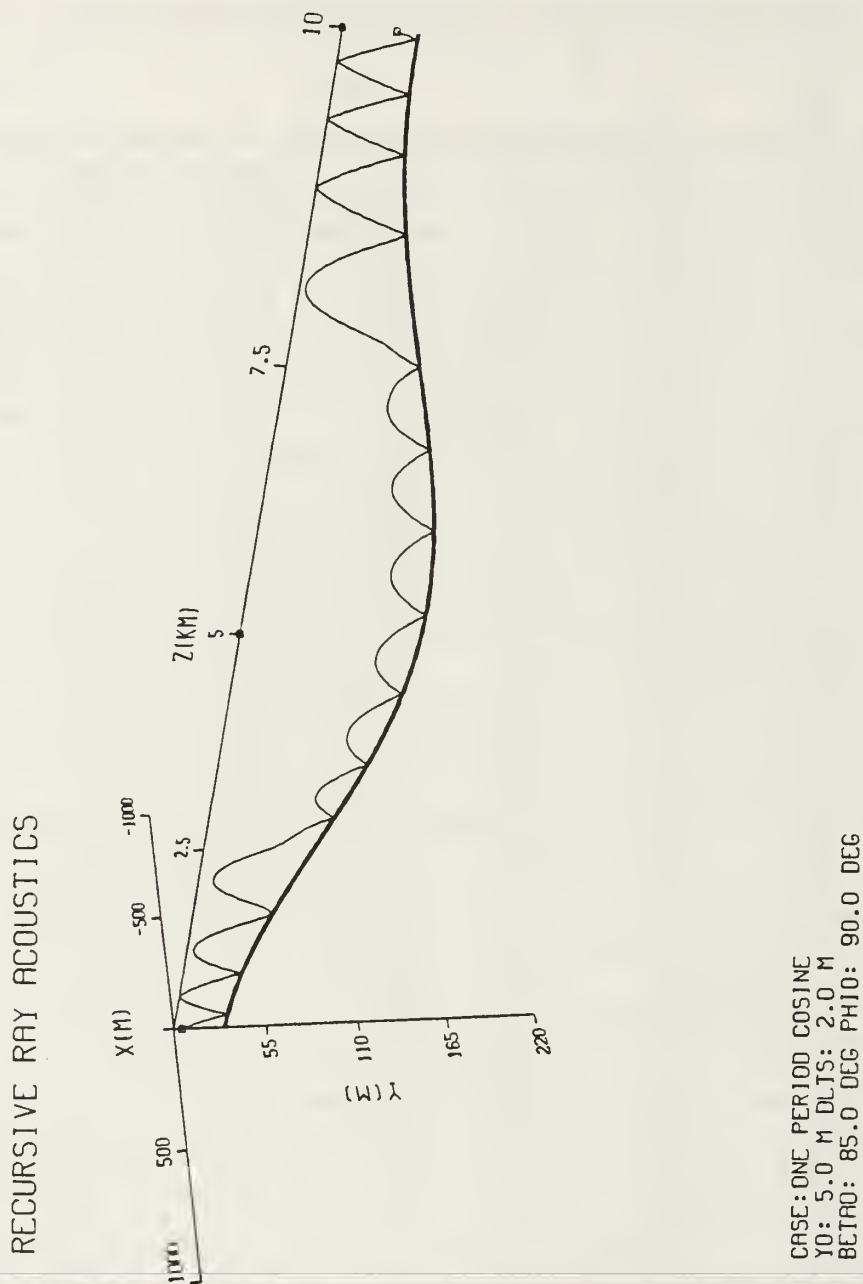
Figure 79. Acoustic Ray Impinging A Cosine Bottom: This figure shows an acoustic ray launched at depth 5 m with initial angle $\beta_0 = 85°$ and propagating in an ocean medium where sound speed varies as a function of depth.
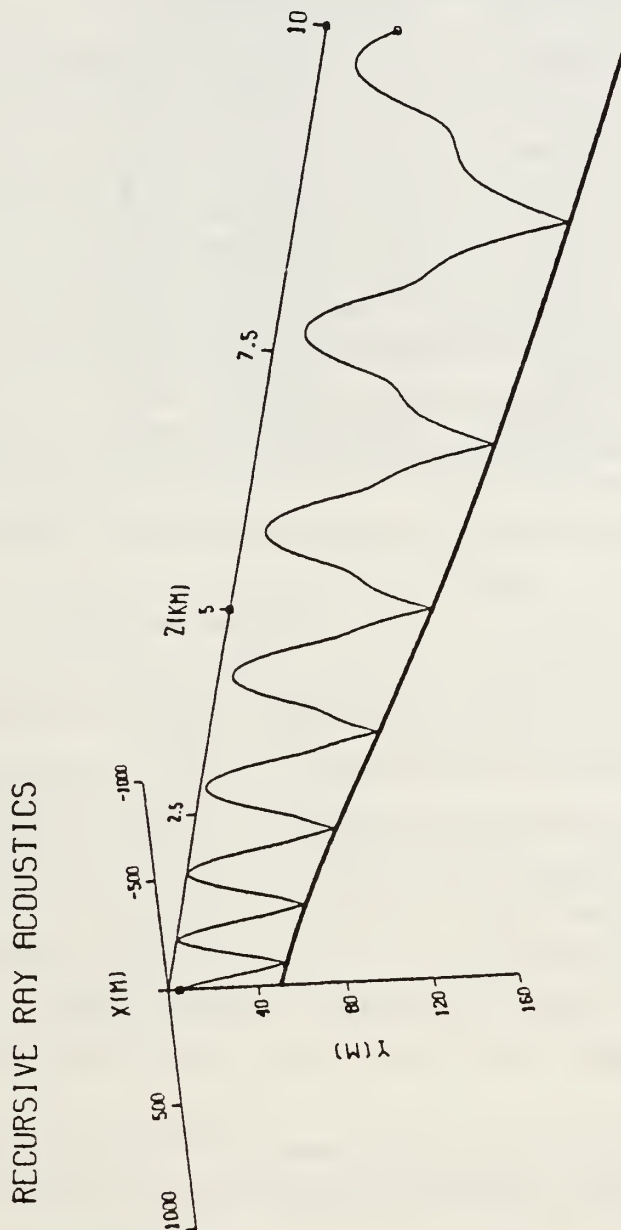
Figure 80.　Acoustic Ray Impinging A Modified Witch Of Agnesi Bottom:　This figure shows an acoustic ray launched at depth 5 m with initial angle $\beta_0 = 85°$ and propagating in an ocean medium where speed of sound is a function of depth.

Table 33.   SOUND SPEED PROFILE

Depth (m)	Sound Speed (m/s)
0.00	1540.00
25.00	1524.00
30.00	1522.00
36.00	1524.00
40.00	1529.00
45.00	1532.00
50.00	1531.00
60.00	1525.75
100.00	1514.75

V. CONCLUSIONS AND RECOMMENDATIONS

The IMSL Version 10 Akima Cubic Spline (ACS) computer computer program had proven useful in modeling ocean bottom contours, but was unable to provide accurate first and second-order derivatives for the one period cosine and modified Witch of Agnesi ocean bottom models. The application of Spatial Fourier Series (SFS) methods as an alternative means of modeling the one-dimensional ocean floor was considered a viable solution to this problem. However, despite several numerical enhancements to the fundamental technique, including Lanczos smoothing and artificial data simulation to eliminate end point anomalies, Spatial Fourier Series failed to achieve the accuracy required for subsequent acoustic ray and reflection angle computations.

Despite the aforementioned difficulties, Spatial Fourier Series methods may yet prove to be a viable numerical tool in modeling ocean bathymetries, but its immediate utility, based upon the analysis conducted, is doubtful.

The divided differences polynomial curve fitting Fortran routine yielded results which were equal to, or better than, both the ACS and SFS modeling techniques that it replaced. Similarly, the central differencing method for determining the first and second-order derivatives of the ocean bottom provided the most accurate estimates when used in conjunction with this alternate approach to bottom contour modeling. Notwithstanding the foregoing observations, this polynomial routine also had deficiencies, the most notable being the introduction of artificial oscillations generated following an imprudent choice of discrete bathymetric data to describe the contour.

The reflection angle algorithm developed in Chapter 2 for an arbitrarily shaped one-dimensional, ocean bottom were validated by the computer simulations given in Chapter 3.

One of the realizations of this research was that no one numerical modeling method studied was definitive. Further investigation of bottom contour modeling techniques, such as the method of least squares, is warranted. This work represents precursory efforts in the development of a two-dimensional ocean bottom model which would enable more advanced study of ray acoustic theory in an ocean medium where sound-speed varies as a function of all three spatial coordinates.

LIST OF REFERENCES

1. Goodman, A.W., *Analytic Geometry and the Calculus*, The Macmillan Company, New York, 1963, pp. 547-549.

2. Strum, R.D. & Kirk, D.E., *First Principles of Discrete Systems and Digital Signal Processing* , Addison-Wesley Publishing Company, New York, 1989, pp.554-557.

3. Lanczos, C., *Applied Analysis*, Prentice Hall, Inc., London, 1956, pp. 219-220.

4. Hamming, R.W., *Digital Filters*, 3rd edition, Prentice Hall, Inc., London, 1989.

5. Officer, C.B., *Introduction to the Theory of Sound Transmission*, McGraw-Hill Book Company, Inc., New York, 1958.

6. Spiegel, M.R., *Mathematical Handbook of Formulas and Tables*, Schaum's Outline Series, McGraw-Hill Publishing Company, New York, 1968.

7. Gerald, C.F., & Wheatley, P.O., *Applied Numerical Analysis*, 4th edition, Addison-Wesley Publishing Company, New-York, 1989.

INITIAL DISTRIBUTION LIST

1.	Defense Technical Information Center Cameron Station Alexandria, VA. 22304-6145	2
2.	Library, Code 52 Naval Postgraduate School Monterey, CA. 93943-5002	2
3.	Professor Lawrence J. Ziomek, Code EC/Zm Department of Electrical and Computer Engineering Naval Postgraduate School Monterey, CA. 93943-5000	2
4.	Professor Hung-Mou Lee, Code EC/Lh Department of Electrical and Computer Engineering Naval Postgraduate School Monterey, CA. 93943-5000	1
5.	Mr. Thomas Martin Undersea Warfare Program Office PRC, Inc. 1555 Wilson Blvd. Arlington, VA 22209	1
6.	Dr. Richard Seesholtz Undersea Warfare Program Office PRC, Inc. 1555 Wilson Blvd. Arlington, VA 22209	1
7.	LCDR T.N. Jones, RAN HMAS BRISBANE c/o Warships Section Central Mail Exchange Redfern, 2890 Sydney, NSW, Australia	1
8.	Director of Surface and Underwater Weapons Building A Russell Offices Canberra, 2600 ACT, Australia	1
9.	Director of Naval Education Building D Russell Offices Canberra, 2600 ACT, Australia	1